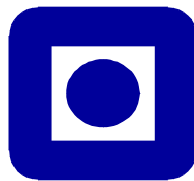# Process Integration Applied to the Design and Operation of Distillation Columns

by

Hilde Kathrine Engelien

A Thesis Submitted for the Degree of Dr. Ing.

Norwegian University of Science and Technology
Department of Chemical Engineering

Abstract

Process integration of distillation columns with focus on multi-effect distillation is studied in this thesis. Columns are integrated by using different pressures, so that the condensing duty of one column can be used to boil a second column. This system of multi-effect integration is applied to a complex distillation system; a prefractionator arrangement. The resulting multi-effect prefractionator arrangement has a much lower energy requirement than a conventional distillation arrangement and it is shown that the savings can be in excess of 70 %.

The emphasis of the work is on the energy savings of such arrangement, looked at mainly in terms of *minimum vapour flow* requirements. Energy savings are considered in terms of both design and operational issues.

The first part of the thesis deals primarily with minimum vapour flow expressions. It is shown how minimum vapour flow of multi-effect arrangements can be visualised in a V_{min}-diagram. These diagrams can be used to find the minimum energy requirement for different multi-effect configurations and can further be used to analyse and understand the multi-effect prefractionator arrangement.

Having shown the potential savings of the multi-effect prefractionator arrangement it is interesting to look at how such integrated arrangements can be operated in practice. A method of self-optimising control is used as a systematic tool to find the variables that should be controlled in order to keep the system close to its *optimal* operating point. Dynamic simulations are used to verify the suggested control structure.

The final part of the thesis looks at an industrial case study to see if the tools and a multi-effect prefractionator arrangement can be implemented for a real separation task.

Acknowledgements

I wish to thank my supervisor Professor Sigurd Skogestad, Department of Chemical Engineering, Norwegian University of Science and technology (NTNU), for his support and advice during my four and a half years at university.

I would also like to thank all my colleagues for their support and help in the last years. I have to especially thank Stathis Skouras, who started at the same time as me, for your help, for all our discussions and for being a good friend. Thanks to Marius Govatsmark for all your help with Matlab and for always having a positive outlook on life. I shall try to look at every day as a new opportunity…

During the first three years of my degree I received funding by the Nordic Energy Research Programme (NEFP). NEFP runs a number of programs related to energy and I was a part of the Process Integration (PI) Group. Being a part of the NEFP and the PI Group has been a really good experience where I have had the opportunity to travel to other Nordic countries and being a part of a Nordic co-operation. I would like to give a big thanks to all the other students and people in the PI Group for your support and encouragement and for all the good times we shared. Through seminars, courses and other events we have formed a Nordic co-operation and friendship.

Sitting here now at the end of four and a half years I have to conclude that as always time passes quicker than you think. I admit, the time has sometimes seemed slower (especially when things were going wrong) and other times quicker (a normal feeling around deadlines). But, as I also have learnt previously in life, time does pass, regardless of what goes on around you.

In my work there have been times with both ups and downs, where my outlook on life often was coloured by the success of the model I was currently working on. Sometimes it felt more like there were more downs than ups, but I think I found my bearing in the end.

This time has also been four and half years where I have experienced many other things apart from working with my thesis. I have had the opportunity to go on many smaller trips to seminars and conferences, where I have visited countries such as Germany, Finland, Iceland and Denmark. These trips have been good and it has been a valuable experience and glimpse into the academic world.

In addition to the academic journey I have also made two great trips of both the mind and body, to Thailand in 2001 and Nepal in 2002, where I experienced the greatness of the East. In August 2002 I got engaged in Prague and I am currently looking forward to getting married to the love of my life in April 2004.

I would say that for me the doctoral degree has maybe been much like walking a steep mountain or taking a difficult trip. At times it is easy, then it is really hard and you feel like turning back. But, when I look back I remember the good times, and the achievement. I may not always have managed to stay the course, but I have tried to go on by following my life motto: "Keep walking, the road knows where you are going".

So, now, at the end of one Chapter and at the beginning of a new one I would like to thank all those close to me who make walking the road that much easier and my life richer. Thanks to my dearest family, for always believing in me, and especially thanks to my mother for her help and support. In my mind you are without a doubt the best mum in the world.

Most of all thank you David. You are the essence of my being and the person that balances my life. You are the constant sun on my horizon. Your love, patience, support, humour and fabulous cooking are some of the things that makes this life so special and makes me remember what a lucky woman I am. I would never have managed this without you and I thank you with all my heart for being you.

Finally, I would like to dedicate this thesis to my father. You are deeply missed and always in my thoughts.

With hands like spades.

And a heart full of gold.

My father, my father.

Irish proverb.

TABLE OF CONTENTS

Nomenclature

The notation has mainly been defined in the text. However, the most important notation used in the thesis is summarised here:

V	Vapour flowrate
L	Liquid flowrate
D	Distillate flowrate
B	Bottom product flowrate
S	Sidestream product flowrate
x	Mole fraction in liquid phase
y	Mole fraction in vapour phase
z	Mole fraction in feed
q	Feed liquid fraction (feed quality)
T	Temperature
P	Pressure
i, j	Components i, j
A, B, C	Components (lightest component is A, heaviest component is C)
N_c	Number of components
J	Cost function (objective function)
Q	Heat duty
α	Relative volatility
γ	Distillate to feed ratio (D/F)
η	Thermodynamic efficiency
θ	Underwood root

Superscripts

C1	Prefractionator column
C21	Upper section of main column in prefractionator arrangement
C22	Lower section of main column in prefractionator arrangement
CD1	First column in integrated direct split arrangements
CD2	Second column in integrated direct split arrangements

| CI1 | First column in integrated indirect split arrangements |
| CI2 | Second column in integrated indirect split arrangements |

Subscripts

min	Minimum
D	Distillate product
B	Bottom product (or bottom of column/column section)
i, j	Components i, j
A, B, C	Components (lightest component is A, heaviest component is C)
i/j	Sharp split between components i and j
T	Top of column (or column section)

Column Notation

DS	Direct split column arrangement
IS	Indirect split column arrangement
DSF	Direct split column arrangement with forward multi-effect integration
DSB	Direct split column arrangement with backward multi-effect integration
ISF	Indirect split column arrangement with forward multi-effect integration
ISB	Indirect split column arrangement with backward multi-effect integration
PF	Prefractionator column with forward multi-effect integration
PB	Prefractionator column with backward multi-effect integration

Chapter 1. Introduction

1.1.   Motivation

The title of this thesis is "Process integration applied to the design and operation of distillation columns". Now, what exactly is **process integration** and how has it been applied in this work ?

The definition of process integration can vary, depending on the field of work or even from person to person in the same field. A common view of what process integration can be, is for example the technique of pinch technology. A more general definition of process integration is that of the International Energy Agency (IEA) which was made at an expert meeting in Berlin (1993):

> *"Systematic and general methods for designing integrated production systems, ranging from individual processes to total sites, with special emphasis on the efficient use of energy and reducing environmental effect."*

This definition has later been expanded, and now includes:

> *"...Process integration also refers to some aspects of operation and maintenance."*

Process integration is thus <u>systematic</u> and <u>general</u> methods that are applied to <u>design</u> and <u>operation</u> of integrated plants with the objective or motivation of saving energy and reducing any environmental impacts.

In this thesis the focus of work has been on one type of heat-integrated distillation system. The work applies systematic and general methods to look at design and operational issues in terms of energy savings and in terms keeping the system operating close to the optimum energy demand. Focus has been on the *energy* savings for both the design and the operation of this integrated system and not on factors that are time dependent, such as energy costs or equipment costs.

The motivation for looking at a heat-integrated distillation design is mainly due to the high-energy demand of distillation processes. In addition, distillation is a very commonly used separation process, which can account for a large portion of the energy consumption in a chemical plant. It is therefore interesting to study different alternative distillation schemes that can save energy (design issues) as well as study how these heat-integrated distillation units should be operated (operational & control issues).

In terms of heat-integration of distillation columns the main questions for each designer is "What is the best energy saving scheme for my separation problem ?" and "How can it best be operated to achieve the promised energy savings ? More specifically, in this thesis, the question is "Is the multi-effect prefractionator arrangement a good solution and how can it be operated ?"

Now, why should we answer such questions and what is (or should be) our motivation ? When solving an engineering question or problem there are many different objectives that have different importance, e.g. profit, safety, environment, flexibility, controllability. One issue or objective that should always concern engineers is the *sustainability* of the process. In this context we should always be thinking about reducing the energy demand of all processes. In my opinion energy efficiency should always be considered, irrespectively of the energy prices. Unfortunately, energy issues are often only regarded as interesting when the energy prices are high.

In terms of operation we have to try to identify the best way a system can be operated so that the energy savings we are expecting are actually achieved. An integrated system that is operated incorrectly can result in a higher energy demand than a simple non-integrated system. When a good energy saving scheme has been identified it is important that the operation is not forgotten. Operational aspects of integrated plants are important as the integration can cause additional control problems.

The multi-effect heat integrated prefractionator arrangement is interesting to study as this arrangement has potential for large energy savings compared with non-integrated arrangements. The control of the system is important as the integration of the two systems result in a linking of the reboiler and condenser of two columns. Also, there have not been many studies on the control and operation of this type of arrangement.

Finally, it should be noted that <u>one</u> "optimal" solution for <u>all</u> cases does not exist. Integration should therefore be done with care and be on a case-to-case basis. Simple shortcut methods exist for screening different alternatives and systematic methods can be used to ensure satisfactory operation of the selected arrangement.

1.2.   Thesis Overview

The system studied in this thesis is a distillation arrangement where pressure is used to heat-integrate two columns using multi-effect. The system consists of a prefractionator column and a main column with sidestream, where the condenser of one of the columns is integrated with the reboiler of the other column. Heat then only has to be supplied to the column running at the higher pressure. This system is here called the *multi-effect integrated prefractionator arrangement*.

The basis for most of the comparisons made between this integrated prefractionator arrangement and other integrated and non-integrated arrangements is *minimum vapour flow* (V_{min}). As shown here this is a useful measure for comparing different arrangements.

The minimum vapour flowrate can be looked on as a measure for the operating costs of a particular distillation arrangement. This thesis does not however, look at the prefractionator arrangement in terms of capital costs. In the real world both the capital costs and operating costs would have to be considered, where the "optimal" solution is usually a trade-off between the two.

The following summary gives an overview of the different chapters in this thesis:

Chapter 2 gives an overview of some of the available heat-integrated distillation systems. The concept of heat integrated distillation is introduced with focus on multi-effect distillation systems. A brief review of the literature on multi-effect distillation is given. Finally, the aim of the thesis is presented.

Chapter 3 presents shortcut methods for minimum energy requirements for six ternary multi-effect distillation systems and three non-integrated systems. The comparison of the different arrangements is based on minimum vapour flowrates at infinite number of stages. A comparison of the energy requirement of the integrated prefractionator arrangement with other integrated and non-integrated systems is made based on the shortcut method. There is also a brief introduction to exergy analysis for multi-effect arrangements.

Chapter 4 looks at how the energy requirement for the multi-effect arrangements can be easily visualised and compared in V_{min}-diagrams. The V_{min}-diagram can be used as a tool for analysis and understanding of the integrated prefractionator arrangement. This Chapter, together with parts of Chapter 3 has been submitted to the AIChE Journal, Feb. 2004.

Chapter 5 is a self-optimising control study for a *forward-integrated* prefractionator scheme. It details the selection of suitable controlled variables with the aim of keeping the system near the optimum energy savings. A control structure is suggested and dynamic simulations are made to verify the selected control structure. The chapter has been presented at ESCAPE 13 (Lappeenranta, Finland, 2003) and will be published in a Special Issue of Computers and Chemical Engineering, May 2004.

Chapter 6 presents an industrial case study. A system of four distillation columns has been studied to see if any could be integrated using an integrated prefractionator arrangement. The methods presented in Chapter 3 and Chapter 4 are used in the analysis to screen the different column options. One case was studied more rigorously using a commercial simulation package, where three arrangements were studied. This Chapter has been submitted for publication to the journal of Chemical Engineering and Processing, February 2004.

Chapter 7 gives the general conclusions of the thesis and recommendation for further work.

Appendix A describes the dynamic simulation model and the optimisation methods used in Chapter 5 of the thesis.

Appendix B presents a self-optimisation study of a methanol/water separation using a direct split with forward integration distillation arrangement. This has previously been presented at the International Conference on Distillation and Absorption (Baden-Baden, Germany, 2002) and published the Trans IChemE Journal, February 2003.

Appendix C presents further results from the energy comparisons made in Chapter 3.

4

The main contributions of this thesis are:

- The comparison of the integrated prefractionator arrangement with the other (conventional) multi-effect arrangements and non-integrated arrangements (including the Petlyuk column).

- The graphical visualisation of the minimum energy requirements of multi-effect distillation arrangements in a V_{min}-diagram. The V_{min}-diagram gives a simple visualisation of complex integrated solutions in one diagram. Figure 4.4 summarises much of the results in Chapter 4. This chapter is the main contribution of the thesis.

- The selection of controlled variables for a forward integration prefractionator arrangement (Chapter 5). This analysis takes one step back from the usual controllability analysis and looks at what variables should be controlled in order to operate the integrated multi-effect arrangement close to the optimum (in terms of minimum energy).

- The analysis of an industrial case study in Chapter 6.

Note

The reference from the International Energy Agency (http://www.iea.org/) is found from the following web page: http://www.tev.ntnu.no/iea/pi/definition.html

Chapter 2. A Brief Overview of Heat-Integrated Distillation Systems

2.1. Introduction

In the chemical industries, the task of separation is a very energy consuming process, where distillation is the process most widely used for fluid separations. Distillation columns are used for about 95% of liquid separations and the energy use from this process accounts for an estimated 3% of the world energy consumption (Hewitt et al., 1999). With rising energy awareness and growing environmental concerns there is a need to reduce the energy use in industry. For the distillation process any energy savings should have an impact on the plant energy consumption.

The use of heat integration and more complex configurations for distillation columns holds a great promise of energy savings up to about 70%. In addition to saving energy, heat integration reduces the environmental impact of a process, reduces site utility costs and can give possible reduction in capital costs. However, there are a number of different methods or designs that can be applied to save energy in distillation, for example integration of distillation columns with the background process, heat pumps, multi-effect distillation and complex arrangements such as prefractionators or thermally coupled columns (Petlyuk columns). Deciding which heat integrated arrangement to use is not a straightforward task as the best arrangement is very much dependent on the given separation task.

This chapter will first give a short summary of some available heat saving schemes and then focus on heat integration using multi-effect distillation, which is the use of different pressures to change the temperature levels to allow for heat integration. For multi-effect distillation an overview of different configurations are given, then follows a short summary of some of the literature available in this area. The topic of column sequencing using optimisation procedures such as MINLP etc., has been considered outside the scope of this work. The last section of this chapter presents the problem statement for the thesis.

2.2. Heat Integrated Distillation Systems

When distillation is the choice of separation for a given mixture there are a number of ways that the separation can be carried out. There are many factors that are important in the design process, such as safety, operating costs, capital costs and operability. Deciding on the most appropriate distillation system can be difficult, as in most cases there are usually trade-offs between the various objectives.

In the chemical and petroleum industry distillation usually accounts for around 25-40 % of the energy usage (Rush, 1980), and it has been estimated that for a wide range of distillation applications 10-15 % of the energy use is in excess (Energy Efficiency Best Practice Programme, 1999). The potential for energy savings therefore exists and design and operation of energy efficient distillation systems will have a substantial effect on the overall plant energy consumption and operating costs.

Any separation requires the addition of work or exergy. In a distillation column the work requirements are supplied indirectly through heating in the reboiler and cooling in the condenser at a lower temperature. If cooling water is used then the problem of optimal operation of individual columns is reduced to minimising the boilup (or even simpler the vapour flowrate in the columns). Usually, if simple columns (no heat integration) are to be used, the first approach may be to use rules of thumb to find a column sequence that has low total energy consumption. A number of potential column sequences can be made based on **heuristic rules** or **short-cut methods** and then the most promising schemes can be tested using more rigorous simulation tools. The description of such rules and methods can be found in many textbooks on distillation, for example King (1980), Smith (1995) and Biegler, Grossmann and Westerberg (1997). The most common methods for heat integration described below can also be found in these textbooks.

When the best column sequence has been identified further energy savings can be made by integrating the reboiler and condensers with other process streams, either by using the product/feed streams from the distillation sequences or integration with the rest of the process. The best combination for **this heat exchanger network** can be found using **pinch methods**. The pinch method looks at the heating and cooling of the whole process and gives targets for the minimum heating and cooling requirements. A distillation column can also be integrated with the process where the heating or cooling duty is provided by the process streams. A grand composite curve (see e.g. Smith, 1995) can be used to see if a distillation column can be integrated with the plant. The rule for integration with the process is that a column should not be integrated across the pinch. Either the condenser should be integrated *above* the pinch (where heating is required) or the reboiler should be integrated *below* the pinch (where cooling is required).

Another method for saving exergy (work) is the use of **interheating** or **intercooling**, where heat is added or removed at intermediate points in the column. There will be no reduction in the total energy requirement, in fact it is likely to increase, however the temperature in the intermediate reboiler will be lower than in the bottom reboiler and the temperature in the intermediate condenser will be higher than the top condenser. This allows for the use of cheaper hot or cold utility, if different heat sources and heat sinks are available. Using intermediate reboilers and condensers may also improve opportunities for heat integration.

An alternative is to use **heat pumps**. There are three different schemes for heat pumps. In the first scheme the overhead vapour is compressed and then condensed in the reboiler. Second, an external working fluid can be used or third, reboiler liquid flashing. Heat pumping can save energy in the distillation of close boiling

mixtures. The disadvantages are for multicomponent mixtures or mixtures with large differences in boiling points as the compression costs will be too high.

For a multicomponent mixture the distillation is usually carried out in a series of distillation columns that are operated in a **direct split** or **indirect split** fashion. In a direct split column the lightest component is split off first (at the top) and in an indirect split column the heaviest column is split off first (in the bottom). This is shown in Figure 2.1a and Figure 2.1b for a ternary separation.

Figure 2.1. Separation of a ternary mixture (ABC)
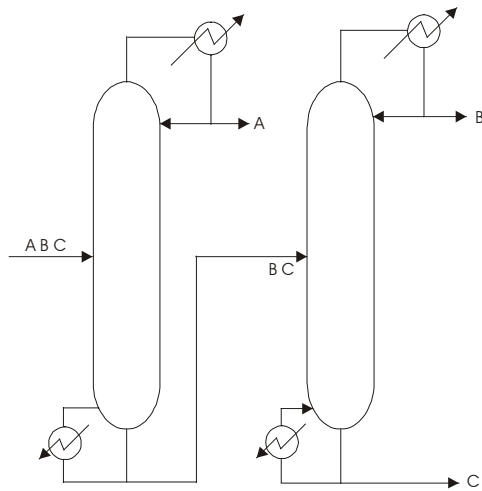
a) Direct split column arrangement   *b) Indirect split column arrangement*
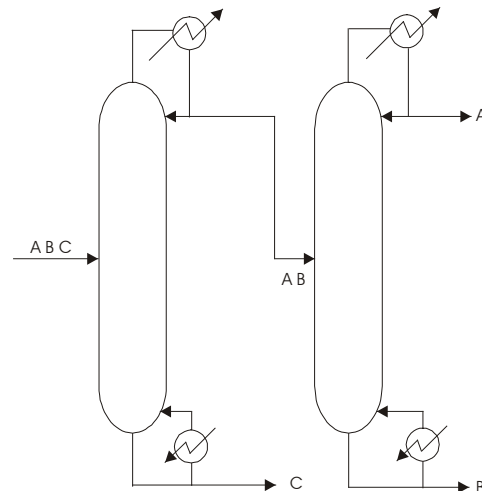
There are also many different **complex arrangements** available for the separation of multicomponent mixtures, especially ternary mixtures. These arrangements can be directly coupled arrangements like prefractionators, side strippers, side rectifiers or Petlyuk columns, the latter which is a thermally coupled prefractionator arrangement (see Figure 2.3). Side strippers and side rectifiers can reduce the energy consumption by 20 % compared with conventional columns.

Using a **prefractionator** is an effective way of reducing energy consumption (see Figure 2.2). Prefractionators are thermodynamically more efficient than conventional two-column arrangements and requires typically 30 % less energy (Energy Efficiency Best Practice Programme, 1999). For a ternary separation (ABC) this arrangement consist of a prefractionator column which splits the lightest (A) and the heaviest (C) component and a main column with a sidestream which carries out the A/B split in the top part and the B/C split in the bottom part. The products are recovered in the main column with A in the distillate, B in the sidestream and C in the bottom stream.

Figure 2.2. Prefractionator arrangement
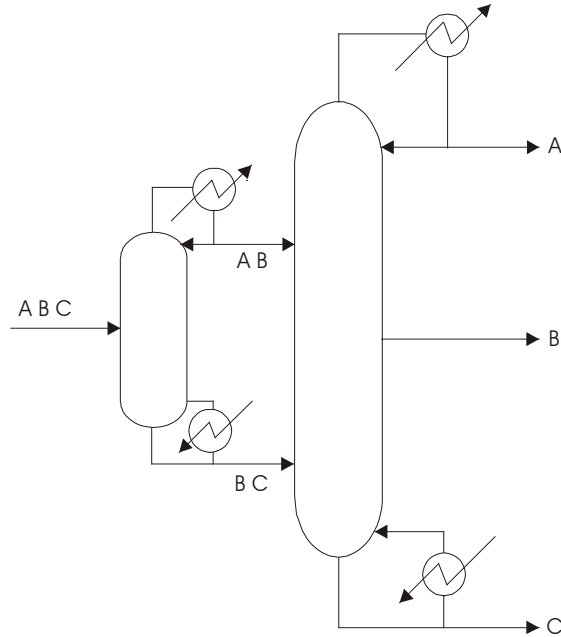
In the thermally coupled **Petlyuk arrangement** (see Figure 2.3) the liquid stream from the second column replaces the condenser of the first column and the vapour stream from the second column replaces the reboiler. The Petlyuk arrangement is equivalent to the prefractionator arrangement in terms of cooling and heating duties. Energy savings in these systems are achieved as the prefractionator prevents the re-mixing effect of the middle component, which otherwise occurs in conventional direct split or indirect split columns.

The Petlyuk column can also be implemented by combining the prefractionator and the main column in a single shell, an arrangement called a divided wall column (DWC). This will in addition to the 30% energy reductions also give a typically 30 % reduction in capital costs (Lestak, 1997).

The method for heat integration that is considered in this thesis is **multi-effect distillation**. Heat integration by using multi-effect columns involves using two (or more) columns with different pressures (see Figure 2.4). The pressures are selected so that the condensation temperature of the overhead vapour is higher than the boiling temperature of the low-pressure column. The overhead vapour stream from the high-pressure (HP) column is then condensed by boiling the bottoms in the low-pressure (LP) column, so rather than having a separate condenser and reboiler these two are combined in one. For this type of arrangement there can be additional large savings in energy; it has been reported to approximately halve the energy costs (Robinson and Gilliland (1950), King, 1980).

Figure 2.3. Thermally coupled columns - Petlyuk arrangement
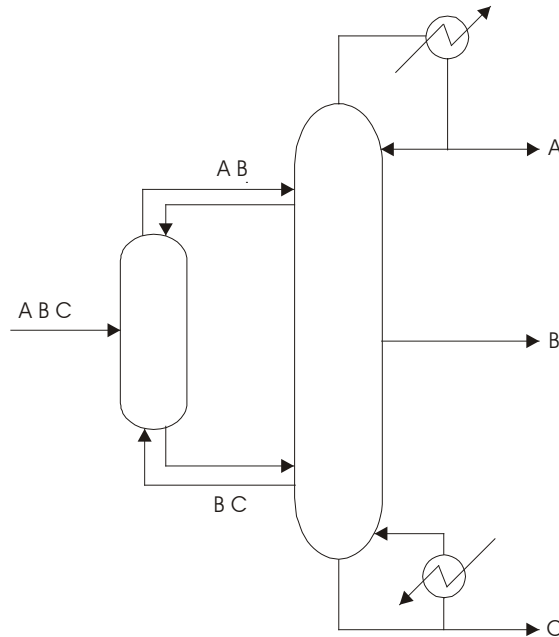
2.3.   **Multi-Effect Distillation - A Description**

As described above, the multi-effect columns use pressure to raise the boiling point of the overhead vapour from a HP column so that this can be condensed in the bottom of a LP column. The reboiler in the LP column and condenser in the HP column are thus combined and heat only has to be supplied at the bottom of the HP column. Heat also has to be removed in a condenser at the top of the LP column.

This type of arrangement has potential for additional energy savings of up to 70 %, depending on the arrangement, feed composition and the difficulty of the separation, which determines how "balanced" the integrated columns are. The disadvantages are added capital costs, an increased temperature of the hot utility and potential control problems.

There are two types (or directions) of multi-effect heat integration: forward integration, where the integration of the energy is in the same direction as the flow and backward (reverse) integration where the energy integration is in the opposite direction of the flow. Distillation sequences are usually termed direct or indirect, where for the direct split the lightest component is split off as the distillate product from the first column and for an indirect split where the heaviest component is split off as the bottom product from the first column. Figure 2.4 and Figure 2.5 shows, for a ternary separation, how the direct and the indirect sequence can be integrated in multi-effect arrangements. Figure 2.4 shows the <u>direct split</u> sequence with forward and backward integration and Figure 2.5 shows the <u>indirect split</u> sequence with forward and backward integration.

The integrated arrangements shown in Figure 2.4 can also be used to achieve multi-effect savings for binary separation, however, this would require one more column than necessary for a non-integrated arrangement. For the binary separation there is also a feed split arrangement, in which the feed is split to both columns. Further description of various schemes for binary separation can be found in several references, see for example, the paper by Wankat (1993).

Figure 2.4. Multi-effect distillation for direct split

a) Direct split with forward integration (DSF)   *b) Direct split with backward integration (DSB)*
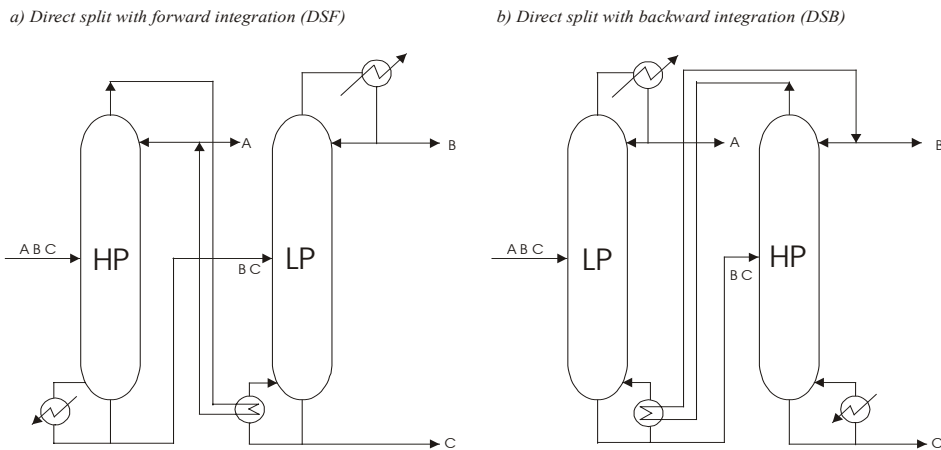
Figure 2.5. Multi-effect distillation for indirect split

a) Indirect split with forward integration (ISF)   *b) Indirect split with backward integration (ISB)*
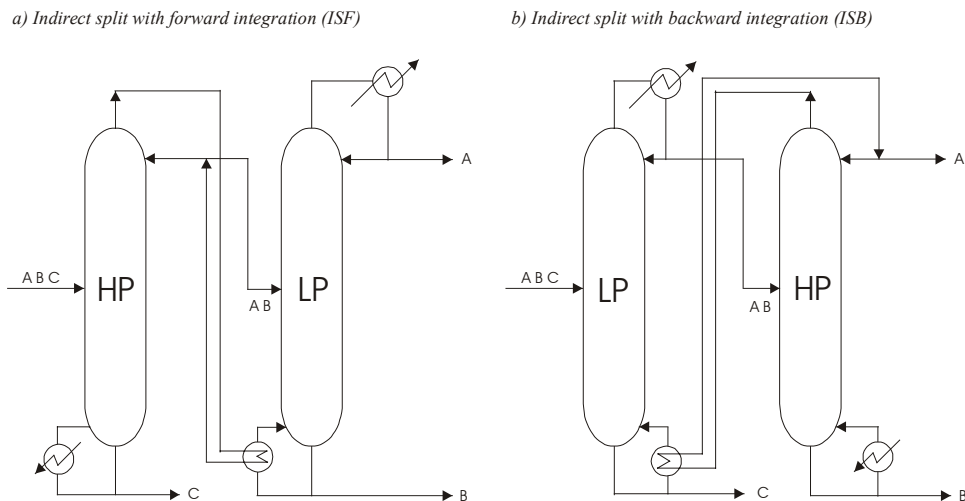
For a ternary separation we can combine the two properties of the prefractionator arrangement and multi-effect distillation in an **integrated prefractionator arrangement** as shown in Figure 2.6. The prefractionator can be run at a higher pressure and then the vapour from the prefractionator can be used to boil the

bottom of the main column in an integrated reboiler/condenser (forward integration, see Figure 2.6a). Alternatively, the main column can be run at a higher pressure and the condenser of the main column and the reboiler of the prefractionator can be integrated (backward integration, see Figure 2.6b).

These integrated prefractionator arrangements have a much higher energy saving than the thermally coupled Petlyuk column and the other multi-effect schemes. The actual savings are dependent on the feed composition and the difficulty of separation (relative volatility). The forward integrated prefractionator arrangement (PF) in Figure 2.6a, has been the main focus of this thesis.

It should be noted that when considering heat integration of distillation columns the distillation unit should also be looked at in terms of the whole process, using pinch analysis. Only then can it be decided whether or not a heat integrated system is the most effective. If there are no possibilities for integration with the process or if it is not desired (which is often the case as the columns then depend strongly on the rest of the process) then heat integration methods like multi-effect can be a good option. In terms of the multi-effect arrangements there may also be further possibilities for integration with the process due to the changes in pressure.

Figure 2.6. Multi-effect heat integrated prefractionator arrangement

a) Forward integrated prefractionator arrangement (PF)   *b) Backward integrated prefractionator arrangement (PB)*
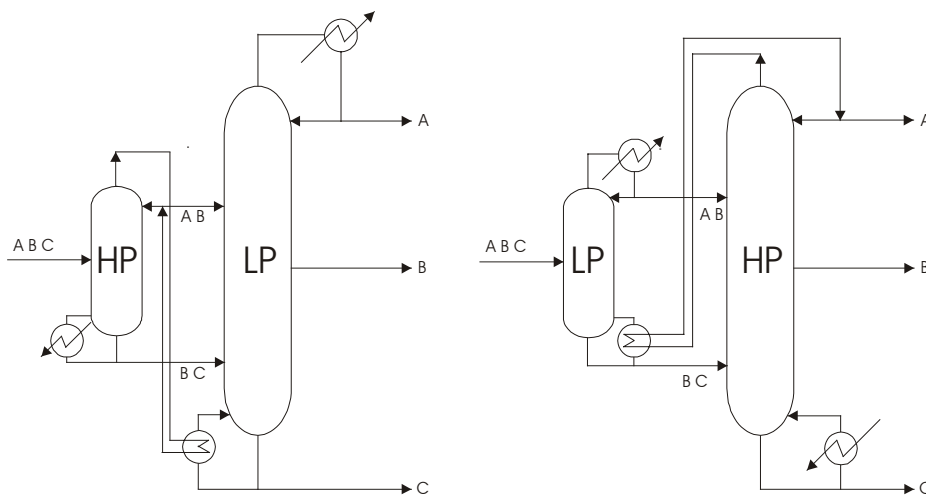
2.4.   Multi-Effect Distillation -A Brief Review of the Literature

This section will briefly summarise some of the studies considering energy and control issues of multi-effect distillation arrangements. First, energy issues for general multi-effect arrangements are briefly discussed. Then energy issues concerning the multi-effect prefractionator arrangement are presented. The second

part deals with control issues for the general arrangements, then the integrated prefractionator arrangement.

The multi-effect distillation system was described in 1950 by Robinson and Gilliland in 'Elements of Fractional Distillation', where they describe various multi-effect distillation arrangements. Other textbooks describing multi-effect distillation are for example King (1980), Smith (1995) and Luyben (1992).

In terms of design and energy consumption there have been many papers for the binary multi-effect system. In 1976 O'Brien presented a study to increase capacity of a solvent recovery system and found that a multi-effect arrangement with backward integration was the most suitable. The new system used 59% of the heat consumption of the original system. Wankat (1993) studied twenty-three different multi-effect systems for binary separations, presented the major design challenges and summarised a number of heuristic rules for selecting the most energy saving configuration based on feed data, i.e. composition and relative volatilities.

Tyreus and Luyben (1975) carried out an economic case study on a propylene-propane separation and a methanol-water separation. They concluded that single column systems that have high steam consumption might qualify for savings in a two-column multi-effect system

Other papers on binary multi-effect distillation include the paper by Tyreus and Luyben (1975) which compares capital and utility costs of a multi-effect feed-split configuration (feed to both columns) with a single column. Chiang and Luyben (1983) compared the energy consumption of five heat-integrated configurations for a methanol/water separation, given different feed compositions. The lowest energy consumption was the backward integrated direct split (DSB) arrangement, especially for low concentrations of methanol. However, the authors concluded that for high methanol concentrations the direct split with forward integration was the best, as it required a lower pressure steam than the backward integrated case.

Many authors have studied the energy consumption and comparison of different distillation configurations for **ternary mixtures**. Annakou and Mizsey (1996) presented an economic parametric study for three different distillation systems: the conventional columns, multi-effect columns (forward and backward integrated DS/IS columns), and the fully thermally coupled column (Petlyuk). The study was performed for three different mixtures, four different feed compositions and three product purity specifications. The comparison was made based on total annual cost. The results showed that the heat-integrated systems were always more economical than conventional distillation. The thermally coupled column gave considerable energy savings compared to the cheapest conventional scheme. However, compared with the multi-effect configurations, the authors concluded that the thermally coupled column was only competitive in a few cases where the concentration of the middle component was high and the A/B split was harder than the B/C split. Also, in the case of sharp separations they found that the heat integrated scheme was always the most economical.

Other authors that have compared and studied different heat integrated distillation systems for ternary separations are for example Cheng and Luyben (1985), Fonyo et al. (1999) and Emtir et al. (1999).

2.4.1. Energy savings of the integrated prefractionator arrangement

The energy consumption of integrated prefractionator arrangements for ternary separations has been studied by many authors. Cheng and Luyben (1985) compared the energy consumption of several multi-effect configurations, including integrated prefractionator arrangements, with non-integrated configurations, for a benzene/toluene/m-xylene separation. They checked configurations with different pressure levels and also included integration between process streams. The authors found for this system that without integration the prefractionator was the best arrangement. For the cases with integration the *prefractionator with the backward integration* was the best, consuming 45 % less energy than the best conventional case (non-integrated prefractionator). Although the forward and reverse heat integrated cases were very similar they concluded that the reverse heat integration seemed to be better for this system. The reverse arrangement had the lowest pressure in the high-pressure column which was proposed as a likely explanation for the backward case being better than the forward case, as the lower pressure can reduce the energy consumption if the relative volatility is a strong function of pressure. In comparison with the case presented by Takama et al. (1982) the most energy saving scheme was found to consume about 30 % less energy that the best solution, with about the same investment.

Fonyó et al. (1999) studied, based on shortcut equations, the energy and exergy loss of different integrated and non-integrated configurations, including integrated prefractionator arrangements and Petlyuk column. They concluded that in terms of energy the so-called "sloppy structures" (structures with A/C split in first column) *with integration* is always capable of achieving as much energy savings as the coupled Petlyuk arrangement. The authors also concluded that in terms of exergy the shortcut calculations showed that the Petlyuk arrangement was best in a significant number of cases, but that detailed studies did not confirm this result.

In terms of *total annual costs (TAC)*, Emtir et al. (1999) compared the non-integrated direct and indirect split arrangements with the corresponding forward and backward integrated direct and indirect split arrangements, a forward-integrated prefractionator and the Petlyuk arrangement. The backward integrated prefractionator arrangement was not included. The system was an ethanol/n-propanol/n-butanol mixture with equimolar feed composition. Rigorous modelling for all systems was carried out using HYSYS. Two types of energy costs were considered: a high energy and a low energy cost. For the high energy cost case the operating costs are dominating and the authors found that the forward integrated prefractionator and the thermally coupled Petlyuk arrangement were the best, with 27-28 % savings in TAC and 33-34 % savings in annual operating costs (compared with the direct split case). For low energy costs the backward integrated direct split

and the prefractionator arrangement were the best, with 27-28 % savings in TAC 42-45 % savings in operating costs.

The work was further expanded (Emtir et al., 2001) to look at three different feed cases: 1) 10% B with equimolar A and C, 2) equimolar feed, and 3) 80 % B with equimolar A and C. In this study, the backward integrated prefractionator arrangement was included. For the first case (10% B) they found that the Petlyuk configuration was the best (in terms of TAC), being 4% and 3 % above the direct split with backward integration, at high and low energy prices respectively. For the equimolar feed case the Petlyuk arrangement is not the best for either of the two cases (high/low energy price). At a low-energy price the forward and backward integrated prefractionator arrangements were the best with 36 % TAC savings. At the high price the direct split with backward integration was the best with 41 % TAC savings. The integrated prefractionator configurations had 36 % TAC savings. For the last case, where only the high-energy prices are included the forward and backward integrated prefractionators were the best with 51 % and 53 % TAC savings, respectively. From the work the authors concluded that the multi-effect structures are sensitive to the heat duty while the Petlyuk system is not (the heat duty requirements increases with increasing concentration of B in feed). For the Petlyuk system the TAC savings are about 30-33 % for all three cases.

Rev et al. (2001) compared integrated and non-integrated structures according to short-cut models, rigorous modelling and operability. From the simple short cut equations they found that for sharp separation, the forward and backward integrated prefractionator arrangements are always capable of achieving as much, or higher, energy savings as that of the Petlyuk configuration. The integrated direct and indirect split configurations were also, in some cases, capable of achieving larger savings than the Petlyuk arrangement. The direct split with backward integration was best in a very small domain, where there were very high ratios of A in the feed. In addition to short-cut equation for the energy use, short-cut equations were also presented for the exergy loss. For the rigorous modelling the structures were compared based on TAC. According to the results the domain where Petlyuk arrangement is the best was even lower, however, the Petlyuk arrangement was better than the multi-effect structures when there was a low amount (10%) of the middle component in the feed. Finally, steady state operability analysis and dynamic simulations are carried out for the backward integrated direct sequence and Petlyuk arrangement. For the steady state analysis controlled and manipulated variables are selected based on engineering judgement and analysis made to find the best pairing. The steady state operability analysis and dynamic simulations showed that both the configurations could be operated. However, the authors showed that the control of the Petlyuk system is significantly poorer.

Agrawal (2000) presents a systematic method for drawing new multi-effect configurations for thermally coupled distillation columns. These new double effect configurations produce pure product streams at both ends of each of the distillation columns and the binary stream transferred from one column to another is taken out at an intermediate location in the column. The paper presents configurations for both ternary and quarternary separations. Approximate calculations showed that a multi-effect fully thermally coupled configuration always had lower heat duty than

any of the other multi-effect configurations. For some of the feed conditions (large amount of B in feed) it was found that the multi-effect prefractionator configuration was very similar to the multi-effect fully coupled configuration.

Takama et al. (1982) presented a procedure for multi-objective optimisation and applied it to an optimal design of a distillation system separating a ternary mixture (benzene/toluene/m-xylene). A number of configurations were tested and optimised considering process system design, control system design and auxiliary subsystems for start-up. The best compromise solution for this separation was found to be the multi-effect backward integrated prefractionator arrangement.

2.4.2. Control Studies

The need for control is motivated by the following quote:

> *"Better regulation can reduce the magnitude and duration of composition upsets and avoid waste of energy while assuring more valuable product" (Ryskamp, 1980).*

The multi-effect distillation columns have added complexity compared to the conventional distillation sequences and can therefore be more difficult to operate and control. This is probably one reason why this type of distillation has not been used much in industry. It is therefore essential to develop good control schemes for these systems that can ensure satisfactory operation and make sure that the promised energy savings are achieved.

Several **control studies** have been presented in the literature for various multi-effect arrangements, for both binary and ternary separations. The studies involve finding the appropriate variable for control, pairing of manipulated and controlled variables, controller selection and tuning and various controllability studies.

Auxiliary reboilers and condensers

Several authors have discussed the inclusion of additional reboilers and condensers for multi-effect columns. This will give additional degrees of freedom for control, however at the expense of a higher capital cost investment and operating costs (energy consumption increases).

Tyreus and Luyben (1976) showed responses to feed composition disturbances and feed rate disturbances using a feed split control system for the propylene/propane and methanol/water separations. They found that this control configuration gave an oscillatory response and concluded that the only process and control configuration that could effectively handle various types of load disturbances was an *auxiliary reboiler and condenser*. An auxiliary reboiler was used to decouple the two columns, thus causing a decrease in the energy savings.

Other authors have discussed the question of whether an auxiliary reboiler and condenser should be used. Lin (1987) found that the use of an auxiliary reboiler

was not a requirement. Lenhoff and Morai (1982) also reported that they did not find the effects reported by Tyreus and Luyben (1976). Gross et al. (1994) used an auxiliary reboiler in their simulations of an industrial case, but noted that even if additional reboilers provides additional manipulated variables they may also lead to severe interaction problems.

Frey et al. (1984) who studied different control schemes for the feed split and a material integrated case, found that the columns can be completely decoupled and effective control can be achieved by properly selecting and pairing the control and manipulated variables.

Rix and Gelbe (2000) also showed that the columns could be decoupled without using an auxiliary reboiler. They showed from steady state analysis that the inclusion of an auxiliary reboiler for a feed-split system *does* remove the control loop interaction between the two columns. However, they also proposed an additional control structure using a feed tank that also showed no control loop interactions. Also, in terms of closed loop simulations this feed tank structure had the best overall performance. The auxiliary reboiler structure had the largest deviations in the bottom concentration as the manipulated variable (heat duty of auxiliary reboiler) reached the upper constraint.

Control structure selection

Many authors have studied the control structure selection of multi-effect arrangements, especially for the feed-split configuration. The topics covered include pairing of manipulated and control variables, investigation into specific control structures and comparison of different control structures for one (or more) integrated arrangements.

Control variable pairing for two integrated systems was studied by Frey et al. (1984). The systems studied was a feed split system and a material integrated feed split design where the bottom from the high pressure column was flashed into the bottom of the low pressure column. The control variables for the two systems were the product purities, i.e. a (4x4) system for the feed split design and (3x3) system for the material integrated design. Four control strategies were studied for the feed split design and three for the material integrated design. From relative gain array (RGA) and sensitivity studies the authors concluded that the feed split design is more easily controlled than the material integration design. They found that the conventional control schemes (LV configuration) were very sensitive to changes in design parameters and showed more interactions than the control schemes that used a ratio of the material flows as the manipulated variables. By properly selecting and pairing the control and manipulated variables they found that the columns can be decoupled and effective control may be achieved.

Al-Elg and Palazoglu (1989) compared a ratio control scheme similar to that of Frey et al. (1984) with a conventional control scheme for a high purity methanol/water separation in feed split columns. The control variables were the four product purities and the manipulated variables the boilup in the high-pressure

column, the reflux flows in both columns and the feed ratio to the columns. The authors found that RGA analysis indicated a high degree of interaction for both schemes. However, for the ratio scheme the interaction was less and the two columns were decoupled. The interaction was also found to be larger than that found by Frey et al. (1984) due to the higher purity separation. Rigorous simulation showed that the columns could be controlled effectively using the ratio control scheme.

The feed split system was also studied by Gross et al. (1994) for an industrial case. In this case however, the system included an additional reboiler on the low-pressure column. The separation was of a ternary mixture ABC, into AB/C with four product concentrations to be controlled. For this case the feed split ratio was not used as a manipulated variable, but was kept constant. The authors investigated three control structures using steady state controllability analysis, dynamic analysis and closed loop simulations. From the analysis they found that a DV-configuration in both columns was the most suitable of the control configurations tested.

Further work on the above system was presented again by the same authors in a later paper (Gross et al., 1998). The new study contains further closed loop simulations and includes a comparison of the three control structures presented earlier with an alternative control structure. The new control structure uses a DB-configuration in the HP column and a DV-configuration in the LP column. The results from closed loop simulations showed that the DB/DV configuration had a fast response and relatively small overshoots. The configuration was also tested out on the plant and the authors concluded that this configuration was a viable alternative to the more conventional structures.

Han and Park (1994) applied a model-based control scheme to a feed split and a direct split system with forward integration, for a high purity methanol/water separation. For the feed split system dynamic simulations were used to compare the proposed control system with the ratio control scheme used by Frey et al. (1984). A 50 % reduction in the feed composition was tested and the authors concluded that the proposed control system had much better performance than the ratio control scheme.

A similar study was presented by Han and Park (1996), but for the feed split scheme and the forward-integrated indirect split arrangement. The authors use a non-linear wave model to develop a profile composition controller that uses a generic model control algorithm. This multivariable controller was compared with the results from Frey et al. (1984) by running different dynamic situations. The feed split system was subjected to a –50 % change in the feed composition and a step change in the setpoint of the bottom concentration. The indirect split system was subjected to a –20 % change in the feed composition. The authors concluded, from the simulations, that the performance of the proposed control scheme was better than the conventional single-input-single-output (SISO) schemes.

Rix and Gelbe (2000) looked at three control structures for the feed-split configuration. For all three cases the distillate concentrations were controlled using the reflux flowrates. The base case was a feed-split structure with no auxiliary reboiler and (4x4) composition control. The bottom concentration in the HP

column was controlled using the feed split and the bottom concentration in the LP column was controlled using the boilup in the HP column. The RGA indicated strong interaction of the two bottom composition loops. The second control structure investigated was the use of a trim reboiler where the boilup in the HP and LP columns were used to control the concentration in the respective bottom streams. The RGA for this structure showed no control loop interaction between the two columns. The final control structure suggested was the use of a feed buffer tank. The feed to the LP column is then used for controlling the bottom concentration in LP column and the feed to the HP column is used to control the level in the feed tank. This structure also removes the control loop interactions. Results from closed loop simulations showed that the feed-split structure had the largest set-point deviation for the bottom concentration (HP column) and that the best structure overall was the feed tank.

The same study (Rix and Gelbe, 2000) also compared the direct split sequence (DS) with the backward integrated direct sequence (DSB) for a ternary separation of benzene, toluene and xylene. A (3x3) composition control structure was compared with a (4x4) structure for the two cases. In terms of energy demands they found that for the DS configuration the (3x3) composition control only gave a 7 % higher energy consumption than the (4x4) structure. For the integrated cases, however, the additional energy demand was 20 % with the (3x3) control structure, leading the authors to conclude that for the DSB a (4x4) structure is justified.

Control comparisons of different configurations

Several comparisons of different integrated multi-effect schemes based on control have been presented. Chiang and Luyben (1988) compared the closed loop response of three different multi-effect arrangements with a conventional single column. For a low purity methanol/water separation they studied a feed split arrangement, in which the feed enters both columns, a direct split arrangement with forward integration and a direct split arrangement with backward integration. In terms of energy the backward integrated case was the best, followed by the feed split arrangement. The selected control variables are the product compositions, which are controlled using the reflux flowrate and boilup. In the feed split the split is also used as an additional manipulated variable. From the closed loop simulations the authors found, in terms of deviations from set point, that the response of the feed split arrangement was the worst. The response of the other two arrangements was worse than the single column, but it was concluded that they were stable and acceptable. Due to the lower energy consumption the backward integrated arrangement was recommended for this system.

Lenhoff and Morari (1982) also studied three different multi-effect systems for a binary mixture of methanol and water. The systems studied were the feed split, the indirect split with backward integration and a prefractionator like arrangement with forward integration. In the last case the first column does a non-sharp separation where both the bottom and top stream (containing both A and B) is fed to the second column where the products are in the distillate and bottom streams. The

assessment is based on steady-state factors, using an economic performance index, and operational factors, using a dynamic performance index. The results from the study showed that if the disturbances in the system are rare then the feed split structure is the best, however, if disturbances are common then the prefractionator arrangement is the preferred structure. The study also tested the use of an auxiliary reboiler and condenser to decouple the columns. However, the dynamic effect of the auxiliary equipment was found to be negligible.

Mizsey et al. (1998) compared the performance of a heat integrated multi-effect column with the Petlyuk arrangement for a pentane/hexane/heptane separation. The heat-integrated system was the backward integrated direct split arrangement (DSB). All three compositions were controlled (3 x 3 system). A number of different control structures were tested using steady state control indices and the three best for both the arrangements were selected for closed loop analysis. For the Petlyuk arrangement the authors found that the concentration controllers had to be detuned in order to prevent instability and achieve a robust system. Comparing the two systems they found that the multi-effect arrangement had smaller overshoots, but that the differences in settling times were not significant. The authors concluded that due to the detuning of the Petlyuk composition controller the control performance of this system is less favourable than the multi-effect structure.

Integration between design and control

Bansal et al. (1998) studied the interactions between design and control on a feed-split methanol/water separation. Two approaches are used for optimising the process design and control system: a sequential approach and a simultaneous approach. For the sequential optimisation the design was optimised first, then the control system was optimised. For the simultaneous approach these were optimised together. A rigorous dynamic model was used. For the simultaneous design they minimised the expected total annual cost of the system, subject to disturbances, dynamic uncertainty profile and system constraints. The results from the study showed that the simultaneous strategy gave a lower capital cost and lower operating costs than the sequential approach. The authors also found that the effect of pressure dynamics is a crucial factor when investigating the design and control.

Further studies were made (Bansal et al. 2000) on the same system where the work was expanded to include a comparison between the sequential and simultaneous design. Again, they concluded that the simultaneous approach gave a cheaper design and a more satisfactorily controlled system than the sequential approach.

Pohlmeier and Rix (1996) studied the interaction of control and design for a methanol water separation in a feed-split configuration and compared the performance of a SISO PI-controller with two MIMO controllers. They showed that the number of trays directly affects the control loop interaction and that a higher number of trays give a lower control loop interaction. Comparisons were made of a SISO PI-controller with an inverse based controller (IBC) and a robust controller (RC). For small disturbances in feed flowrate and composition all three

controllers were satisfactory. However, for larger feed disturbances the authors concluded that the multiple-input-multiple-output (MIMO) controllers were superior.

Start-up of multi-effect columns

The start-up of multi-effect columns has not been studied in great detail. Löwe et al. (1999) presented an experimental study where three different start-up strategies for a multi-effect column were investigated. The first start up strategy investigated was the conventional, with the columns fully thermally coupled and thermally independent. Secondly, a start-up procedure where there is a total removal of the distillate in the HP column was studied and finally a start-up procedure where the HP column reboiler duty is higher than the steady state value was investigated. The experiments showed that for the conventional case running the columns fully thermally coupled gave savings in both energy and start-up time compared with the thermally independent columns. The authors did not find any advantages of the total removal of distillate strategy, however they found that the increased reboiler strategy gave timesaving of 35 % compared with the conventional scheme.

Löwe and Wozny (2001) studied the product switchover and start-up for a methanol/water separation in a direct split system with backward integration (DSB). The authors presented a new product switchover strategy, which for an increase in product concentration from 90 to 99 mol% gave 57 % time saving compared with a conventional switchover procedure. They also presented a new start-up strategy, which compared experimentally with the conventional scheme gave both time saving (57 %) and energy savings.

Integrated Prefractionator Arrangements

There have not been too many papers published on the topic of control of integrated prefractionator arrangements.

Ding and Luyben (1990) studied the controllability of a benzene/toluene/m-xylene separation in a backward integrated prefractionator arrangement, comparing it with a simple direct split system as a base case. Two cases were studied: low and high product purity. Feed preheating with product and intermediate streams was included for both designs. For both purity cases the integrated prefractionator arrangement reduces the energy consumption by about 50 %. For the integrated prefractionator arrangement two impurities in the sidestream (from main column) was controlled by manipulating the sidestream flowrate and the sidestream draw-off tray. In terms of controllability the two structures was found to be dynamically about the same for the low purity case. For the high purity case the authors found that both systems are controllable, but the direct split gives much better load rejection. They also found that the control of the purity of toluene in the main column sidestream was particularly poor.

Bildea and Dimian (1999) studied the interactions between the design and control of forward and backward integrated prefractionator arrangements for a pentane/hexane/heptane mixture. Four different designs were considered depending on the recovery from the prefractionator: 1) a sharp A/C split, 2) A allowed in bottom and C in the top, 3) A in the bottom, 4) C in the bottom. To mach the duties in the two columns the column design (reflux, number of trays) were manipulated. The main control objective was to maintain the product concentrations at their set points. The results from the study showed that the total energy consumption only varied slightly in all the cases, however, the authors found that the dynamic behaviour showed significant difference. They found that the forward-integrated design has very good controllability properties and that the design that yielded a short prefractionator column gave the best performance. For this case it was also possible to use temperature measurements to control the compositions. The backward integrated scheme, however, was not controllable using only temperature measurements. They found that the sidestream composition had to be controlled directly, rather than using indirect temperature control. For this scheme the performance was better when the prefractionator performs a sharp A/C split, resulting in a tall column. The general conclusion from the study was that *the forward-integrated arrangement is easier to control*.

Emtir et al. (2003) presented economical and controllability studies of the forward and backward integrated direct split, integrated prefractionator arrangements and the Petlyuk arrangement. The direct split with no integration was also included for comparison. The mixture studied is the same as in the previous studies, an ethanol/n-propanol/n-butanol separation. All the systems were optimised in terms of total annual costs and the optimised structures were used for the controllability study. In terms of TAC the backward integrated direct split sequence had the highest savings, however, in terms of utility demand, the integrated prefractionator structures were the best. For the control studies the product compositions were selected as the controlled variables and pairing with possible manipulated variables was done based on steady state indices. Ratio control structures were not considered. The results from the steady state analysis indicated that serious interactions can be expected for the integrated prefractionator arrangements and the Petlyuk column and that the integrated and non-integrated direct split schemes show less integration. Dynamic simulations were then carried out for an equimolar feed composition with feed flowrate and feed composition disturbances. Both open and closed loop simulations were made. The results from the open loop simulations showed that the backward integrated prefractionator was the slowest scheme and had the highest time constant. The closed loop simulations showed that the more complex structures (integrated prefractionator and Petlyuk) were more difficult to control as there were serious internal interactions between the control loops. The authors also concluded that the forward-integrated schemes are easier to control. This is in accordance to what Bildea and Dimian (1999) found for the integrated prefractionator arrangements.

2.5. Thesis Problem Statement

As mentioned in Chapter 1 the focus in this thesis is the application of process integration tools to heat-integrated distillation columns. The idea of the thesis was to look at systems where the effect of different pressures (though *multi-effect* columns) was used together with good integrated solutions, like the Petlyuk arrangement. The system studied is the multi-effect integrated prefractionator arrangement described in Section 2.3. This arrangement has been studied in terms of design issues, using shortcut calculations, and in terms of operational issues, using optimisation.

Some of the questions that are important in this thesis are:

- Is the multi-effect prefractionator arrangement a good energy saving scheme ?

- How can we easily analyse the multi-effect prefractionator arrangement and screen it against other different heat integrated arrangements ?

- How can the multi-effect prefractionator arrangement be controlled so that the energy savings are reliably achieved during operation ?

- Can this arrangement be used for a typical industrial example ?

Other studies in literature have shown that this system has large potentials for energy savings (Cheng and Luyben, 1985, Fonyo et al. 1999, Emtir et al. 1999) and it is therefore an interesting arrangement to study in terms of energy savings. Also, only a few studies have been made on the control and operation of the multi-effect prefractionator arrangement (Ding and Luyben, 1990, Bildea and Dimian, 1999, Emtir et al., 2003). The control of such arrangements is important in order to achieve the promised savings. Here the focus has been on the selection of controlled variables, with the aim of keeping the system close to the optimum in terms of energy consumption.

2.6. References

Agrawal, R., 'Multi-effect distillation for thermally coupled configurations', *AIChE Journal*, 2000, Vol. 46, No. 11, 2211-2224

Al-Elg, A.H., Palazoglu, A., 'Modelling and control of a high purity double-effect distillation column', *Computers and Chemical Engineering*, 1989, Vol.13, No. 10, p. 1183-1187

Annakou, O., Mizsey, P., 'Rigorous comparative study of energy-integrated distillation schemes', *Ind. Eng. Chem.* Res., 1996, 35, 1877-1885

Bansal, V., Ross, R., Perkins, J.D., Pistikopoulos, S., 'Interactions of design and control: double-effect distillation systems', 5th IFAC Symposium on Dynamics and Control of Process Systems, 1998

Bansal, V., Ross, R., Perkins, J.D., Pistikopoulos, S., 'The interactions of design and control: double-effect distillation', *J. Proc. Contr.*, 2000, Vol.10, No. 2-3, 219-227

Biegler, L.T., Grossmann, I.E., Westerberg, A.W., 'Systematic methods of chemical process design', Prentice Hall PTR, 1997

Bildea, C.S., Dimian, A.C., 'Interaction between design and control of a heat-integrated distillation system with prefractionator', *Tans IChemE,* 1999, Vol. 77, Part A, pp. 597-608

Cheng, H. C., Luyben, W., 'Heat-integrated distillation columns for ternary separations', *Ind. Eng. Chem. Process Des. Dev.*, 1985, 24, 707-713

Chiang, T.P, Luyben, W.L., 'Comparison of the dynamic performances of three heat-integrated distillation configurations', *Ind. Eng. Chem. Res.*, 1988, 27, 99-104

Chiang, T.P, Luyben, W.L., 'Comparison of the energy consumption in five heat-integrated distillation configurations', *Ind. Eng. Chem. Process Des. Dev.*, 1983, 22, 175-179

Ding, S.S., Luyben, W., 'Control of a heat-integrated complex distillation configuration', *Ind. Eng. Chem. Res.*¸1990, 29, 1240-1249

Emtir, M., Mizsey, P., Fonyó, Z., ' Economic and controllability investigation and comparison if energy integrated distillation schemes', *Chem. Biochem. Eng. Q.,* 2003, 17(1), 31-42

Emtir, M., Rév, E., Fonyó, Z., 'Rigorous simulation of energy integrated and thermally coupled distillation schemes for ternary mixture', *Applied Thermal Engineering*, 2001, 21, 1299-1317

Emtir, M., Rév, E., Mizsey, P., Fonyó, Z., 'Comparison of integrated and coupled distillation schemes using different utility prices', *Computers and Chemical Engineering Supplement,* (1999), S799-S802

Energy Efficiency Best Practice Programme, Good Practice Guide No. 269, 'Efficiency improvements to existing distillation equipment', 1999, Energy Efficiency Enquiries Bureau, UK.

Fonyó, Z., Rév, E., Szitkai, Z., Emtir, M., Mizsey, P., 'Energy savings of integrated and coupled distillation systems', *Computers and Chemical Engineering Supplement*, 1999, S89-S92

24

Frey, R.M., Doherty, M.F., Douglas, J.,M., Malene, M.,F., 'Controlling thermally linked distillation columns', *Ind. Eng. Chem. Process Des. Dev.*, 1984, 23, p.483-490

Gross, F., Baumann, E., Geser, A., Rippin, D.W.T., Lang, L., 'Modelling, simulation and controllability analysis of a heat-integrated industrial distillation system', IFAC Workshop on Integration of Process Design & Control, June 27-28, 1994, Baltimore, USA

Gross, F., Baumann, E., Geser, A., Rippin, D.W.T., Lang, L., 'Modelling, simulation and controllability analysis of an industrial heat-integrated distillation process', *Computers and Chemical Engineering.*, 1998, Vol. 22, No.1-2, 223-237

Han, M., Park, S., 'Multivariable control of double-effect distillation configurations', Proceedings of PSE '94, 989-994

Han, M., Park, S., 'Multivariable control of double-effect distillation configurations', *Journal of Process Control,* Vol. 6, No. 4, 1996, 247-253

Hewitt, G., Quarini, J., Morell, M., 'More efficient distillation', *The Chemical Engineer*, 21 Oct. 1999

King, C.J., 'Separation Processes', 2nd ed. McGraw-Hill Book Co., 1980

Lenhoff. A.M., Morari, M., 'Design of resilient processing plants - I: Process design under consideration of dynamic aspects', *Chemical Engineering Science*, 1982, Vol. 37, No.2, p.245-258

Lestak, F., Collins, C., 'Advances in distillation saves', Chemical Engineering, July 1997, p. 72-76

Lin, S.Y., 'Multivariable control of double effect heat integrated distillation columns', PhD Thesis, 1987, Louisiana State University and Agricultural and Mechanical College, USA

Luyben, W.L., 'Practical distillation control', Van Nostrand Reinhold, New York, 1992.

Löwe, K., Wozny, G., 'A new strategy for product switchover and startup for a heat- and mass-integrated distillation system', *Chemical Engineering and Processing,* 40, 2001, 295-302

Löwe, K., Wozny, G., Gelbe. H., 'Startup of heat- and mass-integrated distillation columns: an experimental study', *Pres '99 2nd Conference on Process Integration, Modelling and Optimisation of Energy Saving and Pollution Reduction*, 415-420

Mizsey, P., Hau, N.T., Benko, N., Kalmar, I., Fonyo, Z., Process control for energy integrated distillation schemes, *Computers and Chemical Engineering,* 1998, Vol. 22, Suppl. S427-S434

O'Brien, N.G., 'Reducing column steam consumption', *CEP,* July 1976, 65-67

Pohlmeier, J., Rix, A., 'Interactive plant and control design of a double-effect distillation column', *Computers and Chemical Engineering*, 1996, Vol. 20, No. 4, 395-400

Rev, E., Emtir, M., Szitkai, Z., Mizsey, P., Fonyo, Z, 'Energy savings of integrated and coupled distillation systems', *Computers and Chemical Engineering,* 2001, 25, 119-140

Rix, A., Glebe, H., 'On the impact of mass and heat integration on design and control of distillation column systems', *Trans IChemE,* 2000, Vol. 78, Part A, 542-548

Robinson, C.S., Gilliland, E.R., 'Elements of Fractional Distillation', 4th. edn., McGraw-Hill Book Co., 1950, 168-191

Rush, F.E., 'Energy-saving alternatives to distillation', *Chemical Engineering Progress,* 76 (7), 1980, 44-49

Ryskamp, C.J., 'New strategy improves dual composition column control', *Hydrocarbon Processing*, June 1980, 51-59

Smith, R., 'Chemical process design', McGraw-Hill Book Co, 1995

Takama, N., Kuriyama, T., Niida, K., Kinoshita, A., Shiroko, K., Umeda, T., 'Optimal design of a processing system', Chem. Eng. Prog., 1982, 78 (9), 83.

Tyreus, B.D., Luyben, W.L., 'Controlling heat integrated distillation columns', *Chemical Engineering Progress*, Sept. 1976, 59-66

Tyreus, B.D., Luyben, W.L., 'Two towers cheaper than one?', *Hydrocarbon Processing*, 1975, 54(7), 93-97

Wankat, P.C., 'Multieffect distillation processes', *Ind. Eng. Chem. Res.*, 1993, 32, 894-905CEP

26

Chapter 3. Shortcut Methods for Analysis of Ternary Multi-Effect Distillation Columns

Abstract

The minimum energy requirements of six different heat-integrated multi-effect and three non-integrated distillation arrangements for separating a ternary mixture have been considered. The focus of this Chapter is on a heat-integrated complex distillation configuration; called a multi-effect prefractionator arrangement. The comparison of the different arrangements is based on the minimum vapour flowrates at infinite number of stages. The shortcut equations that can be used for calculating the minimum vapour flowrate for each arrangement is summarised. Calculations show that in terms of minimum energy, when assuming constant relative volatility, that the multi-effect integrated prefractionator arrangement is superior to the other integrated and non-integrated arrangements.

3.1. Introduction

When looking at the design of integrated distillation systems there are many different factors that have to be considered in order to achieve an optimal design for the required separation. One of the most common factors is the *energy consumption* and what savings can be achieved when using one arrangement rather than another. To compare the energy consumption of different distillation arrangements it is convenient to use minimum vapour flowrates, which are often expressed in terms of simple shortcut equations. Such equations are given for different multi-effect arrangements by Rev et al. (2001) and for the prefractionator column they can be found in e.g. Carlberg and Westerberg (1989).

However, when considering energy, it is also necessary to consider the *quality* of the energy, i.e. at what temperature does the heating and cooling media have to be delivered and at what temperatures levels are they actually available. This gives rise to the use of the term *exergy*. Another factor affecting the design is for example the pressure level, which will affect the capital cost of the column and other equipment such as heat exchangers. It is also important to consider the operation and control of the selected arrangement and how it compares to the other systems. For each case a decision has to be made as to which basis should be used to select between the different designs. Usually a trade off between different factors is used.

This Chapter summarises shortcut equations that can be used for calculating the minimum vapour flowrate in different multi-effect integrated distillation arrangements. The shortcut equations were used to analyse a number of different

28

feeds for different difficulties of separation (different relative volatility). The energy savings of the integrated prefractionator arrangement are compared with other integrated and non-integrated arrangements. Also, a brief introduction is given on the exergy analysis and thermodynamic efficiency of such columns. These tools can be used as a basis for screening various alternatives where the best can be studied further using more rigorous simulation methods.

Figure 3.1. Non-heat integrated schemes for separating a ternary mixture (ABC)
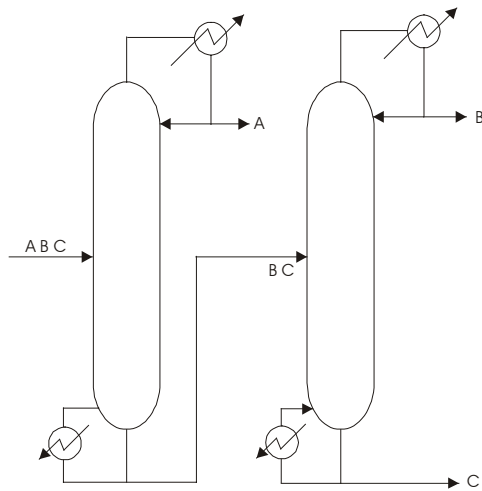
a) Direct split (DS) arrangement   *b) Indirect split (IS) arrangement*
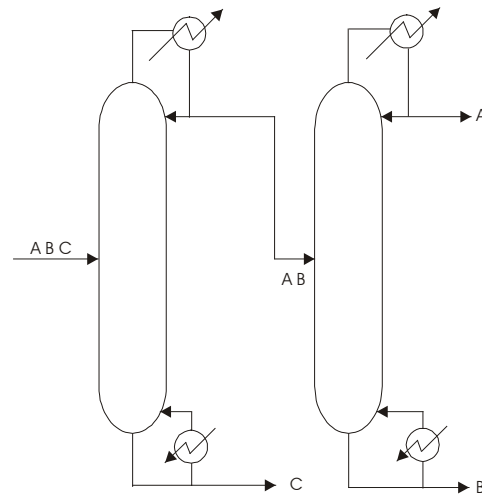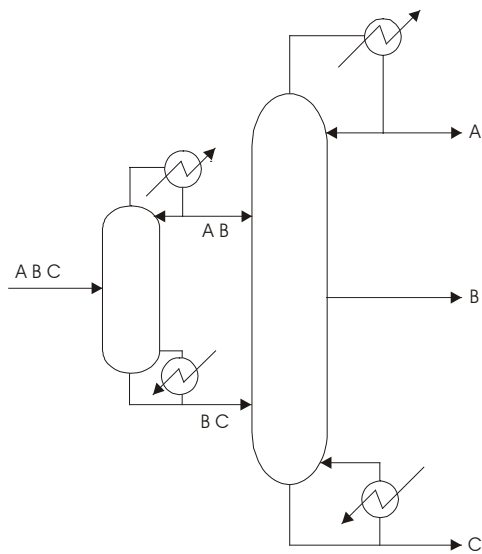
c) Prefractionator arrangement   *d) Petlyuk arrangement*
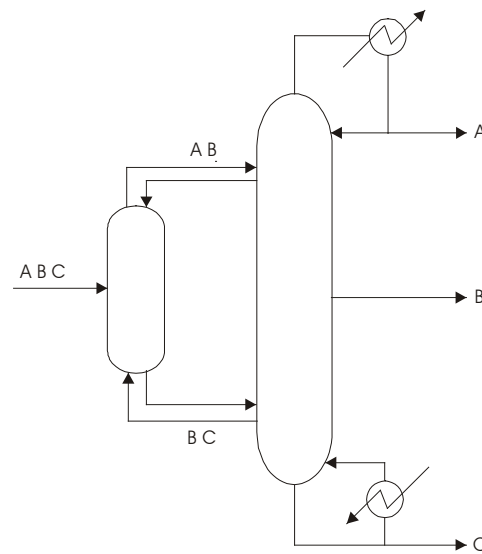
3.2. Multi-Effect Column Arrangements

Figure 3.1 shows four non-heat-integrated schemes for separation of a ternary mixture (ABC): a direct split (DS) arrangement, an indirect split (IS) arrangement, a prefractionator (P) arrangement and a directly thermally coupled prefractionator (Petlyuk column). In the DS arrangement (Figure 3.1a) the lightest component (A) is split off in the first column. For the IS arrangement (Figure 3.1b) the heaviest component (C) is split off in the first column. For the prefractionator and Petlyuk arrangement (Figure 3.1c and Figure 3.1d) the split in the first column is between the lightest (A) and the heaviest (C) component, with the middle component (B) distributing between the two products.

The three first arrangements shown in Figure 3.1 can be heat integrated in a multi-effect fashion by running one column at a higher pressure and then combining the condenser of the high-pressure (HP) column with the reboiler of the low-pressure (LP) column. Each of these can be integrated in a <u>forward</u> or <u>backward</u> fashion, giving us 6 different schemes to consider:

> ***Direct split columns***. Two possible configurations are possible for the direct split: a forward integration (DSF) as in Figure 3.2a and a backward integration (DSB) as in Figure 3.2b.
>
> ***Indirect split columns***. Two possible configurations are possible for the indirect split: a forward integration (ISF) as in Figure 3.3a and a backward integration (ISB) as in Figure 3.3b.
>
> ***Prefractionator arrangement***. The two column options considered are: a forward split (PF), see Figure 3.4a and a backward split (PB), see Figure 3.4b.

It should be noted that an additional scheme is available for the prefractionator design if the separation is carried out in three columns with three pressure levels. This arrangement, called a *dual* scheme, has not been considered here, as the energy consumption is the same as for the two-column multi-effect prefractionator arrangement and as this three-column arrangement would result in a higher capital cost.

In all cases the products and flows between the integrated columns are assumed to be liquid. This may seem non-optimal, but because of the multi-effect integration there is no advantage for these columns in using vapour flows between the columns. This follows because (i) it is better to supply the vapour in the reboiler (ISF, PF) and (ii) it is not economical to compress vapour going from the LP to the HP column (ISB, PB).

In the shortcut equations for minimum vapour flowrate in Section 3.3 the following notation has been used (see Figure 3.2 to Figure 3.4). For the direct split arrangement (integrated and non-integrated) CD1 refers to the first column where the feed enters and CD2 refers to the second column in the distillation sequence. For the indirect split arrangement (integrated and non-integrated) CI1 refers to the first column and CI2 refers to the second column. For the prefractionator arrangement C1 is the feed column (prefractionator). The main column is divided

30

into an upper and a lower section, where C21 refers to the upper section above the sidestream and C22 refers to the lower section below the sidestream.

Figure 3.2. Multi-effect direct split arrangements

a) Direct split with forward integration (DSF)

b) Direct split with backward integration (DSB)
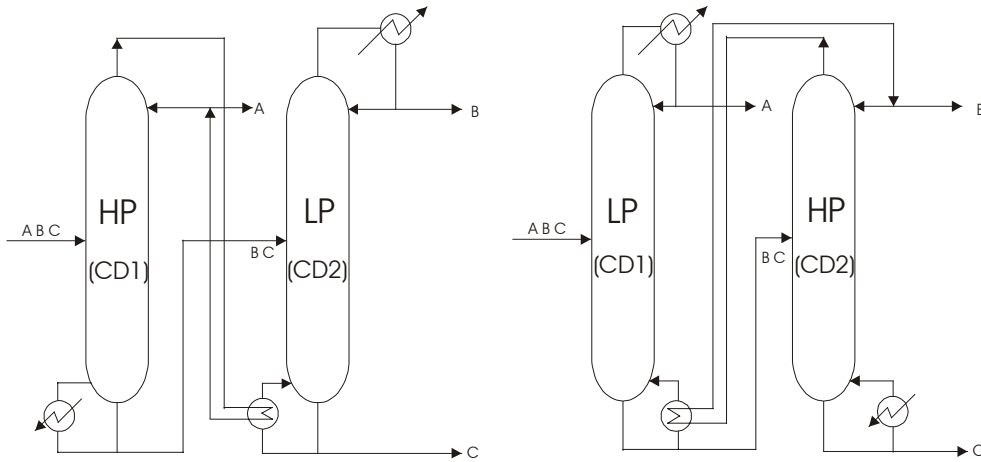
Figure 3.3. Multi-effect indirect split arrangements

a) Indirect split with forward integration (ISF)

b) Indirect split with backward integration (ISB)
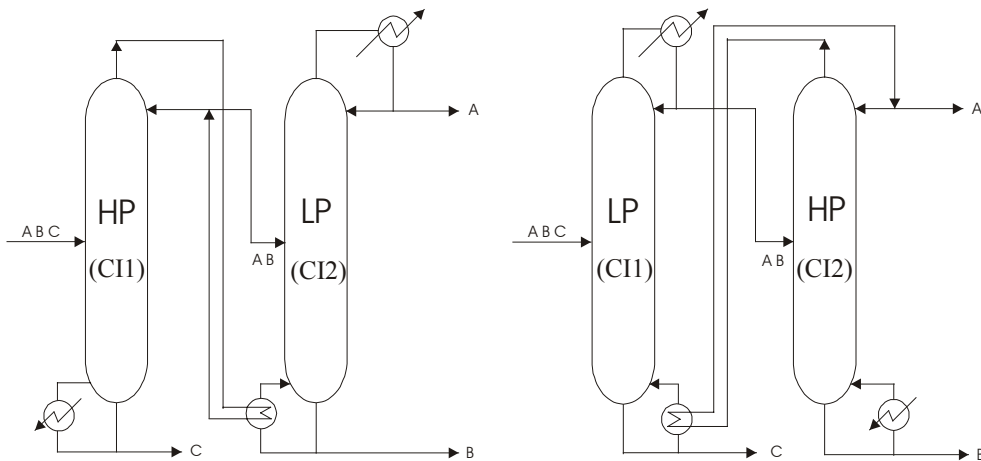
Figure 3.4. Multi-effect prefractionator arrangement

*a) Prefractionator with forward b) Prefractionator with backward
integration (PF)* *integration (PB)*
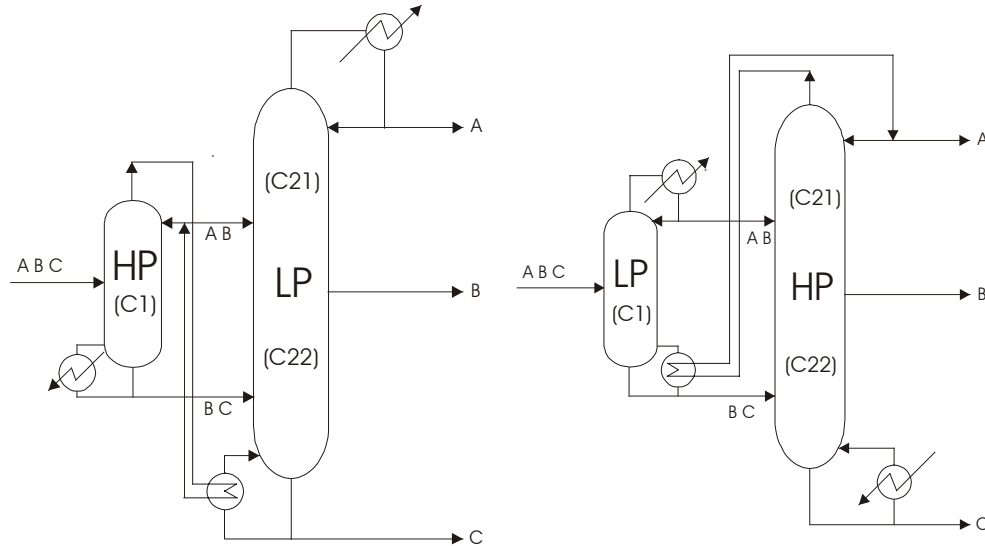
3.3. Minimum Vapour Flow (Energy Requirement)

The following sections considers ideal mixtures with the assumption of constant relative volatility (α_i constant) for the vapour liquid equilibrium and constant molar flows for the energy balance. For all short-cut equations sharp splits are assumed and the vapour flowrate (V) is the bottom flowrate, unless otherwise stated.

The minimum energy required is obtained using column sections with an infinite number of stages. This provides a useful target for distillation where one easily can get within 10% of this target with a reasonable number of stages.

The feed data required for the shortcut calculations are the flowrate (F) and the composition (z), which in this paper has been defined as [z_A z_B z_C] for the ternary mixture ABC. In addition we require the relative volatilities between the components [α_{AC} α_{BC} α_{CC}], which are referenced to the heaviest component (C), so $\alpha_{CC} = 1$. Also needed is the feed liquid fraction, q, where q = 1 is liquid feed and q = 0 is vapour feed.

3.3.1. Minimum Vapour Flow Expressions (Underwood & King)

For a <u>multi-component mixture</u> the vapour flowrate for a given separation can be calculated using Underwood's equations (e.g. King, 1980). The *minimum vapour flowrate* (V_{min}) at the top of the column is given as:

$$V_{T,\min} = \sum_{i=1}^{N_c} \frac{\alpha_{iH} x_{i,D} D}{\alpha_{iH} - \theta} \qquad (3.1)$$

where $x_{i,D}$ is the distillate composition of component i, α_{iH} is the relative volatility with respect to the heaviest component H and θ is the Underwood root. For a mixture of N_c components the $(N_C - 1)$ Underwood roots θ are found as the solution of the so-called feed equation:

$$(1-q) = \sum \frac{\alpha_{iH} z_i}{\alpha_{iH} - \theta} \qquad (3.2)$$

Here z_i is the feed composition of component i and q is the liquid fraction of the feed. The roots lie between the values of neighbouring relative volatilities so: $\alpha_{1H} > \theta_1 > \alpha_{2H} > \theta_2 > \alpha_{3H} > \theta_3 > \ldots > \alpha_{Nc-1H} > \theta_{Nc}$. Equation (3.2) applies for minimum reflux conditions when there are infinite number of stages in the column.

In the *ternary separations* ($N_C = 3$) considered here we first compute the $(N_c-1) = 2$ roots from the feed equation (Equation 3.2). This gives θ_A and θ_B, which are the same for all configurations. The root to be used in Equation (3.1) depends on the split between the components and thus on the configurations considered. If we have a sharp A/BC split as for the DS configurations, then we use θ_A and if we have a sharp AB/C split as for the IS configurations, then we use θ_B in Equation (3.1).

For the special case of a <u>binary separation</u> with components i and j the minimum vapour flowrate at the top of the column ($V_{T,\min}$) for infinite number of stages can be calculated by using Kings formula (King, 1980):

$$V_{T,\min} = \frac{r_{i,D} - \alpha_{ij} r_{j,D}}{\alpha_{ij} - 1} F + D \qquad (3.3)$$

Here $r_{i,D}$ and $r_{j,D}$ are the recoveries of components i and j in the distillate, where the recovery of component i is defined as $r_{i,D} = x_{i,D} D / z_i F$. For a liquid feed the vapour flowrate at the top of the column equals the vapour flowrate at the bottom ($V_{B,\min}$) and for a sharp split we have $r_{i,D} = 1$ and $r_{j,D} = 0$. The minimum vapour flowrate for a binary sharp split with liquid feed is then:

$$V_{T,\min} = \frac{1}{\alpha_{ij} - 1} F + D \qquad (3.4)$$

Note that for liquid feed the vapour flow in the top, V_T equals the vapour flow in the bottom, V_B. Otherwise, if $q \neq 1$ the vapour flowrate in the top is given as: $V_T = V_B + (1-q)F$.

For the ternary separation of ABC the relative volatilities of interest are α_{AC} and α_{BC}. For the binary AB and BC separations the relative volatilities of interest are $\alpha_{AB} = \alpha_{AC}/\alpha_{BC}$ and α_{BC}. If the relative volatilities varies with pressure different relative volatilities should be used in the HP and LP column. In the $V_{\min}$ equations

we use the notation α_{AB}' or α_{BC}' to indicate that the relative volatilities are actually at different pressure levels.

The minimum vapour flow required for the multi-effect configurations in Figure 3.2-Figure 3.4 can be found using the shortcut equations described above. It should be noted that when assuming constant relative volatility independent of pressure the multi-effect configurations with the same split type have the same minimum vapour flow requirements, i.e. DSF = DSB, ISF = ISB and PF = PB. However, if the relative volatility is assumed to be a function of the pressures (and therefore temperatures) in the columns then the relative volatility in the HP and LP columns are different. The V_{min} equations remain the same, but using different volatilities for the HP and LP columns will give different minimum vapour flowrate for same split configurations, i.e. DSF ≠ DSB, ISF ≠ ISB and PF ≠ PB.

3.3.2.   Direct Split Arrangements (DS/DSF/DSB)

With the assumption of sharp splits and liquid flows, from Equation (3.1) the minimum vapour flowrate for the <u>direct split arrangements</u> (DSF and DSB) in Figure 3.2 is expressed for column CD1 as:

$$V_{min}^{CD1} = \frac{\alpha_{AC} z_A}{\alpha_{AC} - \theta_A} F \tag{3.5}$$

In the second column CD2 we have a sharp binary separation between B and C so the minimum vapour flow can be calculated using Kings formula (Equation 3.4). The flowrate and feed composition of B to column CD2 are given by the bottom flow from the first column (CD1):

$$F^{CD2} = F\left(z_B + z_C\right) \tag{3.6}$$

$$z_B^{CD2} = z_B F / F^{CD2} \tag{3.7}$$

There is only B in the distillate of the second column (CD2) so the flowrate is given by:

$$D^{CD2} = z_B^{CD2} F^{CD2} = z_B F \tag{3.8}$$

Substituting into Kings formula (Equation 3.4) gives the minimum vapour flowrate for column CD2:

$$V_{min}^{CD2} = \frac{F}{\alpha'_{BC} - 1}\left(z_B + z_C\right) + \frac{z_B}{z_B + z_C} \tag{3.9}$$

where α'_{BC} is the relative volatility between components B and C column CD2.

The required minimum vapour flowrate for the multi-effect **integrated direct split configurations** is equal to the highest vapour flowrate requirement in the individual columns, i.e.:

$$V_{\min,DSF} = V_{\min,DSB} = \max\left\{V_{\min}^{CD1}, V_{\min}^{CD2}\right\} \tag{3.10}$$

To compare, for the **non-integrated direct split configuration** (Figure 3.1a) the minimum vapour flowrate is the sum of the required vapour rates in each column:

$$V_{\min,DS} = V_{\min}^{CD1} + V_{\min}^{CD2} \tag{3.11}$$

3.3.3. Indirect Split Arrangements (IS/ISF/ISB)

For the indirect-split arrangements (ISF and ISB) in Figure 3.3 the vapour flowrate for column CI1 is expressed as:

$$V_{\min}^{CI1} = \left(\frac{\alpha_{AC}z_A}{\alpha_{AC} - \theta_B} + \frac{\alpha_{BC}z_B}{\alpha_{BC} - \theta_B}\right)F \tag{3.12}$$

Note that for the indirect split the Underwood root used in Equation (3.1) is $\theta = \theta_B$ as the separation is between the two adjacent components B and C.

The second column performs the sharp binary separation between A and B. The feed flowrate and feed composition of component C to column CI2 is given by:

$$F^{CI2} = F\left(z_A + z_B\right) \tag{3.13}$$

$$z_A^{CI2} = z_A F / F^{CI2} \tag{3.14}$$

There is only A in the top of column CI2 (sharp splits) so the distillate flowrate is:

$$D^{CI2} = z_A^{CI2}F^{CI2} = z_A F \tag{3.15}$$

From Kings formula (Equation 3.4) the minimum vapour flowrate in the second column CI2 is then given by:

$$V_{\min(q=1)}^{CI2} = \frac{F}{\alpha'_{AB}-1}\left(z_A + z_B\right) + z_A F \tag{3.16}$$

For the multi-effect **integrated indirect split configurations** with **forward and backward integration** the minimum vapour flowrate required is then the maximum of the two flowrates in the individual columns:

$$V_{\min,ISF} = V_{\min,ISB} = \max\left\{V_{\min}^{CI1}, V_{\min(q=1)}^{CI2}\right\} \tag{3.17}$$

To compare with the non-integrated arrangement (Figure 3.1b) we note that here it is better to partially condense the vapour from the first column so the feed to the second column is vapour ($q = 0$). In this case the minimum vapour flow requirement in the second column will be smaller. The minimum vapour flowrate for a binary sharp split with vapour feed is given by (King, 1980):

$$V_{B,\min} = \frac{1}{\alpha - 1} F \tag{3.18}$$

The vapour flow in column CI2 (q = 0) is thus:

$$V_{\min,(q=0)}^{CI2} = \frac{F}{\alpha'_{AB} - 1} \left(z_A + z_B \right) \tag{3.19}$$

The minimum vapour flowrate for the **non-integrated indirect split configuration** in Figure 3.1b is the sum of the requirements in column CI1 (Equation 3.12) and CI2 (Equation 3.19):

$$V_{\min,IS} = V_{\min,C1} + V_{\min,C2(q=0)} \tag{3.20}$$

3.3.4. Prefractionator Arrangement (P/PF/PB)

In the underlined prefractionator arrangement (Figure 3.4) there is a sharp split between the lightest and the heaviest component, A/C, i.e. $x_{A,D}D = z_A F$ and $x_{C,D} = 0$ in Equation (3.1). However, from Equation (3.1.) the minimum vapour flowrate will depend on the amount of middle (B) component in the distillate, as expressed by $x_{B,D}$. This can alternatively be expressed in terms of the underlined product split from the prefractionator column:

$$\eta \triangleq \frac{D^{C1}}{F} \tag{3.21}$$

Note that $x_{B,D}D = F(\eta - z_A)$ so from Equation (3.1) $V_{\min}$ will depend linearly on η.

For the sharp split between two non-adjacent components (A/C) the Underwood root that should be applied is the root with the value between the relative volatility of the distributing component and the component at the limit of being distributed. Equation (3.2) therefore gives two possible Underwood roots (θ_A θ_B) and the two corresponding values of $V_{\min}$ are from Equation (3.1):

$$V_{\min(\theta=\theta_A)}^{C1} = \left| \frac{\alpha_{AC} z_A}{\alpha_{AC} - \theta_A} + \frac{\alpha_{BC} \left(\eta - z_A \right)}{\alpha_{BC} - \theta_A} \right| F \tag{3.22}$$

$$V_{\min(\theta=\theta_B)}^{C1} = \left| \frac{\alpha_{AC} z_A}{\alpha_{AC} - \theta_B} + \frac{\alpha_{BC} \left(\eta - z_A \right)}{\alpha_{BC} - \theta_B} \right| F \tag{3.23}$$

Note the linear dependency on η.

In the prefractionator the minimum vapour flowrate as a function of the recovery η is the maximum of these two (Fidkowski, 1986):

$$V_{\min}^{C1}(\eta) = \max \left(V_{\min(\theta=\theta_A)}^{C1}, V_{\min(\theta=\theta_B)}^{C1} \right) \tag{3.24}$$

This gives a V-shaped curve as a function of η and the minimum vapour flowrate in the prefractionator column occurs at a specific value of $\eta_{preferred}$, called "the preferred split".

However, to find the optimal value of η for the multi-effect arrangement we also have to consider the vapour flow required in the main column. The two sections of the main column performs sharp binary separations and from Equation (3.4) the minimum vapour flowrate in the upper section (C21) of the main column is:

$$V_{min}^{C21}(\eta) = \left[\frac{\eta}{\alpha'_{AB}-1} + z_A\right] F \qquad (3.25)$$

and in the lower section (C22):

$$V_{min}^{C22}(\eta) = \left[\frac{1-\eta}{\alpha'_{BC}-1} + (1-\eta-z_C)\right] F \qquad (3.26)$$

Note again the linear dependency on η.

As column sections C21 and C22 are connected the minimum vapour flowrate in the main column is the maximum of the two. The minimum flowrate of the integrated prefractionator arrangement (Figure 3.4) is the maximum of the main column and the prefractionator and by adjusting η we have:

$$V_{min,PF} = V_{min,PB} = \min_{\eta}\left[\max\left\{V_{min}^{C1}(\eta),\ V_{min}^{C21}(\eta),\ V_{min}^{C22}(\eta)\right\}\right] \quad (3.27)$$

The "optimum" recovery η occurs at the lowest minimum vapour flowrate for the system.

To compare, for the non-integrated prefractionator arrangement (Figure 3.1c) the vapour flow is the requirement in the prefractionator plus the maximum of the flowrates in the main column:

$$V_{min,P} = V_{min,C1} + \max\left\{V_{min,C21},\ V_{min,C22}\right\} \qquad (3.28)$$

However, here the minimum is always at the "preferred split" ($\eta = \eta_{preferred}$). For the integrated prefractionator arrangements the preferred split will only be optimal in some cases (see below).

3.3.5.   Summary of Minimum Vapour Flow Equations

The vapour flow requirement in the different columns when assuming constant relative volatility in each column, constant molar flows, and sharp splits are summarised in Table 3.1. These can be used as a guideline for deciding which of the multi-effect column configurations is the best, based on energy demands.

It should be noted that in most cases the energy demand of the different columns in an arrangement is different, therefore, the minimum energy is equal to the energy demand of the column that has the largest minimum vapour flowrate. This implies that the columns are not "balanced" and some of the columns or column sections will receive more vapour flow than required for the separation in that section. It may then be possible to perform further integration by, for example, installing an extra cooler to utilise any heat surplus or installing reboilers at different temperature levels. The different cases of unbalance for the multi-effect prefractionator arrangement and the options that exist for these cases are further discussed in Chapter 4.

Table 3.1. Summary of minimum vapour flowrates for sharp split sequences in multi-effect arrangements.

	Overall minimum vapour flowrate	Minimum vapour flowrate in individual columns
DSF/ DSB	$V_{\min,DSF} = V_{\min,DSB}$ $= \max\left\{ V_{\min}^{CD1}, V_{\min}^{CD2} \right\}$	$V_{\min}^{CD1} = \dfrac{\alpha_{AC} z_A}{\alpha_{AC} - \theta_A}\ F$ $V_{\min}^{CD2} = \dfrac{F}{\alpha'_{BC} - 1}\left(z_B + z_C\right) + \dfrac{z_B}{z_B + z_C}$
ISF/ ISB	$V_{\min,ISF} = V_{\min,ISB}$ $= \max\left\{ V_{\min}^{CI1}, V_{\min}^{CI2} \right\}$	$V_{\min}^{CI1} = \left(\dfrac{\alpha_{AC} z_A}{\alpha_{AC} - \theta_B} + \dfrac{\alpha_{BC} z_B}{\alpha_{BC} - \theta_B} \right)\ F$ $V_{\min}^{CI2} = \dfrac{F}{\alpha'_{AB} - 1}\left(z_A + z_B\right) + z_A F$
PF/ PB	$V_{\min,PF} = V_{\min,PB}$ $= \min_{\eta}\left[\max\left\{ \begin{array}{l} V_{\min}^{C1}(\eta), \\ V_{\min}^{C21}(\eta), \\ V_{\min}^{C22}(\eta) \end{array} \right\} \right]$	$V_{\min}^{C1}(\eta) = \max\left(V_{\min,(\theta=\theta_A)}^{C1}, V_{\min,(\theta=\theta_B)}^{C1} \right)$ $V_{\min,(\theta=\theta_A)}^{C1} = \left(\dfrac{\alpha_{AC} z_A}{\alpha_{AC} - \theta_A} + \dfrac{\alpha_{BC}(\eta - z_A)}{\alpha_{BC} - \theta_A} \right) F$ $V_{\min,(\theta=\theta_B)}^{C1} = \left(\dfrac{\alpha_{AC} z_A}{\alpha_{AC} - \theta_B} + \dfrac{\alpha_{BC}(\eta - z_A)}{\alpha_{BC} - \theta_B} \right) F$ $V_{\min}^{C21} = \left[\dfrac{\eta}{\alpha'_{AB} - 1} + z_A \right] F$ $V_{\min}^{C22} = \left[\dfrac{1 - \eta}{\alpha'_{BC} - 1} + \left(1 - \eta - z_C\right) \right] F$

3.3.6. Case Studies (Minimum Vapour Flowrate)

The minimum vapour flowrate expressions above have been used to calculate the vapour flow for the nine different distillation systems in Figure 3.1a, b and d, Figure 3.2, Figure 3.3 and Figure 3.4. The calculations have been made for five different relative volatilities and five different feeds (equimolar feed, feeds with large amount of the intermediate component, feed with a small amount of the intermediate component and a feed with large amount of the lightest component). The relative volatilities considered for the different feed cases are; equal difficulty between A/B and B/C, difficult A/B, difficult B/C, difficult A/B and B/C and easy A/B and B/C. The results are summarised in Table 3.2.

The minimum energy requirements (V_{min}) are expressed in terms of the percentage improvement compared to the best of the non-integrated direct (DS) or indirect split (IS) arrangement for that separation.

From these results the following general observations were made, in terms of "*first law*" energy requirements:

- The integrated prefractionator arrangements (PF/PB) are always better than the other arrangements.

- The highest energy savings for the integrated prefractionator arrangements occur when there is a high concentration of the middle component in the feed. The percentage savings for some of the cases exceed 70 %. The highest savings with high concentration of B occur when the relative volatilities are more or less "balanced" (i.e. same level of difficulty between the A/B and B/C separation).

- The lowest energy savings for all arrangements are when the feed contains a lot of the light component (A), or small amounts of heavy component (C), or small amounts of the middle component.

- There is generally a large difference between the integrated prefractionator arrangement and the Petlyuk arrangement, which is the best of the non-integrated arrangements (Halvorsen, 2003). The improvement of the integrated prefractionator compared with the Petlyuk arrangement ranges from about 5 % to 47 %, depending on the difficulty of separation and feed composition. The lowest savings are when there is a large amount of light component in the feed and the highest savings are when there is a high amount of the middle component in the feed.

For the calculations in Table 3.2 the same relative volatility has been used for both columns. This is the simplest assumption and it is in agreement with the assumption of equal heat of vaporisation made when assuming constant molar flows. For real mixtures, the relative volatility is usually reduced when we increase the pressure, but this is not always the case (e.g. mixture of methanol and ethyl acetate).

Further results for different feed compositions can be found in Appendix C.

Table 3.2. Energy savings in percent compared with the best of the conventional DS or IS (without multi-effect heat integration), assuming α constant with pressure

z_F	Column Arrangement	$\alpha = [4\ 2\ 1]$	$\alpha = [5\ 4.5\ 1]$	$\alpha = [5\ 1.5\ 1]$	$\alpha = [2\ 1.5\ 1]$	$\alpha = [10\ 5\ 1]$
1/3	DS	-1.94	0.00	-4.98	0.00	-0.28
1/3	IS	0.00	-0.51	0.00	0.00	0.00
1/3	Petlyuk	32.80	7.59	12.76	39.54	32.71
1/3	DSF/DSB	47.26	7.59	25.56	39.54	32.71
	ISF/ISB	32.80	8.21	12.76	44.65	34.03
	PF/PB	**61.73**	**37.44**	**47.41**	**59.06**	**50.05**
0.10	DS	-0.09	0.00	-0.23	0.00	-0.01
0.10	IS	0.00	-0.03	0.00	0.00	0.00
0.80	Petlyuk	32.99	11.39	12.43	47.37	44.23
0.10	DSF/DSB	37.69	11.39	16.20	47.34	49.62
	ISF/ISB	32.99	11.63	12.43	49.02	44.23
	PF/PB	**65.55**	**52.83**	**54.54**	**71.71**	**71.80**
0.20	DS	0.00	0.00	-1.06	0.00	0.00
0.20	IS	-0.66	-0.49	0.00	-2.11	-0.52
0.60	Petlyuk	33.40	8.50	13.41	40.03	37.72
0.20	DSF/DSB	48.91	8.50	25.70	40.03	37.72
	ISF/ISB	33.40	8.89	13.41	43.12	38.53
	PF/PB	**64.43**	**42.87**	**52.40**	**62.01**	**57.39**
	DS	-6.25	0.00	-17.42	0.00	-0.78
0.45	IS	0.00	-1.38	0.00	0.00	0.00
0.10	Petlyuk	34.38	4.53	14.19	34.78	18.39
0.45	DSF/DSB	34.38	4.53	27.74	34.78	18.39
	ISF/ISB	34.38	4.90	14.19	39.13	19.26
	PF/PB	**42.58**	**18.40**	**37.29**	**45.65**	**26.45**
0.80	DS	0.00	0.00	0.00	0.00	0.00
0.10	IS	-10.25	-2.14	-3.75	-17.43	-4.07
0.10	Petlyuk	14.96	1.73	19.04	12.45	8.10
	DSF/DSB	14.96	1.73	29.55	12.45	8.10
	ISF/ISB	15.23	1.77	19.04	12.86	8.18
	PF/PB	**19.92**	**10.78**	**32.34**	**19.68**	**13.27**

3.4. Required Pressure and Temperature Levels

In order to determine whether or not a particular integrated arrangement is suitable for a specific task it is also necessary to find the approximate pressure and temperature levels in both columns. This can easily be calculated from simple flash equations, by using the following procedure:

1) Calculate the temperature in the bottom of the LP column.

The temperature in the bottom of the LP column can be calculated from a simple flash calculation, usually by assuming atmospheric pressure in the LP column. This requires the concentration in the bottom of the column to be known. In four of the six integrated arrangements this is simply the product concentration of stream C. For the remaining two structures, the backward-integrated direct split (DSB) and the backward-integrated prefractionator arrangement (PR), the concentration is the BC mixture from the bottom of the LP column. For the DSB arrangement the concentration can be calculated from a simple mass balance by assuming a sharp A/B split in the first column. For the prefractionator arrangement we need to calculate or assume the product split, η, from the prefractionator column. This is found as the product split at the minimum vapour flowrate (see Section 3.3.4).

2) Specify a minimum temperature difference for the integrated reboiler/condenser.

Assume a minimum temperature difference between the integrated reboiler (T_{reb}) and condenser (T_{cond}): $\Delta T = T_{cond} - T_{reb}$.

3) Calculate P_{HP} from flash calculations.

Having assumed a minimum temperature difference the temperature in the top of the HP column is $T_{cond} = T_{reb} + \Delta T$. The pressure in the top of the column is then calculated using a simple flash calculation. The concentration in the top of the HP column is the product specification of the distillate product. In four of the cases this is the product specification of stream A or B. For the two remaining schemes, the forward integrated indirect split (ISF) and forward integrated prefractionator (PF), the concentration is the AB mixture from column CI1 and C1, respectively. For the ISF arrangement the concentration can be calculated from the mass balance by assuming a sharp B/C split CI1. For the prefractionator arrangement it is necessary to find the product split, η, (see Section 3.3.4).

4) Calculate the remaining temperatures.

Having calculated the required pressure in the HP column the other temperatures in the two columns can be calculated using the product specifications and the product split, η, assumed above.

3.5. Alternative Method for Comparing Column Arrangements

When deciding which arrangement is the best for a specific separation task we have to ask questions like: "At what temperatures is the cooling and heating required ? At what temperatures are the required utilities actually available ? What

integrated distillation system is most suitable for this separation ?" These questions are very important in any design procedures and the answer can vary from case to case.

Minimum energy demand is one measure that can be used for comparing different distillation arrangements. The above relationships for minimum vapour flowrate is looking at energy in a *quantitative* fashion, called "first law effects". An alternative to this is to look at the *quality* of the energy required, the "second law effects".

Usually there are trade-offs between the two effects. This can be seen when integrating two columns using multi-effect, as increasing the pressure in one column will lead to a decrease in the energy requirement (first law). However, at the same time there is an increase in the temperature span of the reboiler and condenser (second law effects). Sometimes the increased temperature of the utilities is acceptable, e.g. if existing utilities can still be used, but sometimes it is not acceptable, e.g. if the required hot utility temperature is higher than the utility temperature available.

The second law effects can be used to compare different column arrangements, in terms of the *thermodynamic efficiency*. This is usually called an *exergy analysis*. Many textbooks describe the exergy analysis, e.g. King (1980), and Henley and Seader (1981). Here material from 'Prosessteknikk', Skogestad (2003) has been used.

For a distillation column W_s^{id} is the *minimum work* that has to be supplied to the system. In many cases the enthalpy change, ΔH, is approximately zero and the ideal minimum work is given by the entropy change, which for a distillation process with pure products is given by:

$$\Delta S_{sep} = R \sum_i x_i \ln \gamma_i x_i \qquad (3.29)$$

where x_i is the concentration of component i and γ_i is the activity coefficient. The summation is for all i components in the feed.

Exergy is defined as:

$$B = H - T_o S \qquad (3.30)$$

so it follows that:

$$W_s^{id} = \Delta B = \Delta H - T_o \Delta S \qquad (3.31)$$

Meaning that the *change in the system exergy* is equal to the maximum theoretical work that can be produced by this change of state in relationship to the surroundings at constant temperature T_o.

An exergy analysis compares the changes in the exergy, ΔB, of the process with the (net) added work, W_s (dependent on the given process). We have that the lost work (or *exergy loss*) is:

$$W_{lost} = W_s - W_s^{id} = W_s - \Delta B \qquad (3.32)$$

However, in the expression for W_s^{id} (Equation 3.39), it is assumed that the surroundings are at a constant temperature T_o. This is not the case for distillation where heat, Q_H is transferred *from* a heat sink at a temperature T_H in the reboiler and heat, Q_C is transferred *to* a cold sink at temperature T_c in the condenser. In addition to this there may be other heat transfer (Q_i) taking place at temperatures T_i.

To deal with transfer of heat Q_i at a temperature T_i different from T_o we may compute the minimum work needed to generate this heat based on heat at T_o. This may be done using an ideal heat pump that operates between the temperatures T_i and T_o. This ideal work is given by:

$$W_i^{'} = Q_i \left(1 - \frac{T_o}{T_i}\right)$$

(3.33)

Then considering the losses of the distillation column by itself, this ideal should be included in the *total added work*:

$$\tilde{W} \triangleq W_s + \sum_i W_i^{'}$$

(3.34)

Equation (3.41) can also be used to avoid the problem of different temperatures for the inlet and outlet streams.

The thermodynamic efficiency should then be calculated as the ratio of *the ideal minimum work* to the *total added work*:

$$\eta = \frac{W_s^{id}}{\tilde{W}_s}$$

(3.35)

The topic of exergy is further considered in Chapter 6 where the thermodynamic efficiency is compared for different column arrangements in the context of an industrial application.

3.6.   Conclusion

Shortcut equations for minimum vapour flowrate for six conventional multi-effect configuration have been presented, including the equations for multi-effect prefractionator arrangements.

Using these shortcut equations it was shown that the multi-effect prefractionator arrangements (PF/PB) are always better than the other multi-effect arrangements considered, when assuming constant relative volatility, constant molar flows, liquid feeds and sharp splits. The highest energy savings for the integrated prefractionator arrangements occurred with a high concentration of the middle component in the feed with the percentage savings in the range of 50-70 %. The percentage savings for some of the cases exceed 70 %. In terms of improvement compared with the

Petlyuk arrangement, which is the best non heat-integrated arrangement, the improvement ranged from 5-50 % depending on the difficulty of separation and feed composition.

The lowest energy savings for all the multi-effect arrangements were found when the feed contained a lot of the light component, or small amounts of the heavy component, or small amounts of the middle component.

Thermodynamic efficiency was briefly presented as an alternative measure for comparison between different distillation arrangements.

3.7.   References

Biegler, L.T., Grossman, I.E., Westerberg, A.W., 'Systematic Methods of Chemical Process Design', Prentice Hall PTR, 1997.

Carlberg, N.A., Westerberg, A.W., 'Temperature-heat diagrams for complex columns. 3. Underwood's method for the Petlyuk configuration', *Ind. Eng. Chem. Res.*, 1989, 28, 1386-1397.

Fidkowski, Z., Krolikowski, L., 'Thermally coupled system of distillation columns: optimization procedure', *AIChE Journal*, 1986, Vol. 32, No. 4, 537-546.

Halvorsen, I.J., 'Minimum Energy Requirements in Complex Distillation Arrangements', PhD. Thesis Norwegian University of Science of Technology (NTNU), 2001.

Halvorsen, I.J., Skogestad, S., 'Minimum energy consumption in multicomponent distillation. 2. More than three products and generalised Petlyuk arrangements', *Ind. Eng. Chem. Res*., 2003, Volume 42, 616-629.

Henley, E.J., Seader, J.D., 'Equilibrium-Stage Separation Operations in Chemical Engineering', John Wiley & Sons, 1981.

King, C.J., 'Separation Processes', 2nd edition, McGraw-Hill Book Co., 1980.

Rev, E., Emtir, M., Szitkai, Z., Mizsey, P., Fonyó, Z, 'Energy savings of integrated and coupled distillation systems', *Computers and Chemical Engineering,* 2001, 25, 119-140.

Skogestad, S., 'Prosessteknikk', 2nd edition, Tapir Akademisk Forlag, Trondheim, Norway, 2003.

Chapter 4. Graphical Visualisation of Minimum Energy Requirements of Multi-Effect Distillation Arrangements

A revised version of parts of Chapter 3 and the main results from Chapter 4 has been submitted to the AIChE Journal, February 2003.

<u>Abstract</u>

This Chapter shows how the energy requirement for the multi-effect arrangements are easily visualised and compared in a V_{min}-diagram. These tools can be used as a basis for screening and the best arrangement(s) can be studied further using more rigorous simulation methods.

4.1. Introduction

The use of heat integration combined with complex configurations for distillation columns holds a great promise of energy savings up to about 70%. In addition to saving energy, which are accompanied by reduced environmental impact and site utility costs; there is also a possibility for reduction in capital costs. There are a number of different methods or designs that can be applied to save energy in distillation, for example integration of distillation columns with the background process, heat pumps, multi-effect distillation and complex arrangements such as prefractionators or thermally coupled columns (Petlyuk columns). Deciding which heat integrated arrangement to use is not a straightforward task as the best arrangement is very much dependent on the given separation task and the background process.

In this Chapter the focus is on the multi-effect integrated prefractionator arrangement (see Figure 3.4), which several authors, for example, Cheng and Luyben (1985) and Emtir et al. (2001) have shown to have high-energy savings, compared with other distillation arrangements. The other arrangements considered are shown in Figure 3.1-Figure 3.4.

An easy form of comparison for the energy consumption is the minimum vapour flowrate, which is often given in terms of simple shortcut equations. Such equations are given for different integrated multi-effect arrangements by e.g. Rév et al. (2001).

A visual representation of the minimum vapour flowrate in thermally coupled Petlyuk columns has been presented by Halvorsen (2003a), Fidkowski (1986) and Christiansen (1997). In these diagrams the vapour flowrate is plotted against the distillate/feed ratio in the prefractionator column. Defining the feed composition

and the relative volatility of the components being separated, the diagram can be drawn by simply plotting five points (see Figure 4.1). The diagram can be used to find the minimum vapour flowrate for the Petlyuk column, as well as the recovery for the preferred split.

As shown in this Chapter, the V_{min}-diagrams developed for the Petlyuk columns can be used for multi-effect heat-integrated systems if they are modified to also include the minimum vapour flowrate for a sharp binary A/B and B/C split. The diagram can then be used to find the minimum vapour flowrate for all conventional multi-effect columns. Also it can be used for find further information about the multi-effect heat integrated prefractionator arrangement, such as the optimal recovery of middle component, if the columns are balanced and compare the savings from the integrated arrangement with the Petlyuk arrangement.

4.2. Visualising the Vapour Flow Requirements in a V_{min}-Diagram

For a ternary feed we can draw a V_{min}-diagram (see Figure 4.1) for the prefractionator in Figure 3.1c where the top vapour flow (V_T/F) is plotted against the product split ($\eta = D/F$) (Halvorsen, 2003a).

The required data for plotting this diagram is the feedrate (F), the feed composition, $z = [z_A \; z_B \; z_C]$, the feed quality (q), the relative volatility, $\alpha = [\alpha_{AC} \; \alpha_{BC} \; \alpha_{CC}]$ and the Underwood roots ($\theta_A \; \theta_B$) that are the solution to the Underwood feed equation (e.g. King, 1980):

$$(1-q) = \sum \frac{\alpha_{iH} z_i}{\alpha_{iH} - \theta} \tag{4.1}$$

Equation (4.1) applies for minimum reflux conditions when there are infinite number of stages in the column. For a more in depth presentation of the minimum vapour flow equations see Chapter 3.

To draw the V_{min}-diagram in Figure 4.1 for the prefractionator column (C1) we have to identify five points [η, $V_{T,min}/F$]. For sharp splits and liquid feeds these are from the equations in Chapter 3 (see also Halvorsen and Skogestad, 2003a):

$$P_{AB}: \quad [z_A, \frac{\alpha_{AC} z_A}{\alpha_{AC} - \theta_A}] \tag{4.2}$$

$$P_{BC}: \quad [z_A + z_B, \frac{\alpha_{AC} z_A}{\alpha_{AC} - \theta_B} + \frac{\alpha_{BC} z_B}{\alpha_{BC} - \theta_B}] \tag{4.3}$$

$$P_{AC}: \quad [\eta_{preferred}, \frac{\alpha_{AC} z_A}{\alpha_{AC} - \theta_B} + \frac{\alpha_{BC}(\eta_{preferred} - z_A)}{\alpha_{BC} - \theta_B}] \tag{4.4}$$

Point P_{AC} is at the "preferred" split where:

$$\eta_{preferred} = z_A - \frac{\alpha_{AC} z_A \left(\alpha_{BC} - \theta_A\right)\left(\alpha_{BC} - \theta_B\right)}{\alpha_{BC}\left(\alpha_{AC} - \theta_A\right)\left(\alpha_{AC} - \theta_B\right)} \tag{4.5}$$

Finally, we have the points P_o and P_1. These are actually not used in this paper, but they complete the diagram for the prefractionator:

$$P_0: \quad = [0,0] \tag{4.6}$$

$$P_1: \quad = [1,(1-q)] \tag{4.7}$$

Figure 4.1. V_{min}-diagram for ternary separation.
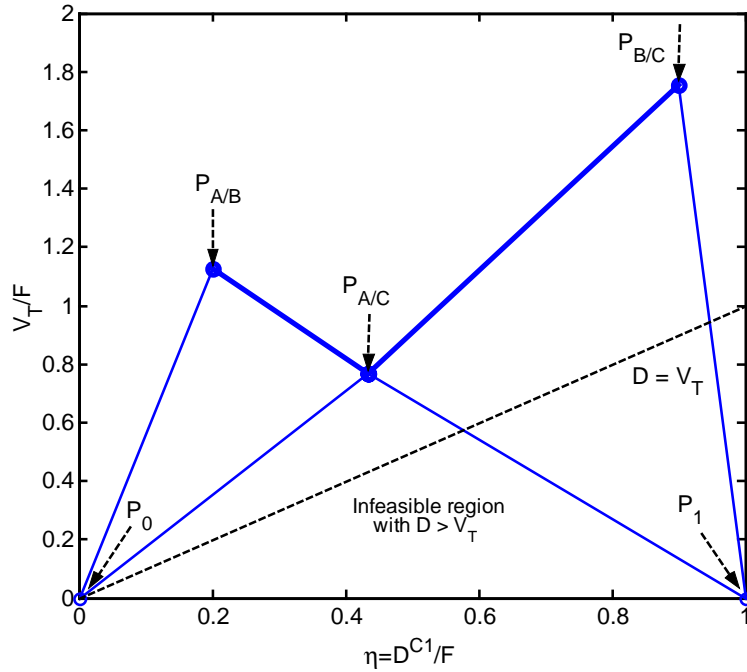
In the V_{min}-diagram (Figure 4.1) the peak $P_{A/B}$ is the minimum vapour flow for a sharp split between A/B with C present (A/BC) and the peak $P_{B/C}$ gives the minimum vapour flow for a sharp B/C split with A present (AB/C). The curve between the points P_{AB}-P_{AC}-P_{BC} gives the minimum vapour flowrate for sharp split between A and C for different recoveries of B in the distillate from the prefractionator. Along and above this line the split between A and C is sharp, with B distributing between the top and bottom product. The "preferred split" at point $P_{A/C}$ gives the minimum vapour flowrate for a sharp split between the lightest component (A) and the heaviest component (C) in the prefractionator. Note that below the dotted line where $D = V_T$ the separation in the prefractionator is infeasible as we must have that $V_T < D$.

For the Petlyuk column the minimum vapour flowrate is the highest of the peaks in the Vmin diagram (Halvorsen and Skogestad, 2003a), i.e.:

$$V_{\min,Petlyuk} = \max[V_{A/B}, V_{B/C}] \tag{4.8}$$

where $V_{A/B}$ and $V_{B/C}$ correspond to the points $P_{A/B}$ and $P_{B/C}$, respectively, in Figure 4.1.

The diagram in Figure 4.1 corresponds to the prefractionator column (C1) in Figure 4.2. In Figure 4.3 the $V_{\min}$-diagram is extended to the entire multi-effect arrangement by including the relationships for the minimum vapour flowrate in the two sections of the main column.

Figure 4.2. Multi-effect prefractionator notation
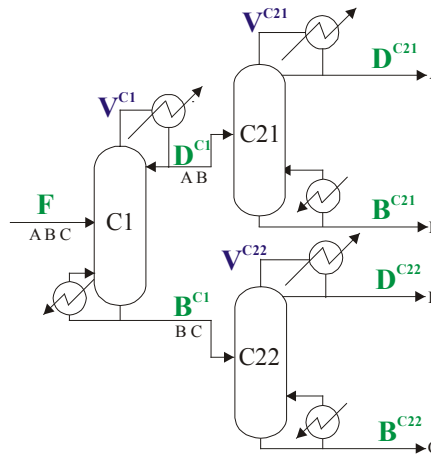
The co-ordinates for the main column sections are found from the minimum vapour flowrate expression for sharp binary separation with liquid feed (q = 1):

$$V_{B,\min} = V_{T,\min} = \frac{1}{\alpha - 1}F + D \tag{4.9}$$

The amount of B in the feed to the upper section of the main column (C21) varies depending on how the prefractionator is operated in terms of the product split $\eta = D^{C1}/F$. One possibility is to have no middle component B in the distillate from C1, so that $\eta = z_A$. Alternatively, all of B could go to the prefractionator distillate, giving $\eta = (z_A + z_B)$. In between these two "extremes" we have different recoveries of B in the distillate from the prefractionator.

Thus, the two points [η, $V_{T,min}/F$] for the **upper section of the main column (C21),** are:

$$P_{M1}: \quad [z_A, \frac{z_A}{\alpha'_{AB} - 1} + z_A] \tag{4.10}$$

$$P_{M2}: \quad [z_A + z_B, \frac{z_A + z_B}{\alpha'_{AB} - 1} + z_A] \tag{4.11}$$

and the two points for the **lower section of the main column, (C22)**, are:

$$P_{M3}: \quad [z_A, \frac{z_B + z_C}{\alpha'_{BC} - 1} + z_B] \tag{4.12}$$

$$P_{M4}: \quad [z_A + z_B, \frac{z_C}{\alpha'_{BC} - 1}] \tag{4.13}$$

It should be noted that in Figure 4.3 the lines for V^{C21} and V^{C22} go from $\eta = z_A$ (points P_{M1} and P_{M3}) to $\eta = z_A + z_B$ (points P_{M2} and P_{M4}). To the left of points P_{M1} and P_{M3} there is no B present in the feed to the upper part of the main column so all of B goes to the lower part of the main column. To the right of points P_{M2} and P_{M4} all of B is fed to the upper part of the main column and no B goes to the lower part.

Figure 4.3. Extended Vmin diagram for the multi-effect prefractionator arrangement in Figure 4.2 (Case 1).
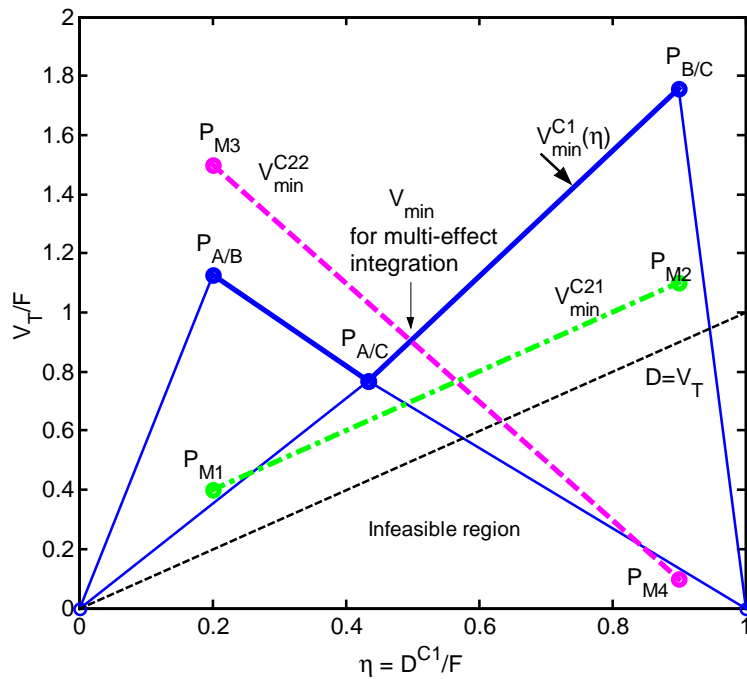
4.3. Using the V_{min}-Diagram for Multi-Effect Prefractionator Columns

In the multi-effect prefractionator arrangement in Figure 3.4 the vapour flow in all the three column sections must be equal. It then follows that the minimum vapour flow for a *given* recovery of component B in the prefractionator (given value of $\eta = D^{C1}/F$) is the maximum of the minimum flowrates in the three sections. The value of η should be adjusted such that V_{min} is minimised. The minimum vapour flow for the multi-effect prefractionator arrangement is then (see also Section 3.3.4):

$$V_{min,PF} = V_{min,PB} = \min_{\eta}\left[\max\left\{V_{min}^{C1}(\eta),\ V_{min}^{C21}(\eta),\ V_{min}^{C22}(\eta)\right\}\right] \quad (4.14)$$

Importantly, this value can easily be found using the V_{min}-diagram in Figure 4.3, as is further illustrated in Table 4.1.

When we require sharp split the points $P_{A/B}$, $P_{A/C}$ and $P_{B/C}$ span the minimum vapour flowrate for the prefractionator column (shown in bold). The points for the main column are shown as P_{M1}-P_{M2} (C21) and P_{M3}- P_{M4} (C22). For the specific case in Figure 4.3 the minimum vapour flow as a function of η, $V_{min,PF}(\eta)$, follows the V^{C22}_{min}-line from the point P_{M3} and down to the crossing with the V^{C1}_{min}-line and then goes up to the point $P_{B/C}$. The minimum vapour flowrate for the overall multi-effect integrated prefractionator arrangement is then where the V^{C22} and V^{C1}-lines cross (indicated as V_{min} in the figure).

The case shown in Figure 4.3 is referred to as Case 1. More generally, we have the following five possibilities for the multi-effect prefractionator arrangements:
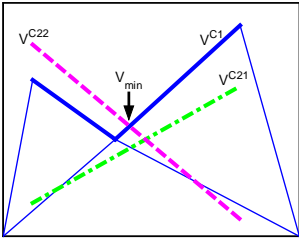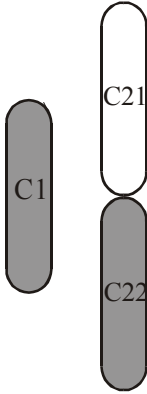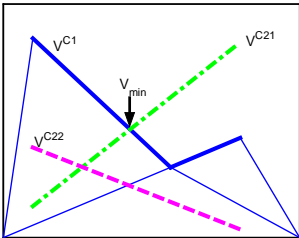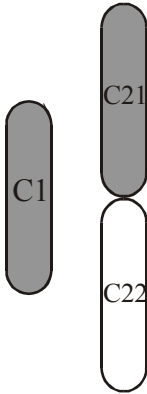
Case 1: Lines for V^{C22} and V^{C1} cross at optimum: $V^{C1} = V^{C22} > V^{C21}$

Case 2: Lines for V^{C21} and V^{C1} cross at optimum: $V^{C1} = V^{C21} > V^{C22}$

Case 3: Lines for V^{C21} and V^{C22} cross at optimum: $V^{C21} = V^{C22} > V^{C1}$

Case 4: Optimum at "preferred split", no lines cross: $V^{C1} > V^{C21}$ and V^{C22}

Case 5: All lines cross in the same point at optimum: $V^{C1} = V^{C1} = V^{C22}$
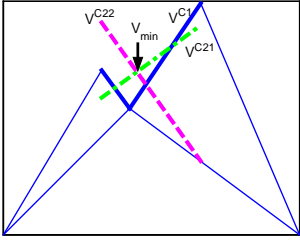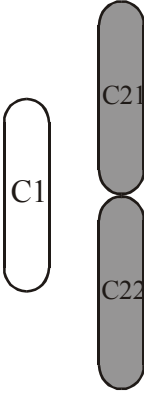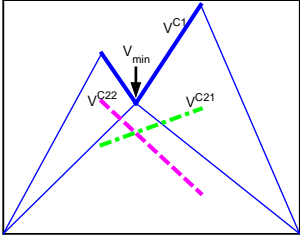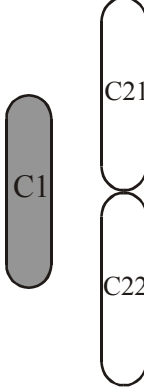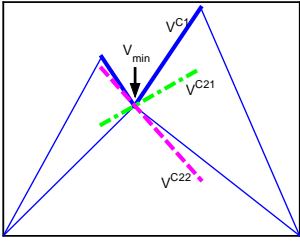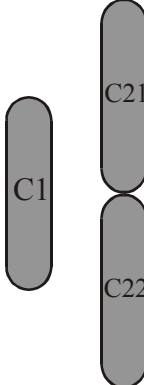
The left column in Table 4.1 shows the V_{min}-diagrams for these different cases. We can also use the information from the V_{min}-diagram to find the column sections that receive excess vapour ("unbalanced sections"). The column sections receiving excess vapour are shown in white in the middle column in Table 4.1. The "limiting" column sections, which operate at minimum flows, are shown in grey.

Except for Case 5 there will always be an excess (or "unbalance") of vapour flow requirement in some column section. The last column of Table 4.1 summarises the design or operational options that are available for the different classes. Note that the options available can differ depending on the arrangement, PF or PB, used. The difference occurs as for the PF arrangement the heat input is to the prefractionator column (C1) whereas for the PB arrangement the heat input is to the lower section of the main column (C22).

The different options for design and operation for the multi-effect prefractionator arrangement are further discussed in Section 4.4.

Table 4.1. Possible V_{min}-diagrams for multi-effect prefractionator arrangement (note: white sections receive excess vapour, i.e. are over-refluxed).

V_{min}-diagram	Limiting column sections	Possible use of excess vapour
Case 1 ($V^{C1} = V^{C22} > V^{C21}$)		PF a) Intermediate condenser between C22 and C21. b) Overpurify C21 product. c) Vapour sidestream product. d) Shorter column section C21. PB a) Overpurify C21 product. b) Shorter column section C21.
Case 2 ($V^{C1} = V^{C21} > V^{C22}$)		PF a) Overpurify C22 product. b) Shorter column section C22. PB a) Intermediate reboiler between C22 and C21. b) Overpurify C22 product. c) Shorter column section C22.

Case	Diagram	Configuration	Notes
Case 3 ($V^{C21} = V^{C22} > V^{C1}$)	(V^{C22}, V_{min}, V^{C1}, V^{C21})	C1; C21; C22	<u>PF</u> Not common, unless α increases with pressures. <u>PB</u> Overpurification in C1 is possible, but not important for final products. a) Use shorter column C1. b) Intermediate condenser at top of C21 or C1.
Case 4 ($V^{C21} = V^{C22} < V^{C1}$)	(V^{C1}, V_{min}, V^{C22}, V^{C21})	C1; C21; C22	<u>PF</u> a) Intermediate condenser between C22 and C21, or between C1 and C22. b) Overpurify products from main column. c) Vapour sidestream product. d) Shorter column sections C21 and C22. <u>PB</u> Not common, unless α increases with pressures.
Case 5 ($V^{C1} = V^{C21} = V^{C22}$)	(V^{C1}, V_{min}, V^{C21}, V^{C22})	C1; C21; C22	All column sections are balanced. No special measures needed.

4.4. V_{min}-Diagram for Other Column Configurations

The V_{min}-diagram can also be used to find the **minimum vapour flowrate** of other column arrangements. This is shown in Figure 4.4 for the following multi-effect arrangements (see Figure 3.2 and Figure 3.3):

- Direct split with forward and backward integration (DSF/DSB).

- Indirect split with forward and backward integration (ISF/ISB).

The minimum vapour flowrate for the DSF/DSB arrangement in Figure 3.2 is the maximum of the two points $P_{A/B}$ and P_{M3}. For the ISF/ISB arrangement (Figure 3.3) the minimum vapour flowrate is the maximum of the two points $P_{B/C}$ and P_{M2}. The difference between these points will also indicate how the columns are unbalanced. It is easy to see from the diagram which of the integrated DS or IS arrangement has the lowest energy demand for a given separation.

In this analysis it has been assumed that there is no difference in the relative volatilities for the forward and backward integrated cases, so that $V_{DSF} = V_{DSB}$ and $V_{ISF} = V_{ISB}$. If the relative volatilities are expected to vary with pressure then different relative volatilities for the HP and the LP column should be used (this will give different V_{min}-diagrams for the different same split arrangements).

The V_{min}-diagram can also be used to find the minimum vapour flowrate for the non-integrated single pressure direct split (DS) and indirect split (IS) arrangements. The minimum vapour flowrate for direct split is the sum of $(P_{A/B} + P_{M3})$ and for the indirect split (IS) the sum of $(P_{B/C} + P_{M2})$. Finally, minimum vapour flowrate for the Petlyuk column is, as mentioned earlier, the maximum of the peaks $(P_{A/B}, P_{B/C})$.

In summary we then have, with reference to Figure 4.4:

$$\text{DS(non-integrated)}: \qquad V_{min} = P_{A/B} + P_{M3}$$

$$\text{IS(non-integrated)}: \qquad V_{min} = P_{B/C} + P_{M2}$$

$$\text{DSF/DSB}: \qquad V_{min} = \max\left[P_{A/B}, P_{M3}\right]$$

$$\text{ISF/ISB}: \qquad V_{min} = \max\left[P_{B/C}, P_{M2}\right]$$

$$\text{Petlyuk (non-integrated)}: \qquad V_{min} = \max\left[P_{A/B}, P_{B/C}\right]$$

$$\text{PF/PB}: \qquad V_{min} = \min_{\eta}\left[\max\left\{V_{min}^{C1}, V_{min}^{C21}, V_{min}^{C22}\right\}\right]$$

The V_{min}-diagram in Figure 4.4 can thus be used as a screening method to quickly determine if multi-effect distillation (especially that with a prefractionator) should be investigated further.

From the shape of the V_{min}-diagram it can be seen that with the constant relative volatility assumption (independent of pressure) the multi-effect prefractionator arrangement (PF/PB) will always be better than the other multi-effect arrangements considered here. It will also always be better than the non-integrated arrangements, including the Petlyuk column. This is further confirmed by the data in Table 3.2.

Figure 4.4. Use of V_{min}-diagram to find minimum vapour flowrate for various column arrangements, with relative volatility independent of pressure.

4.5. Discussion on the Use of the V_{min}-Diagram

This section discusses some of the uses of the V_{min}-diagrams in Figure 4.3 and Figure 4.4.

4.5.1. Optimum Recovery

The V_{min}-diagram can be used to find the **optimum recovery** of the middle component in the prefractionator column (for sharp split). Having found the optimum value for $\eta = D^{C1}/F$, corresponding to $V_{min,PF/PB}$, the optimum recovery can be found from:

$$r_{B,D} = \frac{1}{z_{F,B}} \left(\frac{D^{C1}}{F} - z_{F,A} \right) \tag{4.15}$$

From Figure 4.5 we can see that this optimum recovery does not coincide with the preferred split of the Petlyuk column for most cases. It does, however, usually lie between the "preferred split" and the "balanced split" defined for a non-integrated prefractionator arrangement (see e.g. Christiansen, 1997).

For Cases 1 to 5 defined above, the location of the optimum recovery is as follows:

Case 1:   optimum recovery is between the preferred and balanced split

Case 2:   optimum recovery is between the preferred and balanced split

Case 3:   optimum recovery is between the preferred and balanced split

Case 4:   optimum recovery is equal to the preferred split

Case 5:   optimum recovery is equal to the preferred split

In Cases 1-3 operating the multi-effect prefractionator arrangement at the preferred split may result in a much higher energy demand than required, depending on how far the optimum is away from the preferred split.

Figure 4.5. V_{min}-diagram for a non-integrated prefractionator arrangement, showing the preferred and balanced splits (Case 1).
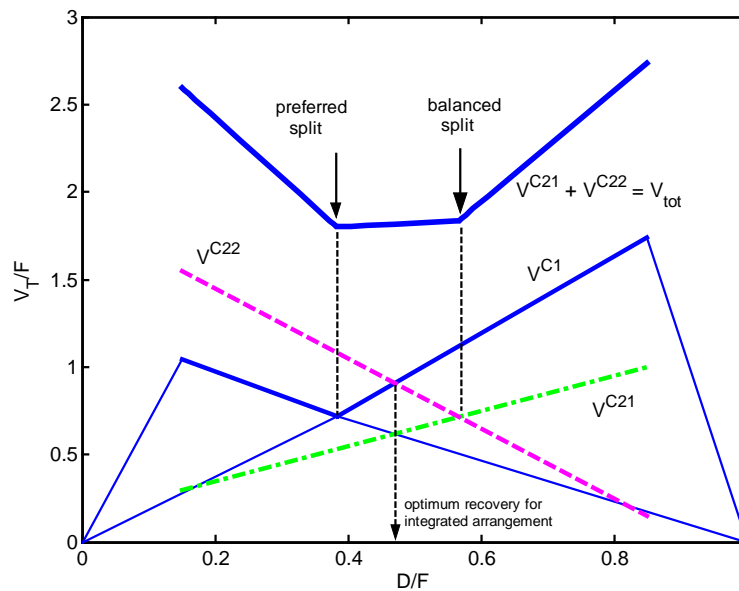
From Figure 4.3 it can be seen that for the multi-effect prefractionator arrangement the optimum as a function of $\eta = D^{C1}/F$ is sharp and not flat as it usually is for a Petlyuk column or prefractionator arrangement with no heat integration (see Figure 4.5). The figure also gives some idea of the shape of the optimum with respect to the recovery. Different separations and feed composition will give different gradients on the curves and they will vary between sharp or not so sharp.

4.5.2.   Unbalanced Columns

The five cases defined in Table 4.1 for the multi-effect prefractionator arrangement are now discussed in more detail. We start with the **forward-integrated case, PF**, where the heat input is to the prefractionator (C1), which is operating at a higher pressure than the main column (C21/C22).

Case 1-PF: The vapour flowrate in the *upper part (C21) of the main column is lower* than the other two sections, which are balanced. Design or operational alternatives for this case can be:

- To use an intermediate condenser between the upper and lower section in the main column to take out some of the excessive heat. The upper section can then be run at the required vapour flowrate.

- To take out some or all of the sidestream as vapour.

- To overpurify the top product from the upper section of the main column. The main section will then run at the higher vapour flowrate.

- To make use of the higher vapour flowrate (reflux) by making the upper section of the main column shorter by reducing the number of stages.

Case 2-PF: The vapour flowrate in the *lower part (C22) of the main column is lower* than the other two sections. Design or operational alternatives are:

- To overpurify the products from the lower section of the main column.

- To make the lower section of the column shorter by reducing the number of stages.

Case 3-PF: The vapour flowrate in the *main column sections (C21 and C22) is balanced* and is *higher* than the vapour flowrate required in the prefractionator column. This is not common for the PF integrated system, as usually the relative volatility is lower in the HP prefractionator than in the LP main column. For both the sections in the main column to have higher vapour flowrates than the prefractionator the relative volatility has to decrease with lower pressures.

Case 4-PF: The vapour flowrate in the *main column sections (C21 and C22) is balanced* but is *lower* than the vapour flowrate required in the prefractionator column. Design or operational alternatives for this case are:

- To use an intermediate condenser between the upper and lower section in the main column or between the prefractionator and lower part of the main column. The latter will be most effective, as the temperature at the bottom of C22 is higher than the temperature between C22 and C21, meaning that the heat is of a higher quality.

- To overpurify the products from the main column.

- To take out some or all of the sidestream as vapour.

- To use the higher reflux in the main column and make the column section smaller by reducing the number of stages.

Case 5-PF: All the column sections are balanced. The prefractionator will in this case run at the "preferred split".

For the **backward-integrated case, PB**, where the heat supply is to the lower part of the main column (C22), which is operated at a higher pressure than the prefractionator (C1), the following options exists for the different cases:

Case 1-PB: The vapour flowrate in the *upper part of the main column (C21) is lower* than the other two sections. Design or operational alternatives are:

- To overpurify the products from the upper section of the main column.

- To make the upper section of the column shorter by reducing the number of stages.

Case 2-PB: The vapour flowrate in the *lower part of the main column (C22) is lower* than the other two sections. Design or operational alternatives are:

- To use an intermediate reboiler between the upper and lower section.

- To make the lower section of the column shorter by reducing the number of stages.

Case 3-PB: The vapour flowrate in the *main column sections (C21 and C22) is balanced* and is *higher* than the vapour flowrate required in the prefractionator column. In this case the prefractionator should be operated at the optimum recovery found from the V_{min}-diagram. It would be possible to overpurify the products in the prefractionator, in terms of A in the bottom stream and C in the top stream. However, this will not have any overall effect on the products in the main column as we are already assuming that the prefractionator is operating at a "sharp" A/C split. The D^{C1}/F ratio (recovery of B) has to be kept at the optimal value otherwise there would be higher energy consumption in one of the sections of the main column. The only option that will result in savings is therefore:

- To make use of the high reflux ratio by reducing the number of stages, making the column shorter.

- Use an intermediate condenser at the top of C21 or C1.

Case 4-PB: The vapour flowrate in the *main column sections (C21 and C22) is balanced* but is *lower* than the vapour flowrate required in the prefractionator column. This is not common for the PB system, as it would require the relative volatilities to be reduced at lower pressures.

Case 5-PB: All the column sections are balanced. The prefractionator will in this case run at the "preferred split".

Note that using an intermediate condenser, which is one of the alternatives in Case 2-PF will mean that some of the condensation can take place at a lower temperature than in the main condenser. This allows for the use of a higher temperature cold stream, which can result in more possibilities for integration with other cold streams on the plant. An intermediate condenser may also allow for the use of a smaller heat exchanger area, but at the expense of an extra heat exchanger.

In the same way, using an intermediate reboiler, as in Case 3-PB, can allow for the use of a lower temperature hot utility. Again, this can result in more possibilities for integration with other process streams.

Note that when talking about overpurifying a product as a possible option this is in terms of *simplifying operation* and is <u>not</u> suggested as a design option. It has been included in Table 4.1 because from a <u>control point of view</u> it may be easier to operate a column section a higher reflux than required and thus obtaining a purer product. As the product is already above the required product purity this means that it is less sensitive to disturbances. This has been discussed by e.g. Skogestad (1997) and Govatsmark and Skogestad (2002). However, in terms of *design,* using a shorter column section would give lower capital costs and utilising the excess heat in other places in the process would give lower operating costs. But, the operation and control of the column should also be considered as a part of the design and overpurification has therefore been included.

Rather than overpurifying it is possible to use the higher reflux to decrease the number of stages in the relevant column section. Usually in a design there is a trade off between reflux ratio and the number of stages. Here the reflux ratio is given by the section(s) requiring the highest vapour flowrate.

It should be noted that Case 3-PF and Case 4-PB could occur, as there are some mixtures where the relative volatility *does* decrease when the pressure is decreased. One such example is the mixture of methanol and ethyl acetate.

From the above analysis we can see that the Vmin-diagram is an important tool for analysis of the multi-effect prefractionator. The Vmin shows quickly the extent of the unbalance between the columns and how the columns can be operated.

4.5.3. Effect Of Disturbances

If the columns are run at the nominal "optimum" vapour flowrate and recovery as found from the diagram, what would the consequences be if there are deviations from the operating point (e.g. due to disturbances) ? The diagram can be used to give an idea.

Assume that we are running with a sharp A/C split in the prefractionator and at the minimum vapour flowrate and "optimal" recovery found from the V_{min} diagram, see Figure 4.6. There are many disturbances or other factors that can move the system from this optimal operating point. This can for example be a disturbance in the duty or measurement errors that affect the control system. The following looks at some scenarios or consequences when there are disturbances resulting in changes of the recovery of the middle component (B).

If a disturbance has resulted in an **increase of the middle component (B)** in the top of the prefractionator then in order to keep a sharp A/C separation there has to be a corresponding increase in the boilup of the prefractionator. In the diagram (Figure 4.6) we will move from point V_{min} along the P_{AC}-P_{BC} line (1). This would lead to a reduction in the vapour requirement in the lower section (C22) of the

main column and an increase in the upper section (C21). As a result the product purity in the upper section C21 may not be achieved, however if the upper column is running at a higher reflux ratio then this may not be a problem as the product is already overpurified.

If, again there were an increase in the middle component, but without an increase in the vapour flowrate in the prefractionator then we would end up in a region of non-sharp splits. We move into the region where the heaviest component (C) will be present in the distillate from the prefractionator (line 2 in Figure 4.6). This will decrease the vapour flowrate requirement in the lower main column section (C22) and increase requirement in the upper section (C21). If too much of the heavy component is allowed to reach the upper section of the main column there may be difficulties in achieving the required purity of the middle product. All of the heavy component that goes over the top will gather in the middle product. There is therefore a maximum amount of C that can be allowed in the distillate from the prefractionator. Keeping a sharp A/C split in the prefractionator will ensure that achieving the purity in the sidestream is possible and will make control easier.

Figure 4.6. Using the Vmin diagram to look at different operating conditions (Case 1).
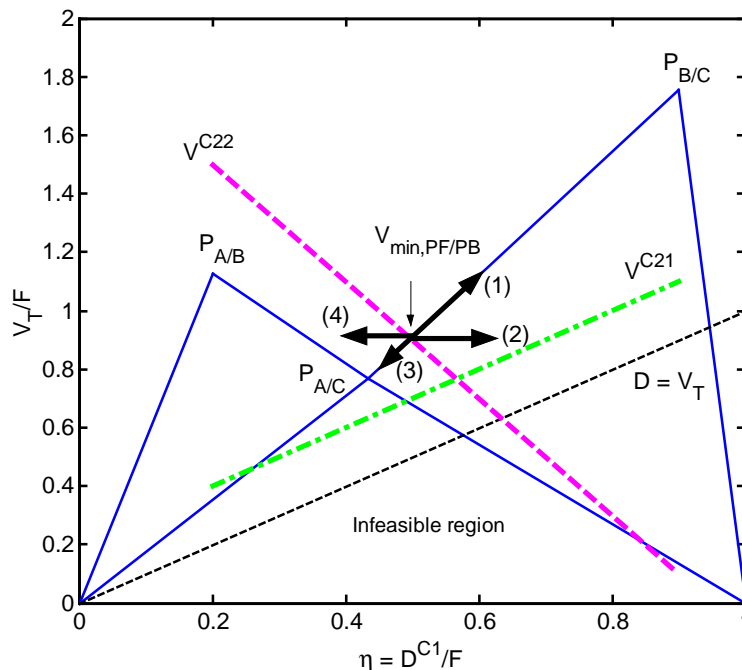
1) increase $r_{B,D}$ and V   2) increase $r_{B,D}$ + keeping V constant

3) decrease $r_{B,D}$ and V   4) decrease $r_{B,D}$ + keeping V constant

Another case would be a **decrease in the recovery of the middle component (B)** in the top of the prefractionator. If the vapour flowrate is decreased along the line towards $P_{A/C}$ (3) then there will still be a sharp A/C split in the prefractionator. The energy requirement in the upper part of the main column (C21) will decrease and the energy requirement in the lower part (C22) will increase. The main column (lower section) will therefore require additional heat input in order to maintain the product specification.

If the vapour flowrate remains the same then we will move along line (4). In this case the A/C split will still be sharp (until we cross the P_{AB}-P_{AC} line). As with the above case the vapour flow requirement in the lower section of the main column will increase and to maintain product specification more heat input is needed in C22.

Going back to the cases in Table 4.1 there can be situations with multiplicities that may give operational problems. In Figure 4.7 the prefractionator column and the upper section of the main column are balanced for two different recoveries. This might occur if the separation between two of the components (in this case A/B) becomes more difficult in the LP column, while the separation between the other two components (B/C) becomes easier. The system shown in Figure 4.7 is a special case of Case 2.

Figure 4.7. Case 2:, V_{min}-diagram with multiplicities.
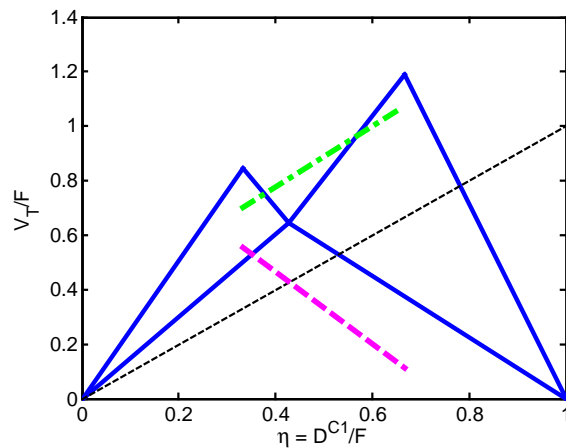
4.6.   Analysis of Two Mixtures

The V_{min}-diagram is here used to analyse the following two mixtures:

Mixture 1: benzene/toluene/m-xylene

Mixture 2: ethanol/n-propanol/n-butanol

The relative volatilities for these mixtures are given in Table 4.2. In this example the pressure variations in the relative volatility has been included. This is important for practical considerations. The relative volatilities have been calculated at HP = 6 bar and LP = 1 bar, using a commercial simulation package (HYSYS). The pressure of 6 bar in the HP column has been selected as it gives a sufficient temperature driving force between the multi-effect integrated columns. For the main column the relative volatilities given are for the upper section of the main column, α'_{AB} and for the lower section of the main column, α'_{BC}.

Table 4.2. Relative volatilities for Mixture 1 and Mixture 2

	Forward integration (PF)			Backward integration (PB)		
	Prefractionator (LP)	Main column (HP)		Prefractionator (HP)	Main column (LP)	
	C1	C21	C22	C1 (HP)	C21	C22
Benzene	3.58	2.43		5.57	1.90	1.88
Toluene	1.88	1.00	2.29	2.29	1.00	1.00
m-xylene	1.00		1.00	1.00		
Ethanol	3.52	2.05		4.55	1.81	1.94
n-propanol	1.94	1.00	2.22	2.22	1.00	1.00
n-butanol	1.00		1.00	1.00		

Figure 4.8 and Figure 4.9 shows the V_{min}-diagrams for Mixtures 1 and 2 for the forward-integrated prefractionator arrangement (PF) at two different feed compositions: $z_F = [1/3\ 1/3\ 1/3]$ and $z_F = [0.15\ 0.7\ 0.15]$. Figure 4.10 and Figure 4.11 shows the same mixtures and feed compositions, but for the backward-integrated arrangement (PB). Note that the reason for the difference between the PF and PB arrangement is the dependency of the relative volatility on the pressure. For the PF system the high-pressure column is the prefractionator whereas for the PB system the high-pressure column is the main column. The relative volatilities used reflect this difference.

Figure 4.8. Vmin diagram for Mixture 1, using PF arrangement (α depends on pressure).

a) $z_F = [1/3\ 1/3\ 1/3]$ - Case 4-PF $z_F = [0.15\ 0.7\ 0.15]$ - Case 1-PF

$V_{min}/F = 0.835$ $V_{min}/F = 0.865$
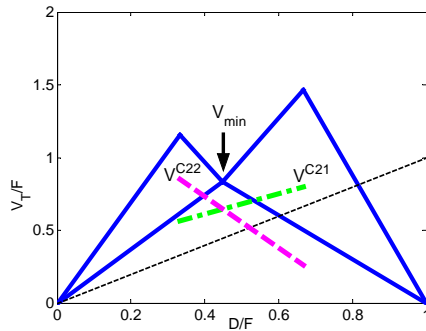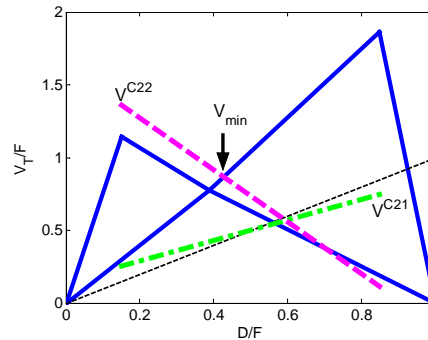
Figure 4.9. Vmin diagram for Mixture 2, using PF arrangement (α depends on pressure).

a) $z_F = [1/3\ 1/3\ 1/3]$ - Case 4-PF $z_F = [0.15\ 0.7\ 0.15]$ - Case 1-PF
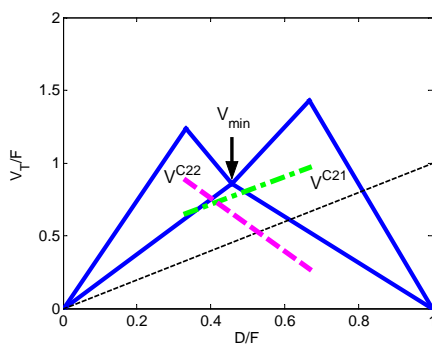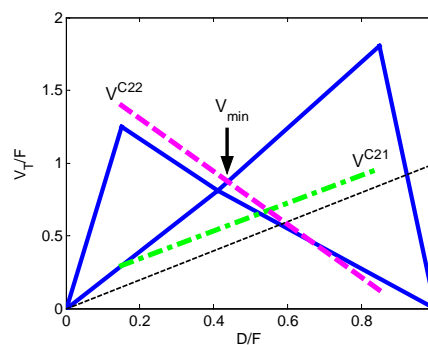
$V_{min}/F = 0.722$ $V_{min}/F = 0.775$

For both Mixture 1 and Mixture 2 we can see that at equimolar feed the minimum energy demand in the prefractionator column is higher than the minimum energy demand in both sections of the main column (see Figure 4.8a and Figure 4.9a). The main column will then have to run at a higher reflux than necessary, with the result that the column can be made shorter (due to the trade off between reflux and number of stages). Alternatively the products in the main column can be overpurified.

In the case of the feed with the high concentration of the middle component the energy demand in the prefractionator and the lower section of the main column is

Figure 4.10. Vmin diagram for Mixture 1 using PB arrangement (α depends on pressure).

a) z_F = [1/3 1/3 1/3] - Case 3-PB z_F = [0.15 0.7 0.15] - Case 1-PB

$V_{min}/F = 0.855$ $V_{min}/F = 0.871$
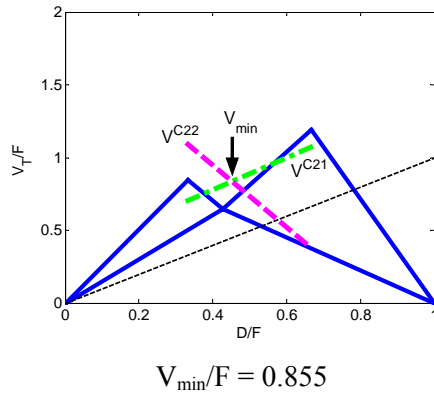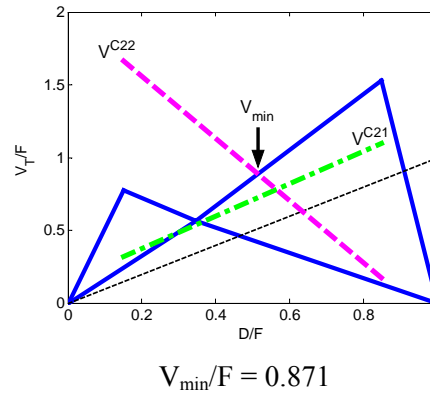
Figure 4.11. Vmin diagram for Mixture 2 using PB arrangement (α depends on pressure).

a) z_F = [1/3 1/3 1/3] -Case 3-PB z_F = [0.15 0.7 0.15] - Case 1-PB

$V_{min}/F = 0.836$ $V_{min}/F = 0.887$
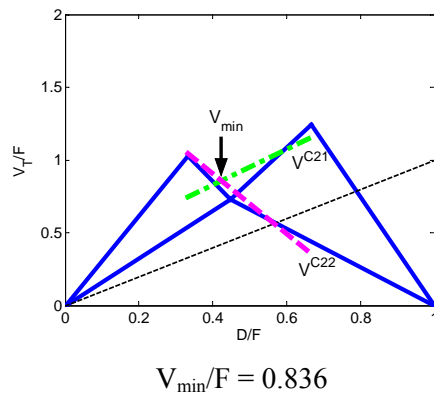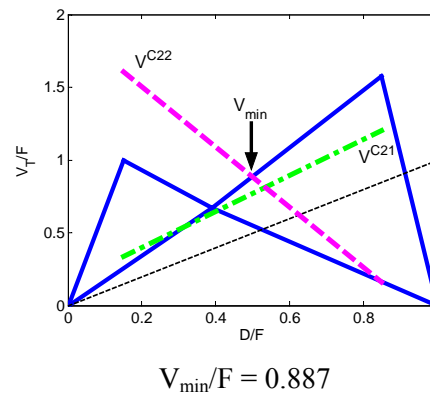
balanced for both Mixture 1 and Mixture 2 (see Figure 4.8b and Figure 4.9b). The energy demand in the upper section of the main column is less than the other two sections. In this case there are two options: to use fewer stages in the upper section (and higher reflux) or to use an intermediate condenser between the upper and lower section of the main column. A third option would be to overpurify the light component.

For the equimolar feed using the PB arrangement the minimum energy demand in the main column is higher than in the prefractionator for both Mixture 1 and Mixture 2 (see Figure 4.10a and Figure 4.11b). This is a backward integrated

scheme so the main column is used to boil the prefractionator column. There are two options for balancing the columns: to condense some of the vapour at the top of the main column (or prefractionator) or to run the prefractionator column at a higher reflux and use fewer stages.

For the feed with the high concentration of the middle component the upper section of the main column has a lower vapour flow demand. We can not install an intermediate condenser between the two column sections and the prefractionator requires a higher vapour flow than the upper section. The option will be to reduce the number of stages in the upper section while running at the higher reflux rate. Another option would be to overpurify the light product.

4.7.   Conclusions

The energy saving of the multi-effect prefractionator has been shown in a V_{min}-diagram. For a prefractionator or Petlyuk column a V_{min}-diagram can be plotted to show the minimum vapour flowrate as a function of the distillate flowrate, when there are infinite number of stages in the columns. For a ternary mixture it has been shown how this diagram can be extended to include heat-integrated multi-effect arrangements. It has been shown how the V_{min}-diagram then can be used to find the minimum vapour flowrate for all conventional non-integrated and multi-effect integrated arrangements. Figure 4.4 summarises these results in a single V_{min}-diagram.

Using the V_{min}-diagram it has been shown that the multi-effect prefractionator has the lowest energy consumption compared with the other arrangements studied.

The calculation of V_{min} assumes infinite number of stages, however, this is not in itself an important limitation since the actual value of V is usually close to V_{min}. Thus, V_{min} provides a good target for comparing energy usage for alternative arrangements. Of course, when the selecting the best arrangements one must also consider other factors such as capital cost, operability and control, product flexibility, available utilities and other often case-to-case specific requirements.

The formulas for the points in the V_{min} -diagrams have in this Chapter been given for sharp splits but they can easily be extended to non-sharp splits (see Halvorsen and Skogestad, 2003b). The lines in the V_{min}-diagram will remain straight, but they will be shifted slightly down, but usually not much since V_{min} is proportional to the purity, e.g. V_{min} for 98% purity is 98 % of that for sharp separation splits. The main effect of purity is on the required number of stages, which increases in proportion to the log of the impurity (e.g. Skogestad, 1997).

The main assumption in this paper is that of constant relative volatility and constant molar flows. For real mixtures, similar diagrams may be generated by simulation.

4.8.   References

Christiansen, A.C., 1997, 'Studies on optimal design and operation of integrated distillation arrangements', PhD. Thesis, Norwegian University of Science and Technology

Fidkowski, Z., Krolikowski, L., 'Thermally coupled system of distillation columns: optimization procedure', *AIChE Journal*, 1986, Vol. 32, No. 4, 537-546.

Govatsmark, M. S., Skogestad, S., 'Optimal number of stages in distillation with respect to controllability', Paper presented at ESCAPE'12 Symposium, The Hague, Netherlands, May 2002

Halvorsen, I.J., 'Minimum Energy Requirements in Complex Distillation Arrangements', PhD. Thesis Norwegian University of Science of Technology (NTNU), 2001.

Halvorsen, I.J., Skogestad, S., 'Minimum energy consumption in multicomponent distillation. 1. V_{min} diagram for a two product column', *Ind. Eng. Chem. Res.*, 2003a, 42, 596-604.

Halvorsen, I.J., Skogestad, S., 'Minimum energy consumption in multicomponent distillation. 2. Three product Petlyuk arrangements', Ind.Eng. Chem.Res., 2003b, Volume 42, 605-615.

King, C.J., 'Separation Processes', 2nd ed. McGraw-Hill Book Co., 1980

Rev, E., Emtir, M., Szitkai, Z., Mizsey, P., Fonyó, Z, 'Energy savings of integrated and coupled distillation systems', *Computers and Chemical Engineering,* 2001, 25, 119-140.

Skogestad, S., 'Dynamics and control of distillation columns: A tutorial introduction', Trans IChemE, 1997, Vol. 75, Part A, 539-562.

66

Chapter 5. Selecting Appropriate Controlled Variables for a Heat-Integrated Distillation System with Prefractionator

Abstract

A multi-effect prefractionator arrangement is studied for a ternary separation of a propane-butane-pentane mixture. Heat-integrated distillation system can be more difficult to control than non-integrated arrangements, so good control systems are essential. In this Chapter the focus is on selecting *control variables* that will ensure that the promised energy savings are achieved. The method of self-optimising control (Skogestad, 2000) has been used to provide a systematic procedure for the selection of controlled variables, based on steady state economics. The results show that the integrated prefractionator arrangement can have large energy savings compared with non-integrated arrangements and that controlling the ratio of the distillate flow to the feed flow has good self-optimising properties.

5.1. Introduction

Distillation is an energy consuming process that is used for about 95% of all fluid separation in the chemical industry and accounts for an estimated 3% of the world energy consumption (Hewitt et al., 1999). However, there are potentials for improvement and heat integration of distillation columns can be a method for achieving large savings.

For ternary separations there are three classical separation schemes: direct split, indirect split and the prefractionator arrangement. Energy savings can be achieved for these separation schemes by running one of the columns at a higher pressure and integrating the condenser of the HP column with the reboiler of the LP column. For these "multi-effect" systems there are two modes of integration: forward integration, where the heat integration is in the direction of the mass flow, and backward integration, where the integration is in the opposite direction of the mass flow.

In this study the focus is on finding self-optimising control variables for a prefractionator arrangement with forward integrated. These type of integrated

arrangements have been shown to have large energy savings compared with both integrated and non-integrated arrangements, see for example Cheng and Luyben (1985) and Emtir et al. (2001). In the literature there are however, only a few articles concerned with the optimisation and control of these integrated arrangements.

Ding & Luyben (1990) presented control studies of a direct split system and a backward integrated prefractionator systems for ternary separation of benzene-toluene-xylene. Two cases were considered: a low and a high purity requirement for the products. For the integrated prefractionator arrangement there is control of the two impurities in the sidestream (from main column) by controlling the sidestream flowrate and the sidestream draw-off tray. For the low-purity case they found that dynamically the prefractionator arrangement is about the same as the conventional direct split configuration. For the high purity case both systems are controllable, but the direct split configuration gives much better load rejection. They also found that the control of the sidestream toluene composition was particularly poor.

Bildea & Dimian (1999) also investigated the controllability for a system with a prefractionator and a sidestream main column. For the forward and backward integrated case they looked at four different designs, depending on the light/heavy split in the prefractionator. The authors concluded that in general the forward heat integration scheme is the easiest to control.

Emtir et al. (2003) compared five different energy-integrated schemes, among them the forward and backward integrated prefractionator arrangement, with a non-integrated direct split sequence. The study compared the total annual costs (TAC) and the controllability of the different schemes. In terms of TAC they found that the backward integrated direct split configuration has the maximum savings of 37 %. The integrated prefractionator arrangements have similar savings of 34 % for the forward-integrated case and 33 % for the backward-integrated case. In terms of controllability the authors found that the integrated direct and indirect split arrangements was similar to the non-integrated direct split. The more complex configurations were found to be more difficult to control due to interactions between the control loops. They also found that in terms of controllability the forward-integrated schemes were preferred.

The work published on the control of the multi-effect prefractionator arrangement is concerned mainly with dynamic controllability issues. In this Chapter we focus on the steady state issues and go one step back from the usual controllability analysis, in that we first look at "<u>what variables should we control</u> ?"

A multi-effect arrangement consisting of a prefractionator and a main column with sidestream is studied for the ternary separation of a propane-butane-pentane solution. The objective of the work has been on the selection of *controlled variables*, that is, finding which variables that should be controlled so that the energy savings can be achieved. The concept of self-optimising control (Skogestad, 2000), which normally is based on steady state economics, is used to provide a systematic framework for the selection of the controlled variables. This method involves a search for the variables that, when kept constant, indirectly lead to near-

optimal operation with acceptable economic loss. In self-optimising control, rather than solving the optimisation problem on-line, the problem is transferred into a simple feedback problem (Skogestad, 2000). In practice, this means that when the plant is subject to disturbances it will still operate within an acceptable distance from the optimum and there is no need to re-optimise when disturbances occur.

5.2.   The Integrated Prefractionator Arrangement

The system studied in this Chapter is a ternary separation of propane-butane-pentane using a forward multi-effect heat-integrated scheme. The separation is carried out in two columns operating at different pressures (see Figure 5.1). The first column is a high-pressure (HP) prefractionator, which performs the propane/pentane split. Both the distillate and the bottom product from the HP column are fed to the second, low-pressure (LP) column. Here propane, butane and pentane are the products from the distillate, sidestream and bottom stream, respectively. The top part of the LP column (above sidestream) performs the propane/butane split while the bottom part (below the sidestream) performs the butane/pentane split. The heat integration between the two columns is in an integrated reboiler/condenser, where the condensing heat from the HP column is used to boil the LP column.

The forward heat integrated scheme was selected for this study because other authors have previously found that it was the most easily controlled (Bildea & Dimian (1999), Emtir et al. (2003)). For a *backward* integrated system the prefractionator would be at a low pressure while the main column would be at the high pressure. The integrated condenser would then be between the top of the main (HP) column and the bottom of the prefractionator (LP). The energy savings assuming constant relative volatility would be identical (see Table 5.2).

The feed data and column specifications are given in Table 5.1.

Table 5.1. Feed data and column specifications

Feedrate (F)	300 mol/s		
Feed composition (z_F)/	Propane	0.15	7.98
Relative volatility (α)	Butane	0.70	3.99
	Pentane	0.15	1.00
Feed liquid fraction:	q = 1 (all columns)		
Number of stages	HP column:	20	
	LP column:	40	

Figure 5.1. The forward heat-integrated prefractionator arrangement.
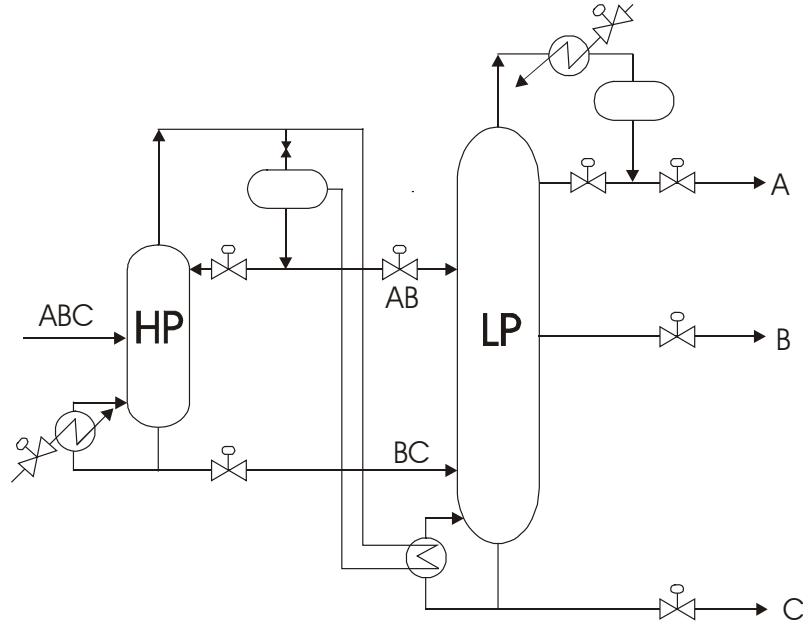
5.2.1. Energy Savings for Integrated Prefractionator Arrangements

For a thermally coupled distillation column (Petlyuk) the energy savings can be typically 30 % compared with the direct or indirect split arrangement (Halvorsen, 1999). However, using a prefractionator which is not only thermally coupled, but also heat integrated with the columns run at different pressures, can have savings of around 50% or more compared to the best of the direct or indirect sequence (Ding & Luyben, 1990).

Minimum vapour flowrate requirements for ternary mixtures may be calculated using the Underwood equations for minimum vapour flowrate for sharp splits and constant relative volatility. In the prefractionator the minimum vapour flowrate as a function of the recovery of the middle component $r_{B,D1}$, is calculated from:

$$V_{min,1} = \left(\frac{\alpha_A z_A}{\alpha_A - \theta} + \frac{\alpha_B r_{B,D} z_B}{\alpha_B - \theta} \right) F \qquad (5.1)$$

The Underwood roots, θ_A and θ_B are found from the feed equation (King, 1980). The break in the prefractionator curve in Figure 5.2 is the point where we go from using θ_A to using θ_B in Equation (5.1). The vapour flowrate in the second column is calculated from Kings equation (King, 1980) for binary mixtures. Note that the effect of pressure on the separation is not included in these formulas.

For prefractionator arrangements the energy saving is dependent on the recovery of the middle component from the prefractionator. Using the Underwood equation for

the prefractionator and Kings equation for the upper and lower part of the main column we can plot the minimum vapour flowrate as a function of the recovery of the middle component from the prefractionator. A sharp split between A/C in the prefractionator and A/B and B/C in the main column has been assumed. Figure 5.2 shows a comparison of the minimum vapour flowrate required for an integrated and a non-integrated prefractionator arrangement as a function of the recovery of the middle component. From the figure it can be seen that in this case both the integrated and non-integrated system has rather sharp optimums. This is not normally the case for the non-integrated scheme, but occurs for the feed composition and relative volatility used in the example, because the recoveries of the "preferred split" and the "balanced split" happen to be the same (see for example Christiansen, 1997). Normally, this does not occur, and the non-integrated prefractionator system has a flat optimum, between the "preferred split" and the "balanced split". For the integrated system the optimum is always sharp, as seen in Figure 5.2 (see Chapter 4).

Figure 5.2. Comparing V_{min} for prefractionator with and without integration.
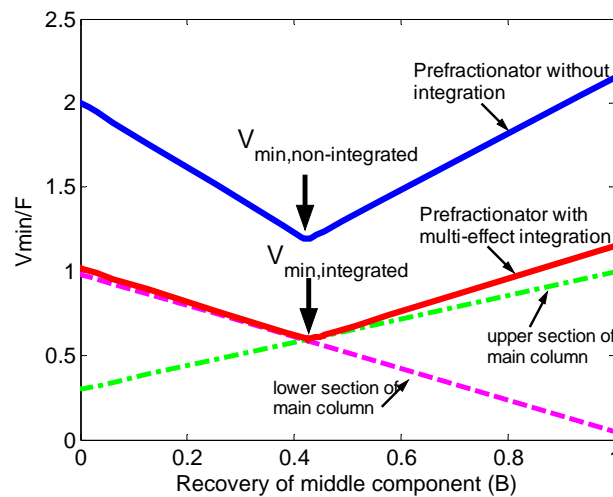
Table 5.2 shows comparisons between energy requirements for integrated and other non-integrated schemes, based on the minimum vapour flowrate expressions described above (sharp splits). The energy savings are given as percentage improvement compared to the best of the non-integrated *direct* or *indirect* sequence. In all cases the integrated prefractionator arrangements have higher energy savings compared to the other schemes. The highest savings occur when there is a high concentration of the middle component. For feed composition [0.15 0.7 0.15] the integrated prefractionator arrangements have savings of 70 %, compared to the best of the direct or indirect *non-integrated* sequence. In terms of energy the best of the other integrated schemes for this feed is a direct split arrangement (with forward or backward integration), which has 49 % savings.

Constant relative volatility has been used in all columns (see Table 5.1). Also, it is optimal for all the cases, except the indirect split (IS), to use liquid feed (q = 1) to all the columns. The indirect split (IS), the indirect split with backward integration (ISB) and the prefractionator arrangement with reverse integration (PB) would require less vapour flow for the A/B split if the feed to this section was vapour. However, for the two integrated cases this would result in a vapour being fed from a LP column to a HP column, something that would require compression. This would lead to added costs and has therefore not been considered as a viable option. Vapour feed is therefore used only in the indirect split case (columns at same pressure); for all the other cases liquid feed is considered to be the optimal operation. In the Petlyuk arrangement there is also vapour feed to the main column, but this is standard for this arrangement.

Table 5.2. Comparison of percentage energy savings (V_{min}) for different feed compositions (compared to the best of the non-integrated direct or indirect sequence) for mixtures with constant relative volatility, α = [8 4 1].

Z_F	DS	IS	Petlyuk	DSF/DSB	ISF/ISB	PF/PB
[1/3 1/3 1/3]	-0.44	0.00	34.86	34.86	36.54	**51.77**
[0.7 0.15 0.15]	0.00	-4.05	13.87	13.87	14.11	**21.65**
[0.1 0.45 0.45]	-3.79	0.00	39.20	46.47	39.20	**66.66**
[0.15 0.7 0.15]	**-0.05**	**0.00**	**42.47**	**49.13**	**42.47**	**70.17**
[0.45 0.1 0.45]	-1.29	0.00	20.85	20.85	22.00	**28.89**
[0.15 0.15 0.7]	-10.70	0.00	35.08	40.08	35.08	**57.64**
[0.45 0.45 0.1]	0.00	-2.41	31.83	31.83	32.22	**49.02**

5.3. Self-Optimising Control

The objective of the study is to implement a simple "optimal" control scheme for the integrated prefractionator arrangement by finding and controlling the variables in the system that will directly ensure optimal economic operation. Then, when there are disturbances in the system, there is no need to re-optimise.

The method of self-optimising control involves a search for the variables that, when kept constant, indirectly lead to *near-optimal* operation with *acceptable loss* (Skogestad, 2000). The procedure consists of six steps: 1) a degree of freedom (DOF) analysis, 2) definition of cost function and constrains, 3) identification of the most important disturbances, 4) optimisation, 5) identification of candidate

controlled variables and 6) evaluation of loss with constant setpoints for the alternative sets of controlled variables.

The first important step in this systematic procedure is to analyse the number of degrees of freedom (DOF) for the system. For the integrated prefractionator arrangement there are eleven dynamic (control) DOF, when assuming a fixed feedrate. These are: the boilup in the HP column, the condensation rate in the HP column, reflux, distillate and bottom flowrate from both columns, sidestream flowrate in the LP column, boilup in the LP column and condensation rate in the LP column (see Figure 5.1).

For this distillation system there are four holdups in the reboilers and condensers that have to be stabilised, but these have no steady-state effects and therefore no effects on the cost function. This then leaves seven degrees of freedom for optimisation.

In the formulation of the objective function there are two 'conflicting' elements: to produce as much valuable product as possible, but using as little energy as possible. For a given feed, the cost function is defined as the amount of propane, butane and pentane from the LP column (at 0.99 mol% or more) multiplied by the relevant product prices, minus the cost of the feed and the cost of boilup:

$$J = p_D D + p_S S + p_B B - p_F F - p_V V \qquad (5.2)$$

From the total mass balance we get:

$$J = (p_D - p_F)D + (p_S - p_F)S + (p_B - p_F)B - p_V V \qquad (5.3)$$

Further, it has been assumed that the products have the same value, so $p_D = p_S = p_B = p$ we have:

$$J = (p - p_F)(D + B + S) - p_V V = (p - p_F)F - p_V V \qquad (5.4)$$

With a given feedrate, F, the first term is fixed. Minimising J is then equivalent to minimising:

$$J' = -V \qquad (5.5)$$

where V is the vapour flow in the bottom of the HP column and $Q_{B,HP} = V \cdot H_{vap}$.

Having defined the objectives, the system constraints must be defined. These are the model equations (equality constraints), i.e. the mass, component end energy balances for the distillation process and the operational constraints (inequality constraints). In addition to requiring positive flows, the following seven constraints have been specified:

- The pressure in the LP column should be greater than or equal to 1 bar.

- The pressure in the HP column should be less than or equal to 15 bar.

- The reboiler duty in the LP column ($Q_{B,LP}$) must equal the condenser duty in the HP column ($Q_{C,HP}$) *(equality constraint)*.

- The product purity of the distillate ($x_{A,D}$), side ($x_{B,S}$) and bottom stream ($x_{C,B}$) should be above or equal to 99 mol%.

The area in the combined reboiler/condenser should be less than or equal to A_{max}, where A_{max} is calculated from the optimal steady state solution assuming ($T_{cond,HP}$ - $T_{reb,LP}$) = 5°C and U = 906 W/m^2 K. In practice the area constraint can, for example, be implemented by allowing the area to vary by using a bypass.

The optimisation problem can then be formulated as: min (-J'(x,u,d)), subject to: g_1(x,u,d) = 0 (model equations) and g_2(x,u,d) ≤ 0 (operational constraints). Here; x are state variables, u are independent variables that can be affected (DOF for optimisation) and d are independent variables that can not be affected (disturbances).

By solving the optimisation problem we find the nominal steady state operating point, i.e. the optimal operating point for the multi-effect distillation when there are no disturbances. This gives us the optimal nominal values for all the variables in the system.

Then the most important disturbances in the system have to be defined. The optimisation is then repeated for the various disturbances to find the active constraints and the objective value at each disturbance. The most important disturbances that have been considered are variations in the feed flow of ± 20 % and variations in feed compositions ($z_{F,B}$ = ± 0.1 mol fraction). The optimal solution for the nominal case and for the disturbances can be seen in Table 5.3.

5.3.1.   Active Constraints

The active constraints of the system are found from the optimisation. For this system we would expect to find that the three product compositions, the pressure in the LP column and the area of the exchanger are active constraints. However, for this problem only the following four constraints were active (see Table 5.3):

- The pressure in the LP column, which is equal to 1 bar

- The product purity of the sidestream, which is equal to 0.99

- The product purity of the bottom stream, which is equal to 0.99

- The area in the integrated exchanger, which is equal to A_{max}

- The pressure in the HP column and the product purity of the distillate were not active constraints.

When a variable is at a constraint then *active constraint control* is implemented, i.e. for this case P_{LP}, $x_{S,LP}$, $x_{B,LP}$, and area (A) will be controlled. For the area it is assumed that there is a bypass that can be manipulated in order to "control" the area and this should be kept "closed" to maximise A.

Table 5.3. The optimum solution for the nominal operating case and for the selected disturbances. Active constants are shown in bold.

Operating case	V_{opt} (mol/s)	$x_{AD,HP}$	$x_{BD,HP}$	$r_{BD,HP}$
Nominal	159.31	0.37	0.61	0.349
F+ 20%	190.70	0.38	0.61	0.346
F-20%	127.75	0.37	0.61	0.351
$Z_{F,B} + 0.1$	162.29	0.23	0.75	0.405
$Z_{F,B} - 0.1$	154.33	0.52	0.47	0.300

$x_{BB,HP}$	$x_{CB,HP}$	$x_{AD,LP}$	$x_{BS,LP}$	$x_{CB,LP}$
0.76	0.24	0.9999	**0.99**	**0.99**
0.76	0.24	0.9999	**0.99**	**0.99**
0.76	0.24	0.999985	**0.99**	**0.99**
0.84	0.16	0.9999	**0.99**	**0.99**
0.68	0.32	0.9999	**0.99**	**0.99**

P_{HP} (bar)	P_{LP} (bar)	$L_{T,LP}$(mol/s)	$L_{T,HP}$ (mol/s)	D_{HP}(mol/s)
7.4	**1.0**	273.6	40.4	119.9
7.6	**1.0**	330.6	48.7	143.3
7.2	**1.0**	217.4	32.2	96.4
6.0	**1.0**	278.2	32.5	129.2
8.8	**1.0**	264.9	42.5	115.4

B_{HP} (mol/s)	D_{LP}(mol/s)	S_{LP}(mol/s)	B_{LP}(mol/s)	B_{HP}/F
180.1	45.0	211.7	43.3	0.600
216.7	54.0	254.0	52.0	0.602
143.6	36.0	169.3	34.7	0.598
170.8	30.0	242.1	27.9	0.569
184.6	60.0	181.2	58.8	0.615

$Q_{B,HP}$ (MW)	$Q_{C,HP}$ (MW)	$Q_{B,LP}$ (MW)	$Q_{C,LP}$ (MW)	A (m^2)
3.3736	-3.1942	3.1942	-5.7292	**821.87**
4.0335	-3.8173	3.8173	-6.9156	**821.87**
2.7086	-2.5660	2.5660	-4.5562	**821.87**
3.4219	-3.3417	3.3417	-5.5414	**821.87**
3.2931	-2.9882	2.9822	-5.8411	**821.87**

This bypass will therefore be fully closed to maximise the area and thus the heat exchange between the two columns. Implementing active constraint control means that we are left with two unconstrained degrees of freedom for which control variables have to be selected.

In this case, where the costs of the products are the same it is the value of boilup that is minimised. In another case where the product prices are different, the purity constraint is likely to be active for the product(s) that has the highest value.

There may also be other cases when the active constraints change. Take, for instance, a case when there are changes in the feed composition, such that the condensation in the HP column is higher than the energy requirements of the LP column. In terms of Figure 5.2 this means that the minimum vapour flowrate curve for the prefractionator will lie above the curve for the main column, for all recoveries of the middle component. In order to balance the columns it may then be optimal to overpurify the least valuable product in the main column, thus one purity constraint is no longer active. Another possible operation is that the prefractionator no longer performs a sharp A/C split and the light component (A) will appear in the bottom stream in order to reduce the prefractionator duty. It is therefore important for the column operation and control system to study the feed composition and the effects of expected disturbances.

If the condensation in the prefractionator is less than the boilup in the main column this can result in the purity requirements of the LP column not being met, or that we get pure A at the top, or pure C at the bottom of the prefractionator.

5.3.2.   Testing Different Control Variables

Above it was found that four of the constraints were active constraints, thereby leaving two degrees of freedom for self-optimising control. This means that there are still two unconstrained variables that we need to control in order to specify the operation. To find out which variables are best suited we calculate the loss when different variables are fixed at their nominal optimal value (found from the optimisation) when there are disturbances. Here it has been decided to keep the product concentration of the distillate stream at its minimum value of 99 mol%. This is justified since fixing the concentration in the distillate stream gives very low loss ($\leq$ 0.0013 %). Thus there is little to gain by overpurifying this product and we may as well keep it at 99 %. This "active constraint" consequently leaves one degree of freedom.

For the remaining unconstrained degree of freedom a number of control variables were tested. The results from the loss calculation are presented in Table 5.4, where the extra cost of duty is presented as the percentage of the optimal duty requirement for each of the disturbances. Here a 1 % extra duty cost corresponds to about $ 25 000 per year when assuming production of 330 days/year and the cost of energy at 0.062 $/MJ.

From Table 5.4 it can be seen that constant setpoint control of many variables, like the pressure in the HP column (P_{HP}), result in large losses when there are disturbances in the feed flowrate or composition. Other variables result in infeasible operation for some of the disturbances. For most of the cases this is caused by the purity constraint not being reached in the sidestream of the main column.

It can also be seen that from the variables tested that the ratio of the distillate or the bottom stream in the prefractionator to the feed stream (D_{HP}/F, B_{HP}/F) has the lowest loss. This indicates that both of these are good self-optimising variables. If

one of these variables is controlled at a constant setpoint then the system will be closer to the optimum energy savings than if, for example, the pressure was to be controlled. The implementation error (± 10%) for D_{HP}/F was also tested and found to result in a loss of 2.9 and 20 %, respectively. The largest implementation error was for the case of D_{HP}/F - 10 %. Including the implementation error this gives an average loss of 4.3 % when controlling D_{HP}/F.

Table 5.4. Loss evaluated for each disturbance.

Control variable, c	Loss (%) (feedrate disturbance)		Loss (%) (composition disturbance)	
	F + 20 %	F - 20%	$z_{F,B}$ + 0.1	$z_{F,B}$ - 0.1
P_{HP}	2.50	0.95	21.94	71.70
$L_{T,HP}/F$	0.02	0.01	0.99	*Infeasible*
D_{HP}/F	**0.03**	**0.02**	**1.3**	**1.47**
$x_{BD,HP}$	0.02	0.06	26.96	38.71
$Q_{B,HP}$	*Infeasible*	24.55	*Infeasible*	2.44
D_{HP}	8.40	19.14	1.33	1.41
B_{HP}	20.80	28.11	1.33	1.41
$Q_{B,HP}/F$	*Infeasible*	*Infeasible*	*Infeasible*	*Infeasible*
B_{HP}/F	**0.03**	**0.02**	**1.30**	**1.47**
$x_{BB,HP}$	0.02	0.14	40.92	*Infeasible*
$L_{T,HP}$	*Infeasible*	1.99	0.97	*Infeasible*
$T_{4,HP}$	3.88	1.09	26.49	*Infeasible*
$X_{AB,HP}$	*Infeasible*	*Infeasible*	*Infeasible*	*Infeasible*

5.3.3.   Proposed Control Structure for Prefractionator Arrangement

A suggested control structure for integrated prefractionator arrangement using D_{HP}/F as the self-optimising control variable is presented in Figure 5.3. The active constraint control loops are shown shaded. It should be noted that this is only a suggestion for the pairing of controlled and manipulated variables. The focus of the study is on identifying the *control variables*, based on steady state economics, and not on the pairing or dynamic issues.

Figure 5.3. Proposed control structure for the integrated prefractionator arrangement.

The control structure has the following features:

(I)   Stabilising level loops (4)

- The reflux flow ($L_{T,HP}$) is used for level control in the HP condenser.

- The distillate flows (D_{LP}) is used for level control in the LP condenser.

- The bottom flowrate from the HP column (B_{HP}) is used to control the level in the HP column.

- The bottom flowrate from the LP column (B_{LP}) is used to control the level in the LP column.

(II) Active constraint control loops (4)

- The bottom product purity ($x_C = x_{CB,LP}$) is controlled using the sidestream flowrate (S_{LP}).

- The sidestream product purity ($x_B = x_{BS,LP}$) is controlled using the boilup in the HP column. To allow for local disturbance rejection this has been implemented in a cascade scheme, where the boilup is used to control the composition $x_{AB,HP}$ in the bottom of the HP column, and the setpoint for

this bottom composition ($x_{AB,HPs}$) is used as an independent variable to control the sidestream purity in the LP column ($x_B = x_{BS,LP}$).

- The pressure in the LP column is controlled using the condensation rate in the LP condenser ($Q_{C,LP}$).

- The maximum area in the integrated reboiler/condenser is used (not actual control loop, bypass valve is fully closed).

(III) "Self-optimising" loops (2)

- The distillate product purity ($x_A = x_{AD,LP}$) is controlled using the reflux flowrate ($L_{T,LP}$).

- The flow ratio D_{HP}/F is controlled at a constant setpoint (self-optimising loop).

5.4. Dynamic Simulations

Dynamic simulations have been carried out in order to verify the proposed control structure in Figure 5.3, where the ratio D_{HP}/F is used as a self-optimising variable. The control loops describes above (and shown in Figure 5.3) were tuned using "Skogestad's tuning rules", described in Skogestad (2003). The loops were first tuned and closed one by one using these rules, then the system was finally tuned by "hand" to achieve a robust response when subject to disturbances.

Figure 5.4 to Figure 5.6 shows the response in the product compositions when the system was subject to the following disturbances:

- 5 % increase in the feedrate F (Figure 5.4)

- 0.05 increase in the middle component feed fraction (Figure 5.5)

- 0.05 decrease in the middle component feed fraction (Figure 5.6).

For all cases the disturbances have been made at time = 10 hours.

The results from the dynamic simulations show that the proposed control system works and that the integrated prefractionator arrangement is controllable, but that the system is quite sensitive to disturbances. If large disturbances are to be expected then other control schemes should also be investigated. It may also be advantageous to use a feed tank before the prefractionator so that the flowrate to the column can be controlled and disturbances in the feed composition evened out. The use of a feed tank to decouple two multi-effect columns has been discussed by Rix and Glebe (2000).

From the figures it can be seen that the distillate composition control is very fast and with small setpoint deviation. The sidestream has a slower response, as expected, since this is normally the case for the sidestream and in addition this loop is the slow cascade loop. The bottom concentration response is the poorest with the largest setpoint deviation. If it is important to keep the concentration close to the setpoint then other alternatives may be investigated.

Figure 5.4. Response to disturbance in feed flowrate F + 5 % at time = 10 hours.

Product composition response in LP column
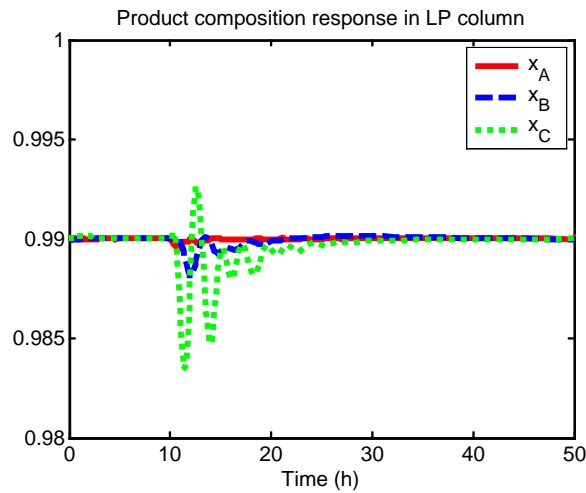
Figure 5.5. Response to disturbance in feed composition, $z_F = [0.175\ 0.65\ 0.175]$ at time = 10 hours

Product composition response in LP column
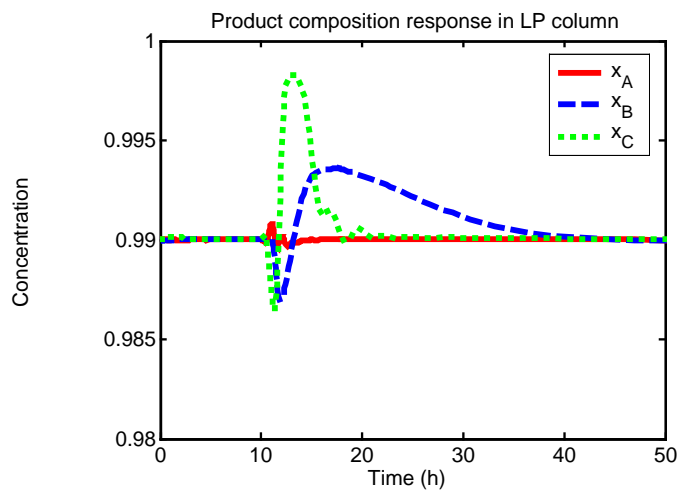
The problem could be alleviated by, for example, using a product tank, which will average out the variations in product composition. Another alternative, which would give a faster response, would be to use an auxiliary reboiler to control the bottom composition. This however, would result in a higher energy demand and as the main objective in this study has been on energy saving this option has not been considered.

According to the results from the optimisation the pressure in the HP column has been kept floating. A typical pressure response in the top of the HP column can be seen in Figure 5.7. The disturbance is a 5 % increase in the feed flowrate.

Figure 5.6. Response to disturbance in feed composition, $z_F = [0.125\ 0.75\ 0.125]$ at time = 10 hours
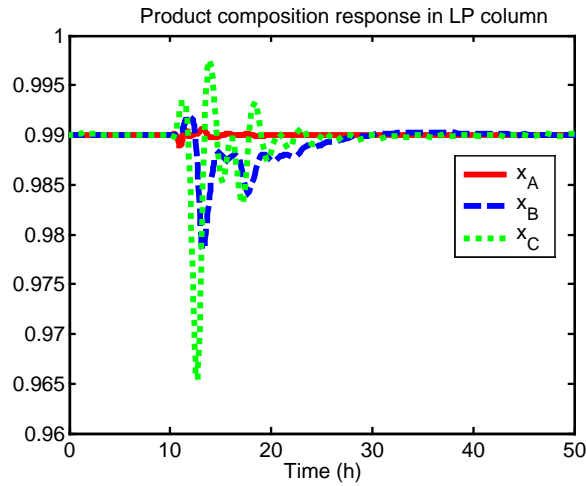
Figure 5.7. Response of pressure in top of HP column response to a 5 % increase in feed flowrate (at time = 10 hours)
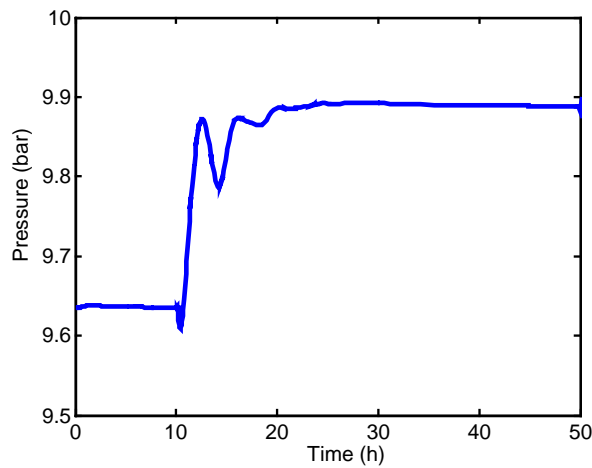
Two other structures with different control for the bottom composition were also tested:

> Alternative structure 1: The bottom composition is controlled in cascade, with a temperature below the sidestream controlled in an inner loop using the sidestream. The temperature setpoint is then used to control the bottom composition.

> Alternative structure 2: The boilup in the HP column is used to control the bottom composition in the LP column. For this scheme the bottom composition in the HP column was not controlled and the sidestream flowrate was used to control the sidestream composition.

None of these alternative structures showed improvement to the proposed structure. Structure 1 was controllable and worked reasonably well, but alternative 2 was very slow and did not work well.

5.5.   Discussion

When considering heat-integrated distillation columns it is important that after the first initial screening of alternatives that a more rigorous analysis is performed. The results will often be on a case to case basis. For instance, when using multi-effect columns the temperature range of the utilities is increased. For the system studied this means that the heat supplied to the HP column must be at a higher temperature than if the system was operating at a lower pressure. This may, for some cases, be within the available utilities on some plants whereas on other plants it may not be acceptable.

The identification and selection of the disturbances may also vary from case to case and this will influence the results. For instance, it may be that composition disturbances are not expected. There may then be variables other than the flow ratio that can be used for the self-optimising control loop. There may also be other disturbances that should be considered, e.g. disturbances in the utilities, such as the steam pressure and feed quality (vapour fraction).

As described earlier the set of the active constraints in the system may also change.

The list of control variable tested is not extensive and further variables should be tested. An alternative method can also be used where the optimal combination of control variables is found (giving no loss) (Alstad & Skogestad, 2002).

Finally, in this study we have only considered the forward-integrated arrangement in Figure 5.1. The backward integrated scheme with the prefractionator operating at the low pressure (LP) and the heat supplied to the main column has similar energy savings, but will otherwise be quite different from an operation point of view. For example, the temperature at the top of the LP-column will be higher, assuming that the LP column is operated at 1 bar. The best self-optimising variable is also likely to change. We found in our study of the forward integrated prefractionator arrangement that the control of the bottom product was somewhat poorer (e.g. see Figure 5.6). The backward integrated scheme is potentially better from this point of view, since the boilup in the main column can be used for control purposes.

5.6. Conclusions

The work presented shows that a heat-integrated prefractionator arrangement has very large energy savings compared with conventional direct or indirect split columns. The focus of the work has been on finding good control variables that will ensure that these promised energy savings are achieved in practice during operation.

The method of self-optimising control is used to find the best control variables. For the prefractionator arrangement there is a total of eleven degrees of freedom with six DOF available for optimisation when variables with no-steady state effects have been excluded and the duties of the two columns are matched. From the optimisation it was found that there are two degrees of freedom left for which control variables had to be found. The active constraints (P_{LP}, $x_{S,LP}$, $x_{B,LP}$, A) were used to implemented *active constraint control*. Also, it was decided to control the top product purity ($x_{D,LP}$) in the LP column as this gave very low loss in the objective function. A comparison of economic loss was then used to find the last self-optimising control variable that will keep the system close to the optimum when there are disturbances. The ratio of the distillate flow to the feed rate (D_{HP}/F) was found to have good self-optimising properties.

Dynamic studies where the D_{HP}/F scheme was implemented showed that the system is controllable, but that the sidestream and bottom stream composition responses are slow and that the system is sensitive to disturbances. For a practical implementation of the multi-effect prefractionator arrangement it would therefore be advisable to use a feed tank so that any disturbances are reduced.

For the selected feed composition the forward-integrated prefractionator arrangement uses only around 30 % of the energy required for the direct or indirect split arrangement. When including the average loss of 4.3 % when controlling the distillate to feed ratio (D_{HP}/F) the forward-integrated prefractionator arrangement will use 31.3 % of the energy required for the direct or indirect split arrangement.

5.7. References

Alstad, V., Skogestad, S., 'Robust operation by controlling the right variable combination', *AIChE Annual meeting*, Paper 247g, Indianapolis, 3-8 Nov. 2002

Bildea, C.S., Dimian, A.C., 1999, Interaction between design and control of a heat-integrated distillation system with prefractionator, *Trans IChemE*, Vol. 77, Part A, 597-608.

Cheng, H. C., Luyben, W., 1985, Heat-integrated distillation columns for ternary separations, *Ind. Eng. Chem. Process Des. Dev.*, 24, 707-713.

Christiansen, A.C., 1997, 'Studies on optimal design and operation of integrated distillation arrangements', PhD. Thesis, Norwegian University of Science and Technology

84

Ding, S.S., Luyben, W., 1990, Control of a heat-integrated complex distillation configuration, *Ind. Eng. Chem. Res.¸* 29, 1240-1249.

Emtir, M., Rév, E., Fonyó, Z., 2001, 'Rigorous simulation of energy integrated and thermally coupled distillation schemes for ternary mixture', *Applied Thermal Engineering*, 21, 1299-1317

Emtir, M., Rév, E., Fonyó, Z., 2003, 'Economic and controllability investigation and comparison of energy integrated distillation schemes', *Chem. Biochem. Eng. Q.*, 17 (1), 31-42

Halvorsen, I.J., 1999, Optimal operation of Petlyuk distillation: steady-state behavior, *J. Process Control*, 9, 407-424

Halvorsen, I.J., 2001, 'Minimum energy requirements in complex distillation arrangements, PhD. Thesis, Norwegian University of Science and Technology

Hewitt, G., Quarini, J., Morell, M., More efficient distillation, *The Chemical Engineer*, 21 Oct. 1999

King, C.J., 1980, Separation Processes, McGraw-Hill Book Co.

Lenhoff. A.M., Morari, M., 1982, Design of resilient processing plants - I: Process design under consideration of dynamic aspects, Chemical Engineering Science, Vol. 37, No.2, 245-258.

Rev, E., Emtir, M., Szitkai, Z., Mizsey, P., Fonyo, Z, 'Energy savings of integrated and coupled distillation systems', *Computers and Chemical Engineering,* 2001, 25, pp. 119-140

Rix, A., Glebe, H., 'On the impact of mass and heat integration on design and control of distillation column systems', *Trans IChemE,* 2000, Vol. 78, Part A, 542-548

Skogestad, S., 'Plantwide control: the search for the self-optimizing control structure', *J. Process Control*, 2000, Vol.10, 487-507.

Skogestad, S., 'Simple analytic rules for model reduction and PID controller tuning', *J. Process Control*, 2003, Vol. 13 , 291-309

Chapter 6. Multi-Effect Distillation Applied to an Industrial Case Study

Chapter 6 has been submitted for publication to the journal of Chemical Engineering and Processing, February 2004.

Abstract

An industrial separation system consisting of four distillation columns has been studied to see if multi-effect integration can be applied to any two columns in the sequence. Shortcut equations and V_{min}-diagrams, as presented in Chapters 3 and 4, have been used for screening purposes to find the columns with the highest potential for energy savings. The most promising case has then been further studied using rigorous simulation tools to verify the results from the shortcut approach. Three cases have been simulated: a non-integrated base case (existing), a multi-effect indirect split arrangement (ISF) and a multi-effect prefractionator arrangement (PF). The results showed that when considering the existing number of stages available the ISF arrangement was the best, however when considering infinite number of stages the PF arrangement was the best (as expected).

6.1.   Introduction

The separation of a hydrocarbon feed into four products using four sequential distillation columns have been studied in this Chapter to see if any of the four columns are suitable for heat integration by using a multi-effect prefractionator arrangement.

Multi-effect integration of prefractionators has been considered in the literature by authors like Cheng and Luyben (1985) and Emtir et al. (2001), who demonstrated that this arrangement can have high energy savings. In terms of industrial examples there is no knowledge of the multi-effect *prefractionator* arrangement being used. There are, nevertheless, examples of other multi-effect arrangements in use. Examples in literature includes a binary multi-effect distillation described by O'Brien (1976), the feed-split arrangement presented by Gross et al. (1998) and the forward-integrated indirect split arrangement (ISF) for the methanol-water separation as described by Larsson and Skogestad (1999).

In this revamp case study we investigate if the multi-effect prefractionator arrangement can be implemented in an industrial context. Three separation tasks from a gas processing facility are investigated, in order to see if an integrated prefractionator arrangement can be suitable for an industrial application.

The methods presented in Chapters 3 and 4 are applied in order to screen the three cases based on minimum vapour flowrate criteria. Also the required pressure levels for multi-effect integration was calculated for each case. From these preliminary calculations a candidate for integration was identified for which further rigorous simulations were carried out to compare energy consumption, pressure and temperature levels for the new multi-effect system with that of the existing distillation arrangement. Finally an exergy analysis was made in order to determine the efficiencies of the different arrangements.

6.2.   Systems Studied

We consider the separation of a light hydrocarbon mixture into five products: ethane, propane, i-butane, n-butane and gasoline (pentane). The four two-product columns presently used for this task are denoted I, II, III and IV in Figure 6.1. The present pressure and temperature levels are indicated in the figure. An example of a multi-effect integration of columns III and IV is shown in Figure 6.2. This is only one possibility as there are three adjacent pairs of columns that are candidates for being replaced by multi-effect prefractionator arrangements in a possible revamp of the plant:

Case 1.   Columns I and II for the separation of ethane, propane and butane (+ higher).

Case 2.   Columns II and III for the separation of propane, butane and gasoline.

Case 3.   Columns III and IV for the separation of i- butane, n-butane and gasoline.

The feed data for all three cases are given in Table 6.1

Figure 6.1. Existing column arrangement.
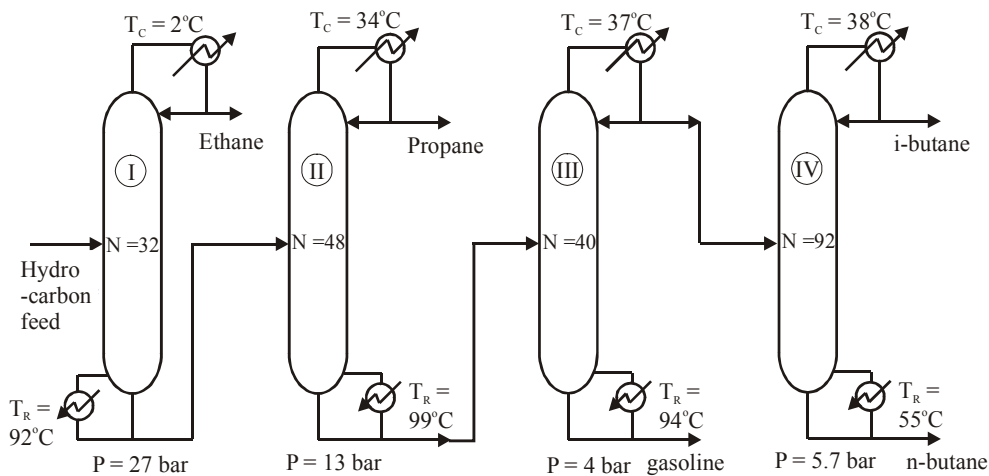
Figure 6.2. Multi-effect integration of two columns (Case 3).

a) *Existing indirect split (IS) arrangement*   b) *Multi-effect prefractionator (PF) arrangement with forward integration*
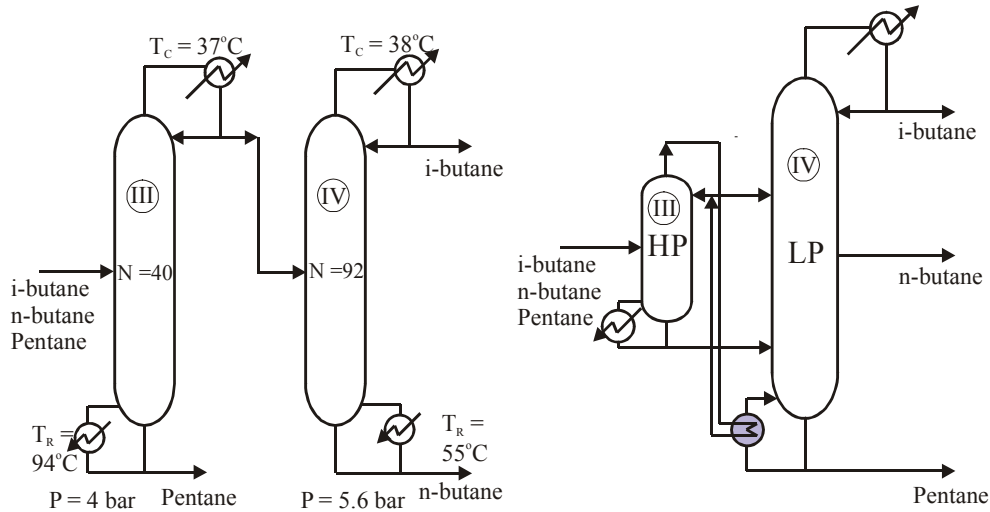
Table 6.1. Feed, product and relative volatility data.

	Case 1	Case 2	Case 3	Product composition
Ethane ($\alpha = 10.0$)	0.3742 A	0.005	1.44e-12	0.9142
Propane ($\alpha = 7.98$)	0.3697 B	0.6212 A	0.005	0.9870
i-butane ($\alpha = 3.99$)	0.0491	0.0827	0.2137 A	0.9723
n-butane ($\alpha = 3.0$)	0.1122 C	0.1889 B	0.5070 B	0.9881
n-pentane ($\alpha = 1.0$)	0.0607	0.1022 C	0.2742 C	0.8414
Feed flowrate (kmol/h)	3228.01	1917.14	714.12	-
Temperature (^{o}C)	49.05	59.42	50.89	-

6.3. Minimum Vapour Flowrate – Shortcut Calculations

The first task is to determine if any of the three cases are suitable for integration using multi-effect distillation. The shortcut methods presented in Chapter 3 and Chapter 4 have been used to calculate the minimum vapour flow requirement for each of the separations. Simple flash calculations have also been made to determine the required pressure levels.

For simplicity the mixtures have been taken as ternary mixtures for the shortcut calculations. Hydrocarbons of C5 or higher have therefore been assumed to be n-pentane and the small presence of CO_2 in the feed to Column (I) has been neglected. Further, in the shortcut simulations for Case 1 the small amounts of i-butane and n-pentane have been lumped together as n-butane. For Case 2 the i-butane and n-butane have been considered to be n-butane. The ternary feeds to each case are marked in Table 6.1 as A, B and C. The specifications of the five products are given in the right hand column. Also given is the relative volatility of each component, relative to the heaviest component consid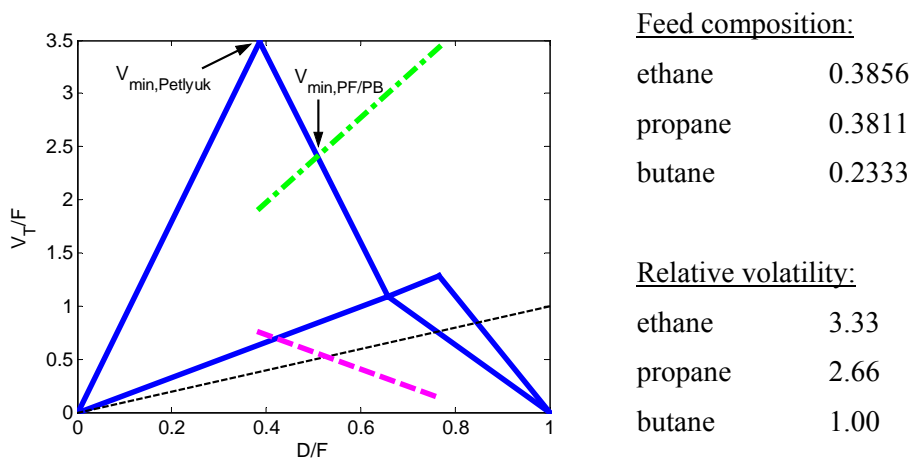ered; n-pentane. These relative volatilities are found from literature (Smith, 1995 and Kister, 1992). For the shortcut analysis the relative volatilities have been assumed to be independent of pressure, but this assumption is relaxed later when studying the most promising alternative in more detail. In addition the analysis assumes sharp splits, liquid feeds, constant molar flows.

The V_{min}-diagram gives the minimum energy requirements (in terms of vapour flow V) as a function of the distillate fraction $\eta = D/F$ for the first column in a two-column sequence. Chapter 4 shows how to draw the V_{min}-diagram and how to use it to compare the multi-effect prefractionator arrangement with other multi-effect systems and the existing non-integrated direct split (Case 1 and 2) and indirect split (Case 3) arrangements. We can also compare the V_{min} to that of the Petlyuk arrangement, which is the best of the adiabatic systems (Halvorsen, 2001).

Using the relative volatility data and the simplified feed compositions in Table 6.1 minimum vapour flow (V_{min}) diagrams for each of the three cases were plotted in Figure 6.3,

Figure 6.4, and Figure 6.5. For clarity the feed composition and relative volatility used are given in each of the diagrams. The results for some other sequences are summarised in Table 6.2.

Figure 6.3. V_{min}-diagram for Case 1: (α independent of pressure).

Feed composition:

ethane	0.3856
propane	0.3811
butane	0.2333

Relative volatility:

ethane	3.33
propane	2.66
butane	1.00

Saving of PB compared with DS: 43.3 %

Figure 6.4. V_{min}-diagram for Case 2 (α independent of pressure).
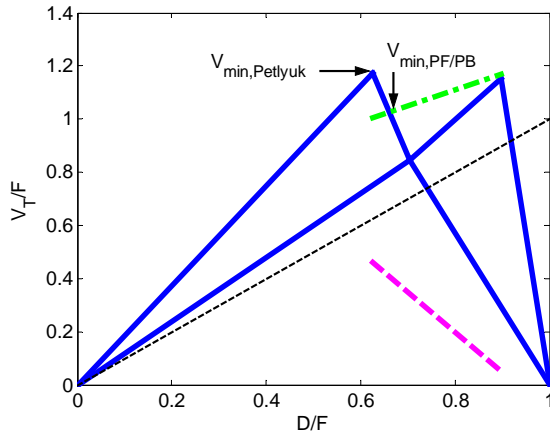
Feed composition:

propane	0.6262
n-butane	0.2716
n-pentane	0.1022

Relative volatility:

propane	7.98
n-butane	3.00
n-pentane	1.00

Saving of PF compared with DS: 37.2 %

Figure 6.5. V_{min}-diagram for Case 3 (α independent of pressure).
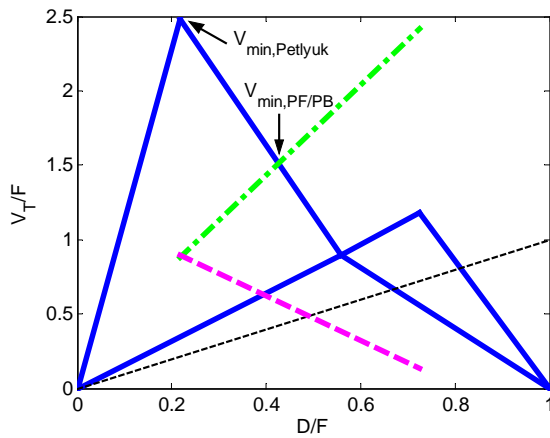
Feed composition:

i-butane	0.2188
n-butane	0.5070
n-pentane	0.2742

Relative volatility:

i-butane	3.99
n-butane	3.00
n-pentane	1.00

Saving of PF compared with IS: 55.3 %

The following savings are found for the integrated prefractionator arrangement, compared with the existing arrangement:

Case 1 (Figure 6.3)   43.3 % savings

Case 2 (

Figure 6.4)   37.2 % savings

Case 3 (Figure 6.5)   55.3 % savings

We see that Case 3 has the highest savings. For case 3 the other multi-effect arrangements also give relative high savings of 28 and 26 % for the indirect and direct multi-effect arrangements, respectively.

From the V_{min}-diagram we can also find how the prefractionator column should be operated in order to achieve the highest energy savings. The value of $\eta_{optimum}$ corresponds to $V_{min,PF/PB}$. The value of $\eta_{optimum}$ can be used as a starting point for further rigorous simulations.

As shown in Chapter 4 the V_{min}-diagrams also indicate how the columns are unbalanced. From Figure 6.3,

Figure 6.4 and Figure 6.5 it can be seen that for all cases the lower section of the main column has "excess" vapour. For the purpose of a retrofit we may then consider using a relatively short section below the sidestream. This would leave more stages for the more difficult separation in the upper section above the sidestream. Alternatively, if the number of stages in the column is sufficient the excess vapour could be utilised by taking out the sidestream as vapour, which can then be used to provide heat elsewhere in the process (if necessary). This could lead to a reduction of the energy consumption of the overall plant.

Table 6.2. Minimum vapour flowrate and percentage improvement for different integrated arrangements (α independent of pressure).

	Case 1		Case 2		Case 3	
	Vmin/F	%	Vmin/F	%	Vmin/F	%
DS	4.23	0.0	1.63	0.0	3.38	-0.2
IS	4.33	-2.2	1.69	-3.76	3.38	0.0
DSF/DSB	3.48	17.7	1.17	28.1	2.49	26.4
ISF/ISB	3.43	19.0	1.16	28.5	2.42	28.4
Petlyuk	3.48	17.7	1.17	28.1	2.49	26.4
PF/PB	2.40	**43.3**	1.02	**37.2**	1.51	**55.3**

6.3.1.   Column Pressure Levels

The pressure levels in the columns were found from flash calculations using the recoveries found from the V_{min}-diagrams. For integrated prefractionator arrangements there are, as mentioned in previous Chapters, two possible types of integration; a forward integration (PF) and a backward integration (PB). In Table 6.3 we have calculated the pressure levels required in both the PF and the PB arrangements.

For Case 2 and Case 3 the temperature of the overhead condenser was assumed to $20^{\circ}C$, so that the existing cooling liquid (seawater) can be used. For Case 1 in the original flowsheet a refrigerant is used in the condenser of the de-ethaniser. For this case the temperature corresponding to using the same coolant has been used for both the PF and PB integrated cases.

Further, a $10^{\circ}C$ temperature difference was assumed between the distillate and bottom stream from the integrated reboiler/condenser and sharp products from the main column was assumed. The concentrations for the prefractionator were found from the optimum product split, η, in Figures 6.4-6.6. The calculated pressure levels for both forward and backward integration are summarised in Table 6.3. Note that for these shortcut calculations the pressure drops in the columns have been neglected.

It can be seen from Table 6.3 that to integrate the columns for Case 1 and Case 2 in a multi-effect fashion would required very high pressure levels. Due to this and the fact that Case 3 has the highest energy savings, these cases were eliminated from further investigation. The rest of the study focuses on Case 3, which, in terms of energy savings and preliminary pressure levels shows potentials for energy integration.

In terms of pressure levels the results in Table 6.3 indicate that the PB arrangement might be a more suitable arrangement for this separation task than the PF arrangement. However, as mentioned in Section 5.3 there are indications that the forward-integrated arrangement is easier to control (Bildea and Dimian, 1999, Emtir et al. 2003). Also, we believe that the forward-integrated arrangement would be easier in terms of start-up. As the heat input is to the first column this can be started up first, e.g. by using a total reflux approach, then when the first column is up and running it will be relatively easy to start the second up. The backward-integrated arrangement would be more difficult.

In light of the control issues it was decided to focus the further study on Case 3 in terms of the forward-integrated prefractionator arrangement. The integrated arrangement for Case 3 is shown on the right hand side in Figure 6.2.

Table 6.3. Pressure levels in integrated columns (from flash calculations). Pressures in bar.

|	Case 1		Case 2		Case 3	
	PF	PB	PF	PB	PF	PB
Prefractionator	153.0	19.2	8.32	8.01	14.0	2.55
Main column	25.1	104.6	66.0	35.37	3.0	6.74

6.4.   Rigorous Column Simulations

After identifying Case 3 as a suitable candidate for integration, further investigations were made using a commercial rigorous simulations program (HYSYS).

The shortcut calculations indicate that the integrated prefractionator arrangement should give approximately 55 % improvement in energy consumption, compared with the non-integrated indirect split (IS) arrangement. In addition to the integrated prefractionator arrangement another multi-effect arrangement has been considered. The second best multi-effect arrangement, according to Table 6.2, is a multi-effect integrated indirect split system. The improvement for this system should be around 28 % compared with the non-integrated arrangement. The forward-integrated indirect split (ISF) system (see Figure 6.6) was selected based on the same arguments that were made when selecting the PF system.

For the simulations the pressure levels were adjusted so that a $10^{\circ}C$ temperature difference was achieved for the integrated reboiler/condenser. This gave a pressure of 19.5 bar in the top of the HP column and 4.17 bar in the LP column for the PF-prefractionator arrangement. The deviation from pressure levels in Table 6.3 is due to impure products. For the multi-effect indirect split arrangement in Figure 6.6 the pressure level is lower with 8 bar in the HP column and 5.2 bar in the LP column.

The energy consumption's for the original base case (IS), the integrated prefractionator (PF) and the integrated indirect split system (ISF) have been found from rigorous simulations. The number of stages in the columns was taken to be the same as the existing number of stages (see Figure 6.5).

Figure 6.6. Multi-effect indirect split arrangement with forward integration (ISF).
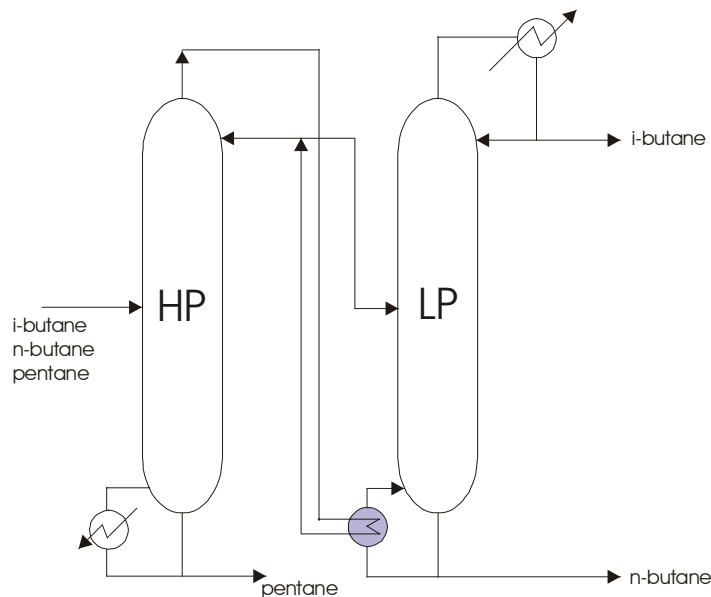
From the results presented in Table 6.4, it can be seen that for the multi-effect prefractionator arrangement (PF) there is an improvement in energy consumption of about 28.6 %, compared with the base case. The multi-effect indirect split (ISF) arrangement has an even higher energy saving, at about 42.7 %. Interestingly, the energy savings of the ISF arrangement are higher than the savings indicated by the shortcut calculations in Table 6.2. This is because in the shortcut equations we have assumed sharp splits for simplicity, whereas for the rigorous simulations the actual product compositions have been used.

On the other hand for the prefractionator arrangement (PF) the energy savings of 28.6 % are significantly lower than the 55.3 % indicated by the shortcut calculations in Table 6.2. However, the shortcut calculations give the minimum energy for infinite number of stages. To confirm that the changes in energy savings for the PF arrangements is due to the number of stages a comparison was made for infinite number of stages (in practice a very large number of stages were used). The results are shown in Table 6.5. From this it can be seen that for infinite number of stages the integrated prefractionator arrangement has a 56.9 % improvement compared with the base case, whereas the integrated indirect split arrangement has a 43.7 % improvement. By comparing Tables 6.4 and 6.4 we see that the ISF arrangement shows little improvement with the increased number of stages, indicating that the existing number of stages already is sufficient for the separation and it is close to the minimum vapour flow target. The PF arrangement shows significant improvement as the number of stages is increased. The results for the PF at infinite number of stages are in good agreement with the V_{min} calculated from the shortcut equations (Table 6.2).

Table 6.4. Rigorous calculations of energy consumption for Case 3 using existing number of stages.

	Base case	ISF	PF
Q_{B1} (MW)	3.853	7.183	8.951
Q_{C1} (MW)	5.464	8.359	8.267
Q_{B2} (MW)	8.682	8.359	8.267
Q_{C2} (MW)	8.735	8.678	10.700
$Q_{B,total}$ (MW)	**12.535**	**7.183**	**8.951**
% Energy Improvement	-	**42.7**	**28.6**

Table 6.5. Rigorous calculation of energy consumption for Case 3 using infinite number of stages.

	Base case	ISF	PF
Q_{B1} (MW)	3.962	6.929	5.309
Q_{C1} (MW)	5.564	8.097	4.608
Q_{B2} (MW)	8.349	8.097	4.608
Q_{C2} (MW)	8.403	8.419	7.068
$Q_{B,total}$ (MW)	**12.311**	**6.929**	**5.309**
% Energy Improvement	**-**	**43.7**	**56.9**

The optimum energy consumption for PF in Table 6.4 and Table 6.5 was found by plotting the recovery of the middle component from the prefractionator against the duty in the bottom of the prefractionator, while keeping the condensing duty from the HP column equal to the boilup duty of the LP column. This is shown in Figure 6.7 where the vapour flowrate required in the prefractionator is plotted against the recovery of the middle component. The diagram is plotted for the case with actual number of stages and the case with infinite number of stages. Also shown is the minimum vapour flowrate calculated from the shortcut equations.

Figure 6.7. Comparing V_{min} from HYSYS using actual number of stages and infinite number of stages with V_{min} from shortcut equations at infinite number of stages.
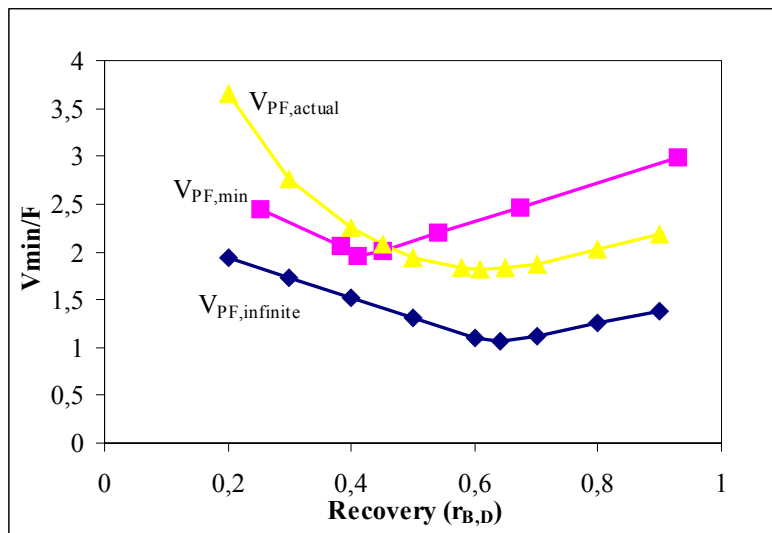
6.5. Number of Stages

From the above results it is clear that the main column of the prefractionator arrangement requires more stages than a conventional column to achieve the potential energy savings. This is seen in Table 6.4 as the ISF arrangement has higher energy savings than the PF arrangement with the existing number of stages.

In a distillation column there is a trade off between the number of stages and the energy usage (vapour/reflux). This trade-off (see Figure 6.8) is illustrated in many textbooks on distillation (e.g. Kister, 1992) and applies to conventional as well as to integrated arrangements. A more careful analysis reveals that the actual V approaches V_{min} for N approximately $2xN_{min}$ or larger. Here N_{min} is the infinite number of stages corresponding to infinite vapour flow, whereas V_{min} is the minimum vapour flow corresponding to infinite number of stages.

Figure 6.8. Trade-off between energy usage(V) and number of stages (N).
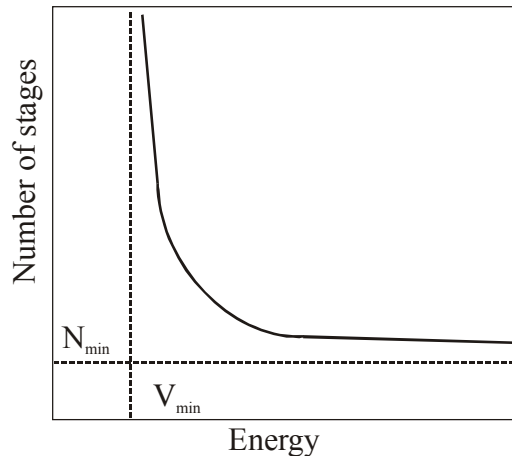
Typically, if we were to operate a column at $2xN_{min}$ (a typical rule-of-thumb for design) then we are already within +20 % of V_{min}. At $3xN_{min}$ we are within about +2 % of V_{min} and at $4xN_{min}$ we are within +0.2 % of V_{min}. The measure of V_{min} is therefore a good target for comparing energy as we are usually operating close to it. However, we can not generally expect that a prefractionator arrangement (PF) will have enough stages if we base it on an existing conventional arrangement (DS or IS) as we did here. This follows since the existing column, which is designed for a 2-product separation, is now required to do a 3-product separation task. On the other hand, the number of stages will be sufficient for the ISF arrangement as illustrated.

The conclusion is that a revamp of a conventional arrangement (DS or IS) to a prefractionator arrangement (PF or PB) should be accompanied by an increase in the number of stages in the main column, for example by changing the column internals or packing.

6.6.   Comparison in Terms of Thermodynamic Efficiency

In addition to looking at the first law effects of the multi-effect distillation, where the *quantity* of energy is considered, it is also interesting to look at second law effects, where the *quality* of energy is determined. The latter is particularly interesting in a plant setting.

When integrating distillation columns by multi-effect we increase the pressure levels in order to integrate a condenser of one column with the reboiler of another column. This increase in pressure results in an increase of the temperature span between where the heat is supplied (reboiler) and where it is removed (condenser). This is illustrated in Figure 6.9 where the temperature span between the reboilers and condensers is plotted against the required heat duties. This is, in terms of energy, the drawback of multi-effect integration.

As we can see from Figure 6.9 the heat in the PF arrangement has to be supplied at a much higher temperature than the heat for the base case. The result of this is that if the required hot utility is supplied at the exact required temperature (+ temperature difference to drive the heat transfer) then in the case of the PF arrangement we would degrade a higher quality heat than in the other cases. The effect of this is seen clearly when comparing the *thermodynamic efficiency* of the three arrangements.

Figure 6.9. Temperature/duty plot for infinite number of stages.
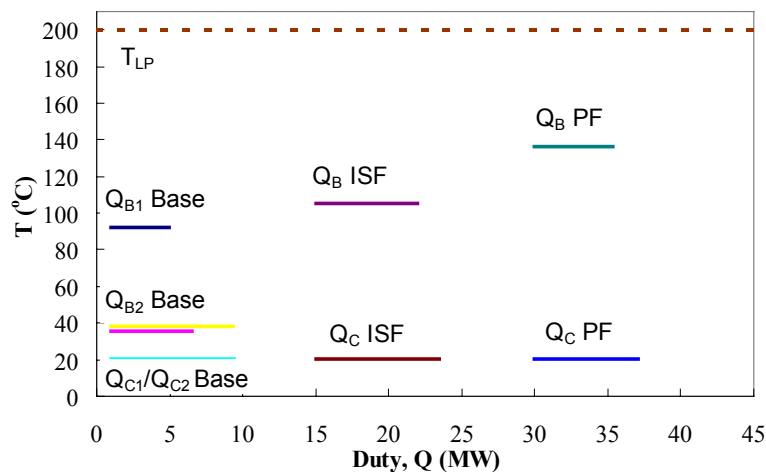
To find the thermodynamic efficiencies we calculate the *ideal minimal work* and the *total added work* for the three different distillation cases.

The ideal (reversible) minimum work for the surroundings at constant T_o is defined as:

$$W_s^{id} \triangleq \Delta H - T_o \Delta S \qquad (6.1)$$

The enthalpy, H and entropy, S were found from the simulation for all streams and the ideal work was calculated. The "actual" work W_s for any ideally integrated distillation column is obtained as the work needed for heat pumps to take the various heats from temperature T_o to the actual temperature:

$$W_s = \sum Q_{R,i} \left(1 - \frac{T_o}{T_{R,i}}\right) + \sum Q_{C,i} \left(1 - \frac{T_o}{T_{C,i}}\right) \qquad (6.2)$$

where $T_{R,i}$ is the temperature of reboiler i and $T_{C,i}$ is the temperature level in condenser i. The thermodynamic efficiency, η_{eff}, is then found from:

$$\eta_{eff} = \frac{W_s^{id}}{\tilde{W}_s} \qquad (6.3)$$

where W_s tilde is the total added work (including any other work, like pump work or compression work).

The thermodynamic efficiency calculated for the three cases are shown in Table 6.6. As expected, due to the larger temperature span in the PF case this arrangement has the lowest efficiency. The base case has the highest efficiency while the ISF case lies between the two.

So, does this mean that the PF arrangement is not a good option ? No, because the exergy analysis assume "ideal integration" with the background process. In an actual setting, for example the actual plant used in this case study, a comparison based on <u>energy</u> is much more relevant. This follows because the utility levels are such that the same hot and cold utility will be used in all cases.

Table 6.6. Thermodynamic efficiencies using ideal utility temperature levels.

	Base case	ISF	PF
Actual number of stages	21.2 %	15.5 %	8.4 %
Infinite number of stages	22.9 %	16.5 %	14.0 %

6.7. Discussion of Some Practical Issues

As indicated by the results in Section 6.4 using the existing number of stages for the PF system is not sufficient for it to be close to the V_{min} target. By increasing the number of stages the energy consumption can be reduced so that it is closer to the minimum. There are limitations on increasing the number of stages, however, in terms of height of the column. If a prefractionator arrangement requires a large number of stages this may mean that the column(s) would have to be divided in

two. Alternatively, it may be possible to use high efficiency packing. Both of these options would result in higher capital costs.

The issue of capital cost has not been discussed here. Instead the focus is on the minimum vapour flowrate requirement as a target (indirectly a measure of operating costs). This target is independent of variations of energy prices and other cost factors. However, when looking at a practical design it is necessary to look at both the capital and operating costs. This important issue of *total annual cost* has been discussed for multi-effect arrangements by Emtir et al. (2001), where the savings in total annual costs are compared for high and low energy prices. They found that for the three feed cases analysed the integrated prefractionator columns (PF/PB) gave high savings. For the case of high amount of middle component B in the feed the PF/PB structures gave the highest savings.

Another issue that has not been discussed, except for the exergy in Table 6.6, is the integration of the columns with the rest of the process. Using pinch methods the overall process, including the distillation columns can be integrated to give the lowest overall energy consumption. However, in practice this integration with distillation columns may be difficult as integrating a column with the rest of the plant may lead to problems in terms of operation and control. To look at the distillation columns as a separate entity may be easier in practice than integrating with the rest of the plant in a heat exchanger network.

Other issues that have to be considered when integrating the columns in a multi-effect fashion are the controllability and operability. Integration may also lead to a loss of flexibility, e.g. in distillation of different products using the same columns.

6.8.   Conclusion

Four industrial distillation columns in sequence have been studied to see if any two were suitable for integration using a multi-effect prefractionator. The methods presented in Chapter 3 and Chapter 4 were used to screen three integrated cases to find the case most suitable for integration, in terms of energy consumption. V_{min}-diagrams were presented for all three cases. From the shortcut comparisons it was found that the multi-effect prefractionator arrangement would have the highest energy savings for all cases.

Based on the shortcut analysis the best case was selected for further analysis using a commercial rigorous simulation program (HYSYS). The rigorous simulations were carried out for the original base case, a multi-effect indirect split arrangement (ISF) and a multi-effect prefractionator arrangement. Using the number of stages in the existing columns it was found that the ISF arrangement had the highest energy savings (43 %). It was concluded that the PF arrangement required more stages in order to get closer to the minimum vapour flow target (V_{min}). An important point however, is that the assumption of V_{min} at infinite number of stages is not an unrealistic target since the actual value of V is close to V_{min} if we are allowed to add stages. At infinite number of stages the results from the rigorous simulations

showed that the PF arrangement was the best with savings of 57% compared with the IS arrangement.

A comparison of the base case, ISF and PF arrangement was also made in terms of thermodynamic efficiency. In the ideal case, where the temperature levels of the reboilers and condensers were used in the analysis it was found, as expected, that the efficiency of the integrated prefractionator arrangement is lower than the non-integrated case. For an ideal integration it is therefore not good to consider the integrated prefractionator arrangements. However, when looking at the practical case where the hot utility is supplied at a set temperature level then the energy consumption is the governing factor. The integrated prefractionator arrangements are then high energy saving solutions that should be considered.

The main conclusion from this study is that a multi-effect arrangement can be a good option for an actual industrial distillation, especially in terms of energy consumption. In practice for this study, due to the limitations of an already existing plant (i.e. number of stages), if a retrofit were to be carried out then the recommendations would be to use the forward-integrated indirect split arrangement (ISF). If however, a new plant were to be built then the integrated prefractionator arrangement (PF) would be recommended as it has the highest potential for energy savings. Rigorous simulations studying the control and dynamic properties would naturally have to be considered in detail.

6.9.   References

Bildea, C.S., Dimian, A.C., 1999, Interaction between design and control of a heat-integrated distillation system with prefractionator, *Trans IChemE*, Vol. 77, Part A, 597-608.

Cheng, H. C., Luyben, W., 'Heat-integrated distillation columns for ternary separations', *Ind. Eng. Chem. Process Des. Dev.*, 1985, 24, pp. 707-713.

Emtir, M., Rév, E., Fonyó, Z., 2003, 'Economic and controllability investigation and comparison of energy integrated distillation schemes', *Chem. Biochem. Eng. Q.*, 17 (1), 31-42.

Gross, F., Baumann, E., Geser, A., Rippin, D.W.T., Lang, L., 'Modelling, simulation and controllability analysis of an industrial heat-integrated distillation process', *Computers and Chemical Engineering.*, 1998, Vol. 22, No.1-2, 223-237.

Halvorsen, I.J., 'Minimum energy requirements in complex distillation arrangements', Dr.ing. Thesis, NTNU, 2001.

Kister, H.Z., 'Distillation Design', McGraw-Hill Book Co, 1992.

Larsson, T., Skogestad, S., Control of an industrial heat integrated distillation column, Presented at the AIChE Annual Meeting, Dallas, November, 1999.

O'Brien, N.G., 'Reducing column steam consumption', *CEP,* July 1976, pp. 65-67.

Smith, R., 'Chemical process design', McGraw-Hill Book Co, 1995.

Chapter 7. Concluding Remarks

7.1. General Conclusions

An arrangement with a prefractionator column and a main column with a sidestream integrated in a multi-effect fashion has been studied. Pressure is used to integrate the two columns by raising the pressure in one column so that the condensing vapours at the top of this column is hot enough to be used to boil the second column. External heat is thus supplied only in the high-pressure column and condensation only in the low-pressure column. Such an arrangement has not been extensively studied in the literature, especially on the issues of control.

In this thesis the focus of the work has been on the *energy savings* of multi-effect systems, in terms of both design and control issues. A number of questions that have been central to this thesis are:

- Can the multi-effect prefractionator arrangement easily be screened against other heat integrated arrangements and how does it compare ?

- Is the multi-effect prefractionator arrangement a good energy saving scheme ?

- How can the energy savings be achieved during operation when there are disturbances and how can we operate the multi-effect arrangement to achieve the promised energy savings ?

- Is it possible to use the multi-effect prefractionator arrangement for a typical industrial application ?

The screening of multi-effect integrated arrangements has been carried out based on *minimum vapour flow* at infinite number of stages. The calculation of V_{min} assumes infinite number of stages, however, this is not in itself an important limitation since the actual value of V is usually close to V_{min}. The assumption of V_{min} is not an unrealistic target since the actual value of V is close to V_{min} if we are allowed to add stages. Thus, V_{min} provides a good target for comparing energy usage for alternative arrangements

In Chapter 3 it has been shown how using simple shortcut methods can be used to calculate the minimum vapour flowrate for the conventional non-integrated arrangements and for multi-effect integrated arrangements. The basis of the equations is infinite number of stages, constant molar flows, constant relative volatility and sharp product splits.

A comparison of energy savings for different separations (relative volatilities) and feed compositions using the shortcut approach showed that the integrated prefractionator arrangement is expected to have the highest savings. When compared with the best of the non-integrated direct or indirect split system the savings were in the range of 50-70 % with the highest energy savings for some of the cases exceeding 70 %. In terms of improvement compared with the Petlyuk

arrangement, which is the best non heat-integrated arrangement, the improvement ranged from 5-50 % depending on the difficulty of separation and feed composition. The results thus showed that the multi-effect prefractionator system is a good energy saving scheme and that it should be considered when designing a separation process.

Chapter 4 presents some of the main results and contributions of this thesis. The energy requirement of multi-effect arrangements is visualised in a V_{min}-diagram. The diagram can be used to analyse and understand the behaviour of the multi-effect integrated prefractionator arrangement. The shape of the diagram confirms the results from the shortcut equations; that the integrated prefractionator arrangement has the lowest energy requirement of the multi-effect arrangements considered (at infinite number of stages and assuming relative volatility independent of pressure). The main results from this chapter are summarised in Figure 4.4.

If the multi-effect prefractionator arrangement has been identified as a good candidate for a specific separation then further rigorous simulations has to be made to verify that the system is suitable. One thing that has to be considered is the control, where we have to make sure that the system is controllable and that the promised energy savings can be obtained. It is very important that the energy savings of heat-integrated arrangements are achieved as these systems often are more complex, involves higher capital costs and can require a more valuable utility to be used. It is therefore important the energy savings (and thus operational savings) are actually achieved, otherwise we might end up using more energy than with the simpler system.

In Chapter 5 we have shown that selecting the right controlled variables for the system can keep the system close to its optimum energy savings. A systematic and general method (*self-optimising control*) is used for screening different control variables showing that it is important to consider what to control in a system, and not only how to control it. Controlling one variable instead of another can lead to higher losses (in terms of the objective, *energy*) during operation. Based on the self-optimising control method a set of controlled variables were identified and a control structure suggested. Dynamic simulations made to verify the control structure showed that the system is controllable, but that the sidestream and bottom stream composition responses are slow and that the system is sensible to disturbances. For practical implementations it is recommended to install a feed tank to reduce the disturbances to the integrated arrangement.

Finally, in Chapter 6 an industrial separation process has been studied to see if the multi-effect prefractionator arrangement can be used for an industrial case. The results from rigorous simulations for the case studied indicated savings of around 29 % at the existing number of stages and 57 % at infinite number of stages. It was shown that the multi-effect arrangements can be applied to an industrial example and that benefits can be in terms of both energy consumption and thermodynamic efficiency (the latter in terms of *actual* utility temperature levels).

7.2.   Recommendations for Further Work

As discussed in Chapter 6 there are a number of practical issues concerned with the multi-effect prefractionator column that could be interesting to look at in more detail. A study into the total annual costs of such integrated arrangements, especially maybe a comparison between the integrated prefractionator arrangement and the *divided wall column* (Petlyuk column in one shell) would be one such topic. In addition to the energy savings the divided wall column has been reported to have savings of around 30 % in capital costs as well (Lestak, 1997).

The multi-effect prefractionator arrangement studied in Chapter 5 this thesis is the *forward-integrated* arrangement (PF) where the prefractionator is at a high pressure and the main column is at a low pressure. The other prefractionator configuration, where the prefractionator is at a low pressure and the main column is at a high pressure, the *backward-integrated* arrangement (PB), was not been studied. The PF arrangement was selected on the basis that previous authors had found that it was easier to control a forward-integrated arrangement than a backward integrated arrangement.

Further study of the PF arrangement is recommended to verify whether or not the system is more difficult to control than the PF configuration. Self-optimisation studies should also be made to see which of the two systems have the highest loss and if controlling the product concentrations is easier than for the PF configuration (as discussed in Chapter 5).

For the PF arrangement further work should carried out on testing other control variables and investigation into what happens when different constraints are active.

In terms of control, a study could be made into the controllability, especially on the pairing of the controlled variables found from the analysis in Chapter 5 with manipulated variables. Practical measures for improving control, for example the installation of a feed tank, could also be investigated in more detail.

Another interesting issue would be to examine at the start-up of the two different PF and PB arrangements, and whether or not one of them is more easy or difficult to start up. As mentioned briefly in Chapter 6 (but not verified) it is believed that the forward-integrated arrangement is easier to start up. Also, to look at start-up in terms of optimisation of time and energy consumption might be another interesting topic. These start-up issues could be deciding factors when determining which integrated prefractionator arrangement to choose (PF or PB).

Finally, it may be interesting to look into other control schemes for the multi-effect prefractionator arrangements. The self-optimising control structure could be implemented using a multi-variable control scheme, such as model predictive control (MPC). It may then be possible to use the multi-effect prefractionator arrangement for a system with larger disturbances.

7.3. References

Lestak, F., Collins, C., 'Advances in distillation saves', Chemical Engineering, July 1997, p. 72-76

Appendix A. Modelling and Simulation

This section contains a description of the dynamic model and the optimisation model used in Chapter 5.

Dynamic Modelling of Distillation Columns

Fundamentals of Rigorous Distillation Models

A rigorous dynamic model for a distillation column can be described as a staged model with mass and energy balances at each stage that includes relationships for the liquid flow dynamics and the pressure dynamics.

On a general distillation stage i (see Figure A.1) the differential equations for the model can be expressed for:

i) the overall mass balance (flow dynamics):

$$\frac{dM_i}{dt} = L_{i+1} + V_{i-1} - L_i - V_i + F_i - S_i \tag{A.1}$$

where M_i is the liquid holdup on stage i, L_i is the liquid flow from stage i and V_i is the vapour flow leaving stage i, F_i is any feed entering stage i and S_i is any side stream from stage i.

ii) the component mass balance (of component j):

$$\frac{dM_i x_{i,j}}{dt} = L_{i+1} x_{i+1,j} + V_{i-1} y_{i-1,j} - L_i x_{i,j} - V_i y_{i,j} + F_i z_i - S_i x_i \tag{A.2}$$

where $x_{i,j}$ and $y_{i,j}$ is the liquid and vapour composition of component j on stage i and z_i is the composition of component j in the feed stream (this may be two-phase).

iii) the energy balance:

$$\frac{dU_i}{dt} = L_{i+1} h_{L,i+1} + V_{i-1} h_{V,i-1} - L_i h_{L,i} - V_i h_{V,i} + F_i h_f - S_i h_i + q_i \tag{A.3}$$

Here U_i is the internal energy on stage i, $h_{L,i}$ and $h_{V,i}$ is the liquid and vapour specific enthalpy on stage i, h_f is the specific enthalpy of the feed (vapour + liquid) and q_i is any heat flowing into or out from stage i.

In addition to the balances the rigorous model includes relationships for the liquid flow dynamics, vapour flow and equations for the vapour/liquid equilibrium (VLE) between the phases on each stage.

Figure A.1. A general distillation stage (i).
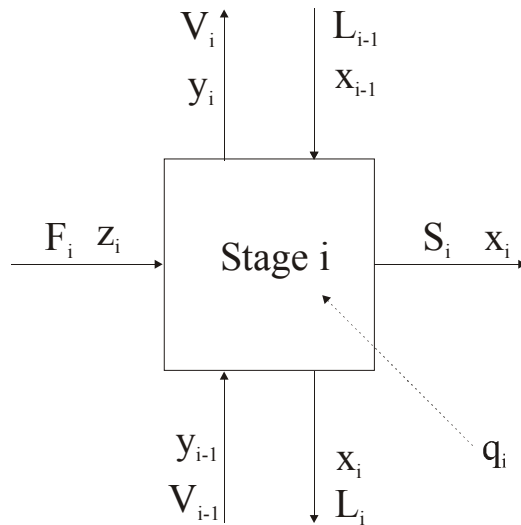
There are no references to be found on dynamic distillation computer programs which solves the dynamic model in a rigorous fashion without making model simplifications (Skogestad, 1997).

A number of *simplified assumptions* are therefore applied to the rigorous model in order to make it easier to solve. The most common model assumptions include simplifications to the vapour dynamics, the energy balance and the liquid flow dynamics (Skogestad, 1997).

For the *vapour flow dynamics* it is common to neglect the vapour holdup on each stage. The assumption is valid when the vapour phase component holdup can be neglected compared to that in the liquid phase. Neglecting the vapour holdup may be a poor assumption for volatile components, columns with high pressure and for cryogenic separations where the liquid density is low. Choe and Luyben (1987) concluded that vapour holdup should be included in models of columns where the vapour density is significant compared to the liquid density and that this typically corresponds to operation at pressures greater than 5-10 bar.

Another common assumption is to fix the *pressure* and neglect vapour holdup or to fix pressure and include vapour holdup. The fixed pressure assumption is common and is often justified as pressure is tightly controlled (Skogestad, 1997). Work by Choe and Luyben (1987) showed that assuming a fixed pressure is valid for moderate to high-pressure systems where the relative changes in pressures are small. However it should be included in vacuum columns and in columns where floating pressure control can cause large changes in operating pressures.

Simplification to the *energy balance* includes neglecting changes in energy holdup ($dU_i/dt = 0$), neglecting changes in liquid enthalpy and assuming equal vapour flows up the column (constant molar flows). The first assumption is quite

commonly used, but should not be used in a rigorous model as the assumption is fundamentally wrong (Skogestad, 1997).

The *liquid dynamics* is commonly neglected. This corresponds to assuming that the system has constant liquid holdups and that $dM_i/dt = 0$. This should, however, not be used for control purposes.

Another simplification is to use *linearised liquid dynamics* where the liquid flow is expressed as:

$$\Delta L_i = \lambda \Delta V_{i-1} + \frac{1}{\tau_L} \Delta M_i \tag{A.4}$$

Here λ represent the initial effect of a change in vapour flow on liquid flow and τ_L is the hydraulic time constant. An alternative to the above equation for liquid flow is to use an expression like the Francis' Weir formula.

Dynamic Model Description for Chapter 5

The main assumptions behind the dynamic model used for the simulations in Chapter 5 are:

- Hold up in the gas phase has been neglected.

- Liquid flows are modelled using Francis weir formula.

- Gas flows are modelled using a valve type equation.

- Vapour pressure has been modelled using Antoine equation.

- Ideal gas phase (no activity coefficients used).

- Equilibrium between the vapour and liquid on each stage.

- No dynamics in the heat exchangers.

The multi-effect distillation columns are modelled using a "rigorous" model where the energy, material (overall) and component material balances are included. The balance equations on a stage i can be written:

Overall material balance:

$$\frac{d\left(M_{L,i} + M_{V,i}\right)}{dt} = L_{i+1} + V_{i-1} - L_i - V_i \tag{A.5}$$

Component material balance:

$$\frac{d\left(M_{L,i} x_{ij} + M_{V,i} y_{ij}\right)}{dt} = L_{i+1} x_{i+1,j} + V_{i-1} y_{i-1,j} - L_i x_{i,j} - V_i y_{i,j} \tag{A.6}$$

Energy balance:

$$\frac{d\left(M_{L,i}u_{L,i} + M_{V,i}u_{V,i}\right)}{dt} = L_{i+1}h_{L,i+1} + V_{i-1}h_{V,i-1} - L_i h_{L,i} - V_i h_{V,i} \quad (A.7)$$

Here $M_{L,i}$ and $M_{v,i}$ are the holdups in the liquid and vapour phase on stage *i*. Index *j* denotes component *j*. L and V are liquid and vapour flows, x and y are component fractions in the liquid and vapour phase and h_L and h_V are the liquid and vapour enthalpies. The internal energy is given in the liquid phase, $u_{L,i}$ and the vapour phase, $u_{V,i}$.

The holdup in the vapour phase has been neglected, so $M_{V,i} = 0$. This considerably simplifies the model and is usually a good assumption when the pressure is below 10 bar (Choe, Luyben, 1987). In the energy balance (Equation A.7) we have also used the approximation $h_{L,i} \approx u_{L,i}$, which holds for liquids (Skogestad, 1997). The energy balance can then be re-written as:

$$M_i \frac{dh_{L,i}}{dt} = \frac{d\left(M_{L,i}h_{L,i}\right)}{dt} - h_{L,i}\frac{d\left(M_{L,i}\right)}{dt} \quad (A.8)$$

substituting for $d(M_{L,i}h_{L,i})/dt$ from Equation (A.7) (assuming $u_{V,i} = 0$) and for $dM_{L,i}/dt$ from the material balance in Equation (A.5) gives:

$$= L_{i+1}h_{L,i+1} + V_{i-1}h_{V,i-1} - L_i h_{L,i} - V_i h_{V,i} - h_{L,i}\left(L_{i+1} + V_{i-1} - L_i - V_i\right) \quad (A.9)$$

The specific liquid enthalpy has been assumed to be a simple function of the specific heat capacity, C_p, where:

$$h_{L,i} = C_p\left(T - T_{ref}\right) \quad (A.10)$$

The specific vapour enthalpy has been assumed to be:

$$h_{V,i} = h_{L,i} + H_{vap} \quad (A.11)$$

where H_{vap} is the heat of vaporisation.

The energy balance has then been re-written in terms of temperature, giving the energy balance on stage *i* as:

$$M_i \frac{dT_i}{dt} = L_{i+1}\left(T_{i+1} - T_i\right) + V_{i-1}\left(T_{i-1} + \frac{H_{vap}}{C_p} - T_i\right) - V_i \frac{H_{vap}}{C_p} \quad (A.12)$$

The liquid streams have been modelled using Francis weir formula, where the liquid flowrate, L at stage i is given by:

$$L_i = k\left(M_i - M_{uw,i}\right)^{1.5} \quad (A.13)$$

where k is a constant, M_i is the holdup on stage i and $M_{uw,i}$ is the holdup under the weir on the tray. To simplify, $M_{uw,i}$ has been taken as half the nominal holdup on the stage. The constant, k, was calculated above and below feed and sidestream stages, using nominal liquid flowrates and holdups.

Ideal gas has been assumed for the mixture modelled in Chapter 5 and the vapour pressures, p_{sj}, for each component j at each stage in the column have been calculated from the Antoine equation:

$$\ln\left(p_{s,j}\right) = A - \frac{B}{C - T_i} \tag{A.14}$$

where A, B, and C are Antoine constants and T_i is the temperature on the stage. The total pressure at the stage has then been calculated from Raoult's law. The VLE relationship for component j between the composition, y_j, in the vapour phase and the composition, x_j, in the liquid phase is then:

$$y_j = \frac{p_{s,j}}{P} x_j \tag{A.15}$$

The vapour flow, V, on a stage *i* has been modelled using a valve type equation for the pressure drop from one stage to the next:

$$V_i = c\sqrt{P_{i-1}{}^2 + P_i^2} \tag{A.16}$$

The constant, c, has been calculated using data from a commercial simulatio (HYSYS) process when a reasonable pressure drop has been assumed.

For the integrated reboiler/condenser we have assumed a maximum area and have calculated the heat duty, Q from:

$$Q = UA\left(T_{D,HP} - T_{B,LP}\right) \tag{A.17}$$

where $T_{D,HP}$ is the temperature at the top of the HP column, $T_{B,LP}$ is the temperature in the bottom of the LP column and U is the overall heat transfer coefficient.

The following state variables for each of the two columns have been used:

- composition x_i on all N_T stages (molar fraction of light component);
- liquid holdups M_i on all N_T stages;
- temperatures T_i on all N_T stages (states for the energy balances)

The simulation starts by guessing an initial vector for the state variables and performing a simulation in order to obtain the steady state conditions. For each iteration the algebraic equations for pressure, vapour and liquid flows are solved and then the derivatives of composition, liquid holdup and temperature are calculated for each stage. Integration of the derivatives is carried out using the

ODE15s integrator in MATLAB. This integrator solves stiff differential equations and DAE's.

Optimisation Model

The model used for the optimisation in Chapter 5 is a steady state model. The balance equations for this model are:

Overall material balance:

$$L_{i+1} + V_{i-1} - L_i - V_i = 0 \tag{A.18}$$

Component material balance:

$$L_{i+1} x_{i+1,j} + V_{i-1} y_{i-1,j} - L_i x_{i,j} - V_i y_{i,j} = 0 \tag{A.19}$$

Energy balance:

$$L_{i+1} h_{L,i+1} + V_{i-1} h_{V,i-1} - L_i h_{L,i} - V_i h_{V,i} = 0 \tag{A.20}$$

The VLE-relationship used for the model is the same as for the dynamic model (Equation A.15) and the vapour pressures have been calculated by Antoine equation (Equation A.14).

The specific enthalpy of the liquid has been calculated using the same relationship as in the dynamic model (see Equation A.10), assuming a constant pressure heat capacity of the liquid. The specific enthalpy of the vapour has been calculated from:

$$h_{V,i} = H_{vap} + H_T \tag{A.21}$$

where H_{vap} is the heat of vaporisation at a reference temperature, T_{ref}, and H_T is the specific enthalpy at temperature T, found from:

$$H_T = \int_{T_{ref}}^{T} C_p dT \tag{A.22}$$

where C_p has been expressed as a power series.

References

Choe, Y.S., Luyben, W.L., (1987) "Rigorous dynamic models of distillation columns", Ind. Eng. Chem. Res., 26, 2158-2161.

Skogestad, S. (1997), "Dynamics and control of distillation columns – a critical survey", Modelling, Identification and Control, Vol.18, No. 3, 177-217.

Appendix B. Implementation of Optimal Operation for Heat Integrated Distillation Columns

Hilde K. Engelien, Truls Larsson and Sigurd Skogestad

Abstract

A multi-effect distillation where the condenser of a high-pressure column is integrated with the reboiler of a low-pressure column has been studied. The method of self-optimising control has been used to provide a systematic procedure for the selection of controlled variables, based on steady state economics. The system has 10 degrees of freedom at steady state. The heat integrated distillation system was optimised to find the nominal operating point. It was found that the constraints on the product composition, area in the combined reboiler/condenser, the purity constraint in the low-pressure column and the pressure in the low-pressure column are active constraints. For the remaining unconstrained variable it was found that a temperature in the low-pressure column has good self-optimising properties. The study also shows how there can be multiplicities in the objective function for certain variables in the system.

Introduction

Distillation is an energy consuming process that is used for about 95% of all fluid separation in the chemical industry and accounts for an estimated 3% of the world energy consumption (Hewitt et al., 1999). Heat integration of distillation columns, where the condenser of one column is coupled with the reboiler of another column, is used to reduce the energy consumption of distillation. Typically the reduction in energy consumption is 50%. It is very important that such heat-integrated columns are operated correctly so that the plant is operational and the energy savings are achieved. However, the task of identifying a suitable control structure for heat integrated distillation columns is not as straight forward as for a single column.

A system (see Figure B.1) is studied where the higher pressure in the first column allows the condensing heat from the top to be used to boil the second column. This is a *forward* integration, as both mass and heat are integrated in a forward

direction. Other multi-effect configurations are for example *dual feed* and *reverse integration* (Wankat, 1993).

A number of studies are concerned about the dynamics and control of multi-effect distillation. Tyreus and Luyben (1976) published one of the first papers in this area addressing the control of the dual feed configuration. Their main conclusion was to decouple the two columns by introducing an auxiliary reboiler and condenser. Other authors have discussed the use of an auxiliary reboiler and condenser. Lenhoff and Morari (1982) questioned their conclusion since they did not find such an effect. Gross et al. (1998) used an auxiliary reboiler in their simulations, but noted that even if an additional reboiler provides an additional manipulated variable it may also lead to severe interaction problems.

The work by Roffel and Fontein (1979) is most similar to our work. They discuss some aspects related to constrained control. Much of their discussion is based on steady state economics and active constraints.

Frey et al. (1984) recommended using ratios of material flows as manipulated variables after examining four different control schemes for the dual feed case with and without mass integration. They used the relative gain array (RGA) as a controllability measure. Much of the above work used simple models that did not include important effects, like flow dynamics and heat transfer area. Gross et al. (1998) presents results for a rigorous model where they used controllability analysis and non-linear simulations for a dual feed industrial heat integrated process. They conclude that a detailed model is needed in order to capture essential details.

The objective of this work is the selection of controlled variables for the heat-integrated system, that is, determining which variables should be controlled. The concept of self-optimising control (Skogestad, 2000) is used, which is based on steady state economics, to provide us with a systematic framework for the selection of the controlled variables. This method involves a search for the variables that, when kept constant, indirectly lead to near-optimal operation with acceptable economic loss. In self-optimising control, rather than solving the optimisation problem on-line, the problem is transformed into a simple feedback problem (Skogestad, 2000). In practice, this means that when the plant is subject to disturbances it will still operate within an acceptable distance from the optimum, and there is no need to re-optimise when disturbances occur. This paper uses this method to find which variables should be controlled for a multi-effect distillation case so that the system will operate near the optimum.

Modelling

The system studied is a multi-effect separation of methanol and water with small amounts of ethanol present in the feed (see Table B.1 for feed and column data). The feed enters the high pressure (HP) column where methanol at 99% is the top product (see Figure B.1). The bottom stream from the HP column containing methanol, water and a small amount of ethanol goes to the low pressure (LP)

column where the final separation between methanol and water takes place. In the LP column the top product is also methanol at 99% and the bottom product is water at > 99% purity. The LP column has also a small side stream, below the feed stage, to prevent ethanol building up in the bottom parts of the column. Heat is transferred from the condenser in the high-pressure column to the reboiler in the low-pressure column.

Figure B.1. The multi-effect distillation system.
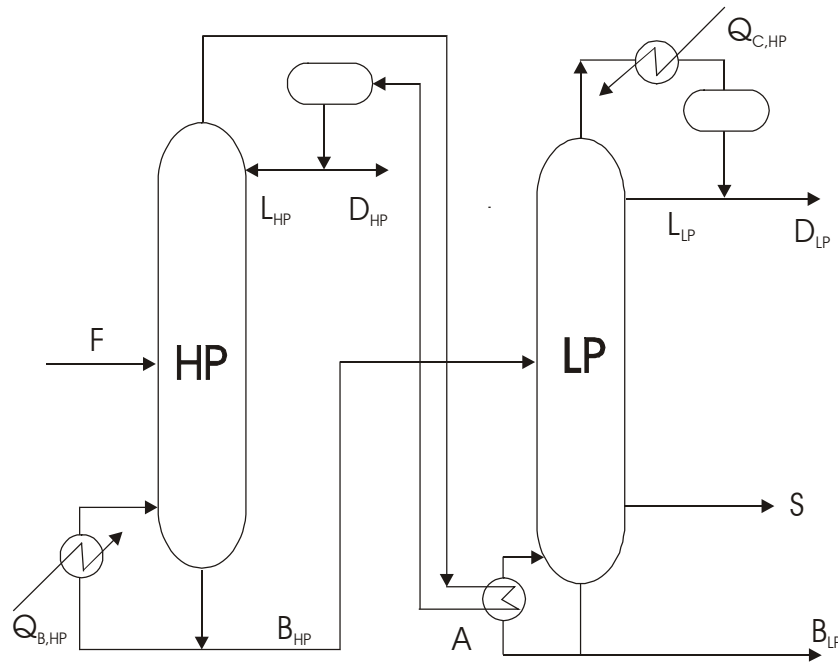
A "rigorous" model is used where the energy, material (overall) and component balances are included. Holdup in the vapour phase has been neglected. This considerably simplifies the model and is usually a good assumption when the pressure is below 10 bar (Choe et al., 1987). The vapour-liquid equilibrium has been modelled by assuming ideal gas and using liquid activity coefficients for the ternary system from the Wilson equation. The parameters used are from Gmehling and Onken (1977). To model the liquid flows we have used a simplified Francis weir formula. In the dynamic model the vapour flow, V, on a stage *i* has been modelled using a valve type equation for the pressure drop from one stage to the next:

$$V_i = c\sqrt{P_{i-1}^2 - P_i^2} \qquad (B.1)$$

For the integrated reboiler/condenser we have calculated the heat duty from:

$$Q = UA\left(T_{T,HP} - T_{B,LP}\right) \tag{B.2}$$

where $T_{T,HP}$ is the temperature at the top of the HP column and $T_{B,LP}$ is the temperature in the bottom of the LP column.

In the optimisation, the area, A, is treated as a degree of freedom and there is a maximum available area for the exchanger (A_{max}). An alternative to using a maximum area would be to specify an allowable temperature difference, ΔT_{min}, for the exchanger. If area is totally unconstrained and with no minimum allowable temperature difference then it would be optimal to have an infinite area.

Table B.1. Feed and column data.

Feed & Column Data	
Feed rate:	1200 mol/s
Feed composition:	73 mol% methanol
	2 mol% ethanol
	25 mol% water
Feed liquid fraction:	$q_F = 1$
No. stages HP column	36
No. stages LP column	48

Self-Optimising Control

The self-optimising control procedure (Skogestad, 2000) consists of six steps: 1) a degree of freedom (DOF) analysis, 2) definition of cost function and constrains, 3) identification of the most important disturbances, 4) optimisation, 5) identification of candidate controlled variables and 6) evaluation of loss with constant setpoints for the alternative sets of controlled variables.

The multi-effect column (*see Figure 1*) has 11 dynamic (control) degrees of freedom: the feed rate, heat duty in the HP column, reflux in HP and LP columns, distillate flows in HP and LP column, heat transfer rate/area in the integrated condenser/reboiler, the bottom flow in the HP and LP column, the cooling in the LP column and the sidestream in the LP column. There are 4 levels (condenser and reboiler in each column) with no steady-state effect (and thus with no effect on the cost) that have to be controlled, and with the feed rate given, this leaves 6 DOFs for optimisation.

In the formulation of the objective function there are two 'conflicting' elements; we would like to produce as much valuable product as possible, but using as little energy as possible. For a given feed, the cost function is defined as the amount of distillate (0.99 mol% methanol) multiplied by the price of methanol, minus the cost

of boilup: $J = P_D(D_{HP} + D_{LP}) - P_V V_{HP}$. As we would like to maximise the profit we have to minimise (-J). To simplify we have used a relative cost of energy, so the object function to be maximised is:

$$J = D_{HP} + D_{LP} - w_r Q_{HP} \qquad (B.3)$$

where $D_{HP} + D_{LP}$ (mol/s) are the top products (methanol) and Q_{HP} (MJ) is the heat load to the HP column and $w_r = 0.6488$ mol/MJ, is the relative cost of energy.

After defining the objective function the system constraints are specified. These are the model equations, i.e. the mass, component and energy balances, for the process (equality constraints) and operational constraints (inequalities) that has to be satisfied at the solution. The following operational constrains have been defined for the multi-effect system:

- The LP column must be operating at a pressure above or equal to 1 bar.

- The HP column must be operating at a pressure below or equal to 15 bar.

- The product (distillate) from both columns must contain at least 99% methanol.

- The bottom stream from the LP column should contain at least 99% water (i.e. no more then 0.1 % methanol and ethanol).

The optimisation problem can then be formulated as:

$$\min_u(-J_x(x,u,d)) \qquad \textit{objective function}$$

$$\textit{subject to}$$

$$g_1(x,u,d) = 0 \qquad \textit{model equations}$$

$$g_2(x,u,d) \le 0 \qquad \textit{operational constraints}$$

where;

    x – state variables

    u – independent variables we can affect (DOF for optimisation)

    d – independent variables we can not affect (disturbances)

By solving the optimisation problem we find the nominal steady state operating point, i.e. the optimal operating point for the multi-effect distillation when there are no disturbances. This gives us the optimal nominal values for all the variables in the system. It is then necessary to define the most important disturbances in the system. For this case we have considered disturbances in the feed flow of $\pm$ 20 %. Feed composition disturbances were not considered as it is assumed that they only have small variations. The optimisation problem was then solved for the disturbances to find the optimal cost (or profit) for each case, used for calculating the loss. The optimal solution for the nominal case and the two disturbances can be seen in Table B.2.

From the optimisation it was found that the following five constraints are *active*:

- the pressure in the LP column - should be 1 bar

- purity in the distillate from the HP column should be at 99 mol% methanol

- purity in the distillate from the LP column should be at 99 mol% methanol

- purity in the bottom stream from the LP column should be at 99 mol% water

- the area should be equal to the maximum area, A_{max}

The pressure constraint for the HP column was not an active constraint as the optimal value of 11.39 bar is below the maximum allowable pressure of 15 bar.

Table B.2. Optimum solution for nominal case and for F +20% and F-20%.

F	J_{opt} (mol/s)	$x_{D,HP}$	$x_{D,LP}$	$x_{B,HP}$
100 %	815.82	0.99	0.99	0.567
120 %	850.37	0.99	0.99	0.594
80 %	664.65	0.99	0.99	0.5013
$x_{B,LP\,(water)}$	P_{LP} (bar)	P_{HP} (bar)	LT_{HP} (kmol/h)	VB_{HP}(kmol/h)
0.99	1.0130	11.39	5468.8	7138
0.99	1.0130	11.41	5753.4	7532.9
0.99	1.0130	11.25	5535.2	7151.5
A (m^2)	LT_{LP}(kmol/h)	VD_{LP}(kmol/h)	QB_{HP} (MW)	ΔP_{HP} (bar)
5360	3744.1	5187.5	66.486	0.76
5360	3619.8.	5084.8	70.165	0.84
5360	4331.7	5284.2	66.612	0.77
$Tb_{,LP}$ (K)	$T2_{LP}$ (K)	$T6_{LP}$ (K)	B_{HP} (kmol/h)	D_{HP}(kmol/h)
412.11	404.69	381.9	2652.5	1667.5
411.99	405.82	378.96	3407.2	1776.8
411.61	401.07	389.04	1838.5	1617.5
D_{LP}(kmol/h)	B_{LP}(kmol/h)	S (kmol/h)	QB_{LP} (MW)	VD_{HP}(kmol/h)
1422.7	993.43	236.43	58.633	7137.4
1445.4	915.62	1046.2	57.472	7531.5
930.67	843.76	64.096	59.725	7153.8

Evaluation of Loss with Constant Setpoints

It is optimal that the system is operated so that the five active constraints listed above are fulfilled. We should therefore use a control system where these variables are controlled at their constrained value ("active constraint control"). This means that there is one steady state degree of freedom left. We now want to find the most suitable controlled variable for this remaining degree of freedom, for which the best choice is not obvious.

To do this a number of candidates for the control variables were proposed. To find out which of the candidates is most suitable we evaluate the loss $L = J(u,d) - J_{opt}(d)$ for the defined disturbances, when the variables are kept constant at their nominal optimal set point. In addition to evaluating the loss at the selected disturbances the loss is also found when there are implementation errors in the controlled variables (c_s) of 20%. The variable selected for self-optimising control should give an acceptable loss.

From the evaluation of we found that the best variable to keep at constant setpoint is the temperature on tray six in the LP column.

Multiplicities in the Objective Function

The results in Figure B.2 give some ideas about the non-linear behaviour of the solution surface for this problem. Using a constant area in the integrated reboiler/condenser it can be seen how some of the variables are varying with the heat load to the HP column. It can also be observed in Figure B.3 that there are multiplicities in the objective function of some variables. The consequence of these multiplicities in the objective function is that if these variables are used for control then a small implementation error could move the plant into a region with a very large loss or infeasibilities in the objective. From this (see also Figure B.3 and Table B.2) we exclude the concentration in the bottom of the HP column, $x_{B,HP}$, and the bottom flowrate from the HP column, B_{HP}, as candidates for the controlled variable.

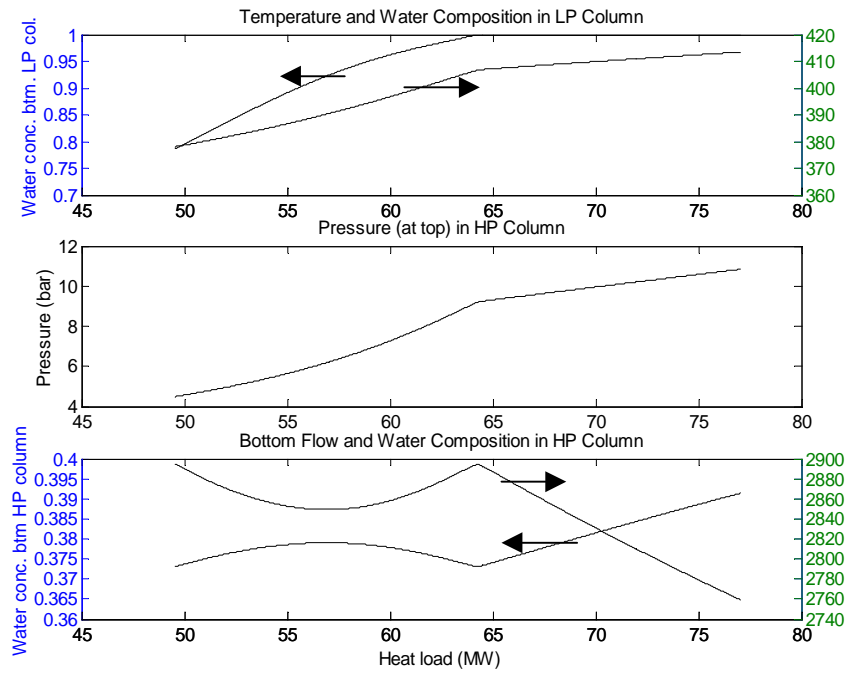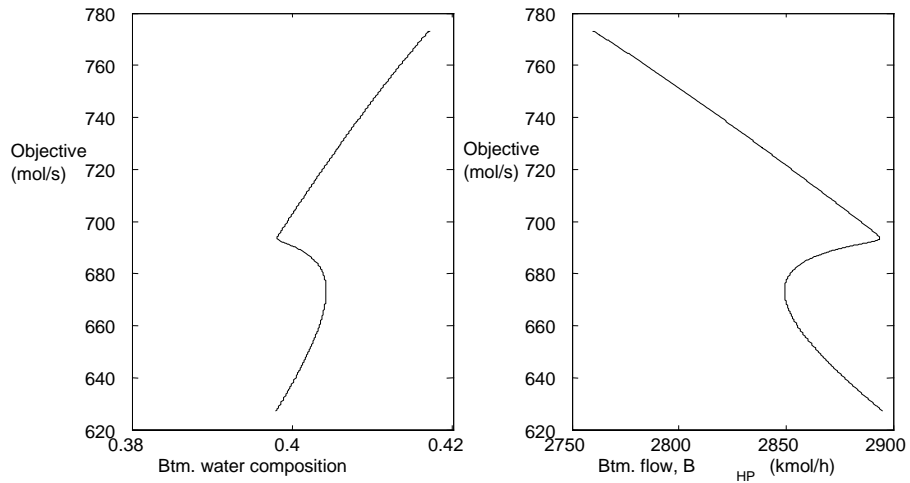*Figure B.2. Selected variables as a function of heat load to HP column.*

Figure B.3. Multiplicities in the objective function.

Proposed Control Structure

Based on the analysis above a control structure is proposed for the multi-effect columns, as shown in Figure B.4. The control structure has the following features:

A)   Stabilising level loops (4)

- The distillate flows are used for level control in the condensers of both columns.

- The bottom flow in the low-pressure column, B_{LP} is used for level control.

- The reboiler level in the high-pressure column is controlled by the boilup in the bottom of the high-pressure column.

B)   Active constraint loops (5)

- The reflux flows are used for final composition control of the distillate streams from both columns.

- The pressure in the LP column is controlled by the condensation rate in the condenser.

- The sidestream flowrate is used for composition control in the LP column bottom stream (controlling the water concentration)

- The maximum area in the integrated reboiler/condenser is used (not an actual control loop)

C)   "Self-optimising" loops (1)

- The bottom flowrate in the high-pressure column, B_{HP} is used for temperature control on tray 6 in the low-pressure column (this is the 'self-optimising control loop').

Discussion

Above, it was have assumed that the feedrate is set at the inlet to the plant. However, this may require reconfiguration of loops if one of the columns becomes a bottleneck. For example if there is an increase in the feedrate to the HP column then eventually this will lead to a case where either the boilup (or the pressure) in this column will reach its constrained value.

If there is a chance that one of these constraints may be reached then boilup is effectively lost as a degree of freedom for control and it will be advantageous to use an alternative control structure. An alternative could for example be to switch to using the feedrate to control the holdup in the bottom of the HP column. This configuration would require that there is a small holdup tank upstream of the HP column so that the feedrate can be manipulated.

In the self-optimisation procedure only the steady state effects of the system has been considered, that is we have found the best control variables for the system

based on the steady state economics. The dynamic effects have not been considered in detail. However, there may be some interesting effects with the selected control structure in Figure 4. Looking at the open loop response in the methanol concentration in the top of the HP column when making a step in the reflux (with holdup loops closed) then the response of the concentration of methanol will first increase with increasing reflux, then decrease. This happens because the boilup is used to control the liquid level in the bottom of the column. An increase in the reflux flowrate will first give an increase in the concentration of methanol, but as the reflux reaches the bottom part of the column the level increases and thus boilup is increased. As a result there will be more of the heavy component going up the column and the methanol concentration will decrease. Dynamic effects of the selected control structure will therefore be considered in further studies.

Figure B.4. The proposed control structure.
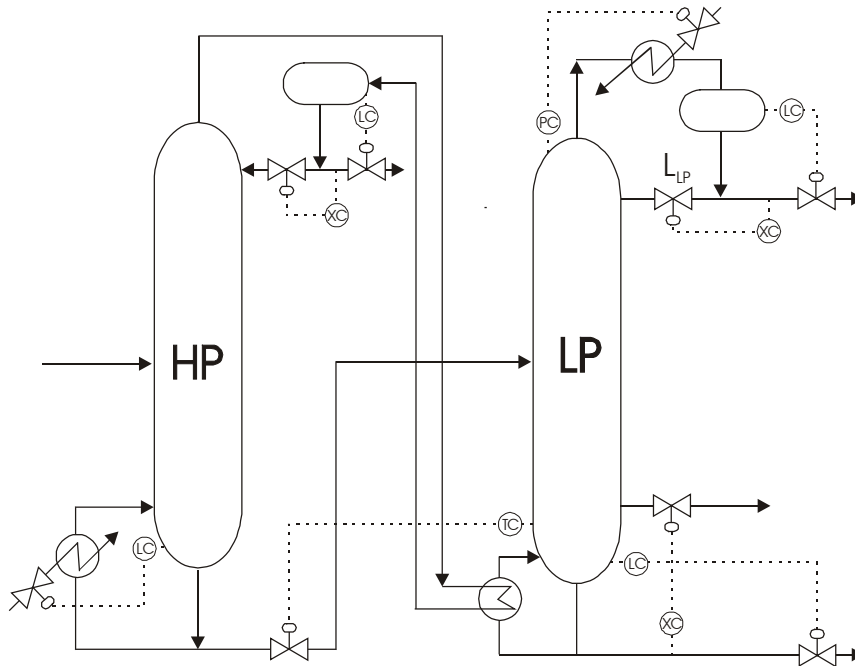
Conclusions

The method of self-optimising control has been applied to a multi-effect distillation case. We have found that five of the system variables should be controlled at their constraints: the top composition in both columns, the pressure in the LP column, the composition in the bottom of the LP column and the area in the integrated exchanger. This left one unconstrained degree of freedom for which the choice of a suitable controlled variable was not obvious. It was found that selecting a temperature in the lower part of the LP column has good self-optimising properties.

It has also been shown that certain variables may have multiplicities in the objective function and they are thus unsuitable for self-optimising control.

References

Hewitt, G., Quarini, J., Morell, M., More efficient distillation, The Chemical Engineer, 21 Oct. 1999

Wankat, P.C., 'Multieffect distillation processes', Ind. Eng. Chem. Res., 1993, 32, 894-905CEP

Tyreus, B.D., Luyben, W.L., 'Controlling heat integrated distillation columns', Chemical Engineering Progress, Sept. 1976, p. 59-66

Lenhoff. A.M., Morari, M., 'Design of resilient processing plants - I: Process design under consideration of dynamic aspects', Chemical Engineering Science, 1982, Vol. 37, No.2, p.245-258

Gross, F., Baumann, E., Geser, A., Rippin, D.W.T., Lang, L., 'Modelling, simulation and controllability analysis of an industrial heat-integrated distillation process', Computers Chem Engng, 1998, Vol. 22, No.1-2, p.223-237

Roffel, R., Fontein, H.J., 'Constraint control of distillation processes', Chemical Engineering Science, 1979, Vol. 34, pp. 1007-1018

Frey, R.M., Doherty, M.F., Douglas, J.M., Malone, M.F., 'Controlling thermally linked distillation columns', Ind. Eng. Chem. Process Des. Dev., 1984, 23, p.483-490

Skogestad, S., Plantwide control: the search for the self-optimizing control structure, J. Proc. Control, 2000, Vol. 10, pp. 487-507

Choe, Y.S., Luyben, W.L., Rigorous dynamic models of distillation columns, Ind. Eng. Chem. Res., 1987, 26, pp. 2158-2161

Gmehling, Onken, DECHEMA Chemistry Data Series, 'Vapor-Liquid Equilibrium Data Collection', Vol. I, Part 1, 1977, Published by DECHEMA

Larsson, T., Skogestad, S., Control of an industrial heat integrated distillation column, Presented at the AIChE Annual Meeting, Dallas, November, 1999

Appendix C. Minimum Vapour Flow of Different Distillation Arrangements

Table C.1 presents energy savings of different multi-effect arrangements, compared in percent with the best of the conventional non-integrated DS or IS arrangement (without multi-effect heat integration). Relative volatility has been assumed to be constant with pressure.

Table C.1. Energy savings of different distillation arrangements.

z_F	Column Arrangement	$\alpha = [4\ 2\ 1]$	$\alpha = [5\ 4.5\ 1]$	$\alpha = [5\ 1.5\ 1]$	$\alpha = [2\ 1.5\ 1]$	$\alpha = [10\ 5\ 1]$
	DS	-1.94	0.00	-4.98	0.00	-0.28
1/3	IS	0.00	-0.51	0.00	0.00	0.00
1/3	Petlyuk	32.80	7.59	12.76	39.54	32.71
1/3	DSF/DSB	47.26	7.59	25.56	39.54	32.71
	ISF/ISB	32.80	8.21	12.76	44.65	34.03
	PF/PB	61.73	37.44	47.41	59.06	50.05
	DS	0.00	0.00	0.00	0.00	0.00
0.80	IS	-10.25	-2.14	-3.75	-17.43	-4.07
0.10	Petlyuk	14.96	1.73	19.04	12.45	8.10
0.10	DSF/DSB	14.96	1.73	29.55	12.45	8.10
	ISF/ISB	15.23	1.77	19.04	12.86	8.18
	PF/PB	19.92	10.78	32.34	19.68	13.27
	DS	-6.59	-1.22	-4.89	-8.63	-3.08
0.1	IS	0.00	0.00	0.00	0.00	0.00
0.45	Petlyuk	27.46	11.01	9.18	40.70	41.46
0.45	DSF/DSB	32.59	11.01	12.33	44.50	47.81
	ISF/ISB	27.46	12.62	9.18	40.70	41.46
	PF/PB	57.09	50.71	43.72	63.52	68.45
	DS	-0.09	0.00	-0.23	0.00	-0.01
0.10	IS	0.00	-0.03	0.00	0.00	0.00
0.80	Petlyuk	32.99	11.39	12.43	47.37	44.23
0.10	DSF/DSB	37.69	11.39	16.20	47.34	49.62
	ISF/ISB	32.99	11.63	12.43	49.02	44.23
	PF/PB	65.55	52.83	54.54	71.71	71.80

z_F	Column Arrangement	$\alpha = [4\ 2\ 1]$	$\alpha = [5\ 4.5\ 1]$	$\alpha = [5\ 1.5\ 1]$	$\alpha = [2\ 1.5\ 1]$	$\alpha = [10\ 5\ 1]$
	DS	-6.25	0.00	-17.42	0.00	-0.78
0.45	IS	0.00	-1.38	0.00	0.00	0.00
0.10	Petlyuk	34.38	4.53	14.19	34.78	18.39
0.45	DSF/DSB	34.38	4.53	27.74	34.78	18.39
	ISF/ISB	34.38	4.90	14.19	39.13	19.26
	PF/PB	42.58	18.40	37.29	45.65	26.45
	DS	-22.49	-4.20	-13.04	-27.32	-14.40
0.1	IS	0.00	0.00	0.00	0.00	0.00
0.1	Petlyuk	16.11	11.54	4.27	23.42	33.56
0.8	DSF/DSB	19.46	11.54	5.43	25.85	40.14
	ISF/ISB	16.11	16.26	4.27	23.42	33.56
	PF/PB	31.90	41.09	18.05	35.35	55.56
	DS	0.00	0.00	0.00	0.00	0.00
0.45	IS	-4.37	-1.07	-1.92	-7.35	-1.93
0.45	Petlyuk	33.60	6.62	14.13	32.56	30.23
0.1	DSF/DSB	42.19	6.62	35.52	32.56	30.23
	ISF/ISB	33.60	6.76	14.13	33.84	30.53
	PF/PB	56.96	36.67	54.88	53.15	47.79
	DS	0.00	0.00	-1.06	0.00	0.00
0.3	IS	-0.66	-0.49	0.00	-2.11	-0.52
0.5	Petlyuk	33.40	8.50	13.41	40.03	37.72
0.2	DSF/DSB	48.91	8.50	25.70	40.03	37.72
	ISF/ISB	33.40	8.89	13.41	43.12	38.53
	PF/PB	64.43	42.87	52.40	62.01	57.39
	DS	0.00	0.00	-1.06	0.00	0.00
0.20	IS	-0.66	-0.49	0.00	-2.11	-0.52
0.60	Petlyuk	33.40	8.50	13.41	40.03	37.72
0.20	DSF/DSB	48.91	8.50	25.70	40.03	37.72
	ISF/ISB	33.40	8.89	13.41	43.12	38.53
	PF/PB	64.43	42.87	52.40	62.01	57.39